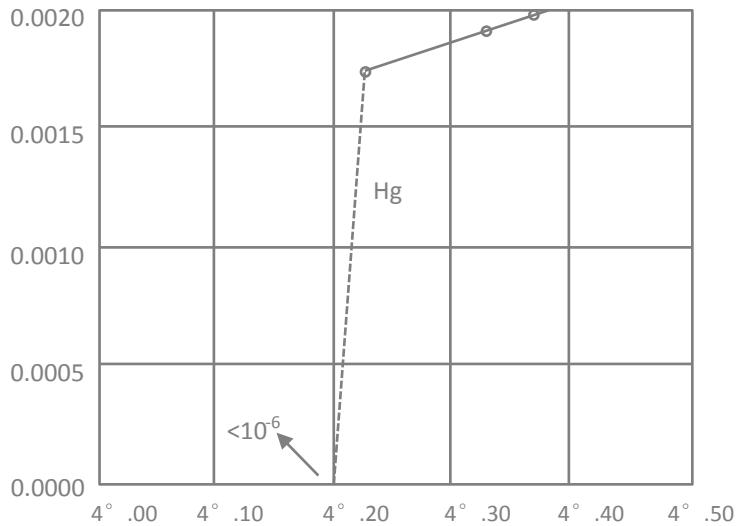




LT26 Schedule

The 26th International Conference
on Low Temperature Physics



August 10 – 17, Beijing International Convention Center, Beijing, China

Thursday Aug.11				
Time Slot	Category	ABSN	Name	Title
Plenary Session(11P)				
11P-1		A1472	Humphrey Maris	Studies of Quantum Liquids in Metastable States
11P-2		D1448	Hans Mooij	Quantum vortices, quantum phase slip and quantum bits
11P-3		D1439	Gerd Schön	Quantum State Engineering with Josephson Junctions
11P-4		B1467	Nikolai B. Kopnin	Vortex Dynamics in Superconductors and Fermi Superfluids
Parallel Session(11a-A) Supersolid I				
11a-A1			Sebastien Balibar	
11a-A2		A1437	Keiya Shirahama	Quantum Criticality of 4He in Nanoporous Media: Effects of Confinement and Disorder
11a-A3		A1383	Anatoly Kuklov	Superclimbing dislocations in solid Helium-4
11a-A4		A1433	Jordi Boronat	Vacancies and 3He atoms in solid 4He
11a-A5		A1389	John Reppy	Torsional Oscillator Studies of the Shear Modulus of Solid 4He
Parallel Session(11a-B) Physical Properties of Fe-based and Cuprate Superconductors I				
11a-B1		B1436	Shin-ichi Uchida	In-Plane Electronic Anisotropy in Iron Pnictides
11a-B2		B0829	Yasutomo Uemura	Comparable energy scales of superconducting charges and spin fluctuations in unconventional
11a-B3			Hong Ding	
11a-B4		B1002	N. C. Yeh	Comparative studies of the field-dependent scanning tunneling spectroscopy in cuprate
11a-B5		B1336	Peter Armitage	Fast vortices in the Cuprates? A vortex plasma model analysis of the THz conductivity and
Parallel Session(11a-C)				
11a-C1			Bela Lake	
11a-C2			Xiaofeng Jin	
11a-C3		C1410	P. Mendels	Quantum Kagome Antiferromagnets : Local NMR and muSR Experiments
11a-C4		C0188	T. Shiroka	Low-temperature features of random Heisenberg spin chains
11a-C5		C0597	S. Maegawa	Quantum Spin Liquid in an Organic Triangular Lattice Antiferromagnet EtMe3Sb [Pd(dmit) 2]2
Parallel Session(11a-D)				
11a-D1		A1476	Oleg Astafiev	Josephson-junction quantum systems in open 1D space

11a-D2		D1449	Marco Aprili	Microwave cooling of Josephson plasma oscillations
11a-D3			Dmitri Averin	
11a-D4		D1348	Shiping Zhao	A two-step transition description of underdamped phase diffusion
11a-D5		D1445	Francesco Giazotto	A quantum electron pump operating at the Josephson frequency
Parallel Session(11a-E)				
11a-E1		E0361	Yuki Sato	Superfluid Helium Quantum Interference Devices: Present Status and Future Prospects
11a-E2		E1429	Pierre-François Cohadon	Optomechanical resonators for cryogenic operation
11a-E3		A1400	Weijun Yao	Search for the Neutron Electric Dipole Moment on SNS
11a-E4		E0346	D. Vasyukov	Nano-sized SQUID-on-tip for a scanning SQUID microscope
11a-E5		E0944	Masamichi Saitoh	Development of Tunnel Junction Micro-SQUID Magnetometer for Investigation of Single-
Poster Session				
11P-A001	A3	A0048	H. R. Glyde, S.O. Diallo, R. T. Azuah, O. Kirichek, and J. W. Taylor	Bose-Einstein Condensation in Liquid Helium under Pressure
11P-A002	A3	A0085	Sergey K. Nemirovskii and Minoru Kubota	Nonlinear Response of the Torsional Oscillation of the Vortex Tangle.
11P-A003	A3	A0100	N. P. Mikhin, A. P. Birchenko, A. S. Neoneta, E. Ya. Rudavskii and Ye. O.	NMR Observation of Disordered Inclusions in the hcp Solid Helium: Evolution from Liquid to Possible Glassy State
11P-A004	A3	A0113	A.A. Lisunov, V.A. Maidanov, V.Yu. Rubanskyi, E. Ya. Rudavskii, S.P. Rubets,	Search for a disordered (glassy) phase in solid \$^3\$He
11P-A005	A3	A0120	S. T. Chui	Supersolidity and AC and DC Rotations
11P-A006	A3	A0124	S. S. Kim, C. Huan, L. Yin, J. S. Xia, N. S. Sullivan, and D. Candela	Nuclear Spin Relaxations of Very Dilute \$^3\$He in Solid \$^4\$He
11P-A007	A3	A0130	I. Iwasa	Dislocation Model for the TO-Period Anomaly
11P-A008	A3	A0131	K. A. Chishko, T. N. Antsygina, I. I. Poltavsky, M. I. Poltavskaya	Two-dimensional hard-core bosons in the superfluid phase: Excitation spectra

11P-A009	A3	A0182	Minoru Kubota, Masahiko Yagi, Nobutaka Shimizu, and Akira Kitamura	Quantized Vortex Physics in the hcp 4He, Studied by Torsional Oscillator with Detailed AC Velocity Dependence and Under DC
11P-A010	A3	A0213	V.Yu. Rubanskyi, V.A. Maidanov, A.A. Lisunov, E.Ya. Rudavskii, and S.P.	Formation of a Glassy Phase in Solid ${}^4\text{He}$: Comparison of Rapidly Quenched and Deformed Samples
11P-A011	A3	A0230	L. Reatto, D.E. Galli, and M. Rossi	Quantum Monte Carlo study of quantized vortices in two-dimensional solid Helium
11P-A012	A3	A0292	J. Ahokas, O. Vainio, J. J?rvinen, V. V. Khmelenko, D. M. Lee and S. Vasiliev	Magnetic resonance study of H atoms in solid H_2 at temperatures below 1 K
11P-A013	A3	A0296	A. Eyal and E. Polturak	BCC vs. HCP - The Effect of Crystal Symmetry on the High Temperature Mobility of Solid ${}^4\text{He}$
11P-A014	A3	A0380	M. Kunimi, M. Kobayashi, and Y. Kato	Dynamics of one-dimensional supersolids
11P-A015	A3	A0439	X. Rojas, A. Haziot, and S. Balibar	Migration of ${}^3\text{He}$ Impurities along Dislocation Lines in ${}^4\text{He}$ Single Crystals
11P-A016	A3	A0443	Xiao Mi, Erich Mueller, and John Reppy	Supersolidity in Solid ${}^4\text{He}$ and the Shear Modulus Anomaly
11P-A017	A3	A0477	P. Gumann, M. C. Keiderling, D. Ruffner and H. Kojima	Hysteretic Response of Torsional Oscillators Containing Solid He-4 at Low Temperatures
11P-A018	A3	A0629	R.B. Hallock	Mass Flux through Solid ${}^4\text{He}$ Induced by Chemical Potential Differences
11P-A019	A3	A0869	K. Yamashita and D. Hirashima	Quantum crystal induced by interparticle repulsive interaction
11P-A020	A3	A0924	G. Nichols, J. Saunders, B. Cowan	Supersolid Measurements using a two-mode torsional oscillator
11P-A021	A3	A1031	A. Penzyev, E. Varoquaux and Y. Mukharsky.	Extreme softness of crystallites in polycrystalline helium-4.
11P-A022	A3	A1033	J. Bossy, M.M. Koza, A. Braslau and Y. Mukharsky	Inelastic scattering of neutron on solid ${}^4\text{He}$ in supersolid regime

11P-A023	A3	A1040	D.E. Zmeev and A.I. Golov	Simultaneous Measurements of the Torsional Oscillator Anomaly and Thermal Conductivity in Solid ${}^4\text{He}$
11P-A024	A3	A1078	A.A. Levchenko, L.P. Mezhov-Deglin	Boundary and Phonon-Dislocation Scattering\\ in Thermal Conductivity of HCP ${}^4\text{He}$ Crystals
11P-A025	A3	A1122	H. Lauter, V. Apaja, I. Kalinin, E. Katz, M. Koza, E. Krotscheck, V. Lauter and A. Puchkov	Quasi-2D superfluid helium in solid helium in aerogel
11P-A026	A3	A1251	Y. Shibayama, H. Fukuyama and K. Shirahama	Hysteresis of Non-Classical Rotational Inertia in 2D ${}^4\text{He}$ Films on Graphite
11P-A027	A3	A1279	Yu Yongle	Onset Properties of Supersolid Helium
11P-A028	A3	A1328	D. Takahashi, T. Harano, K. Kono, and K. Shirahama	Rotation Measurement of Supersolid in Nanoporous Media
11P-A029	A3	A1335	A.D. Fefferman, X. Rojas, A. Haziot, J. West, M.H.W. Chan, S. Balibar	Torsional oscillator studies of helium-4 single crystals
11P-A030	A3	A1373	Minoru Kubota, Masahiko Yagi, Akira Kitamura, Krzysztof Rogacki, and Robert M.	A quest for the Critical Angular Velocity, $\Omega_{\text{c}1}$, and the Landau State in the Supersolid State of hcp ${}^4\text{He}$
11P-A031	A3	A1392	E. Pratt, B. Hunt, V. Gadagkar, M.Yamashita, M. J. Graf, A. V. Balatsky	Interplay of Rotational, Relaxational, and Shear Dynamics of Solid ${}^4\text{He}$
11P-B001	B1	B0079	V. Meerovich, V. Sokolovsky, T. Prikhna ,W. Gawalek and T. Haberreuther	Voltage-current characteristic and transport current AC losses measured by the transformer method in high pressure synthesized MgB₂
11P-B002	B1	B0098	K. K. Choudary, D. Prasad and N. Kaurav	Interpretation of optical conductivity in normal state of Iron-Based Superconductors CeOFeAs
11P-B003	B1	B0101	N. Kaurav, K. K. Choudhary and Y. K. Kuo	Analysis of heat transport in the of iron oxyarsenide TbFeAsO_{0.85}
11P-B004	B1	B0163	Paola Arevalo and Roberto Escudero	Superconductivity in a topological Insulator doped with Pd and H.
11P-B005	B1	B0186	P. M. Shirage, K. Kihou, C. H. Lee, H. Kito, H. Eisaki, A. Iyo	New Iron-based Perovskite-type Superconductors of (Ca₄Al₂O_{6-y})(Fe₂Pn₂) and (Ca₃Al₂O_{5-y})(Fe₂Pn₂) (Pn=As,P)

11P-B006	B1	B0187	J. Haenisch, K. Iida, S. Trommler, F. Kurth, S. Haindl, V. Matias, R. Huehne, J. Engelmann,	Electrical transport properties of clean and pinning-improved Co-doped Ba- 122 thin
11P-B007	B1	B0221	Bhanu Joshi, S.Ramakrishnan,Arumugam Thamizhavel	Study of superconductivity in a single crystal of noncentrosymmetric BiPd
11P-B008	B1	B0246	H. Kaneko, Y. Yun, N. Shumsun, A. Savinkov, H. Suzuki, Y.K. Li, Q. Tao, G.H. Cao, and	Quantum Criticality and Superconductivity in SmFe(1-x)CoxAsO
11P-B009	B1	B0315	P. Mandal, P.Choudhury	Vortex phase diagram of PrFeAsO0.60F0.12 superconductor
11P-B010	B1	B0381	B. Shinozaki, S. Takada, N. Kokubo, K. Makise, T. Asano, K. Yamada, K. Yano, and	Characteristics of T_c and $\rho(T)$ of polycrystalline (In₂O₃)-(ZnO) films with low carrier density
11P-B011	B1	B0422	Sahana Roessler, Dona Cherian, H. S. Nair, H. L. Bhat, S. Elizabeth, F. Steglich	Electronic properties across the first-order phase transition in Fe1.05Te
11P-B012	B1	B0436	J.P. Rodriguez, M.A.N. Araujo and P.D. Sacramento	Spin-wave excitations and Fermi surfaces of iron-pnictide superconductors from the local magnetic moment limit
11P-B013	B1	B0438	D. J. Gawryluk, J. Fink-Finowicki, A. Wisniewski, R. Puzniak, V.	Superconducting and structural properties of pure FeTe1-xSex (0.3 < x < 0.5) and Co, Ni, and Cu substituted Fe1+/-delta Te0.65Se0.35
11P-B014	B1	B0487	Y. Oda, G. Motoyama, M. Shiotsuki, and A. Sumiyama	Superconductivity and Magnetic Aftereffects in
11P-B015	B1	B0491	R. Yoshizaki, T. Yamamoto, H. Ikeda, and K. Kadowaki	A New Aspect of Single Layered Cuprate Superconductors - 90 K Superconductors for Ca-Doped Bi₂Sr₂CuO_{6+delta} Single Crystals
11P-B016	B1	B0528	A. Iyo, P. M. Shirage, K. Kihou, C.H. Lee, H. Kito, and H. Eisaki	(Eu₃Sc₂O_{5-y})(Fe₂Pn₂) (Pn = As, P): new possible iron oxypnictides for superconductors
11P-B017	B1	B0541	Q.T. Meng, S. Komaki, T. Tsuneoka, H. Hanada, S. Maeda, T. Murano, F. Ichikawa,	Tunnel Spectroscopy and microstructure on Bi₂Sr₂Ca_{1-x}Y_xCu₂O_{8+y} crystals
11P-B018	B1	B0562	Yu. N. Chiang, M. O. Dzyuba	POINT-CONTACT CONDUCTANCE OF THE NS HYBRID SYSTEM MO(N)/MO-C(S)
11P-B019	B1	B0572	Y. Ihara, Y. Kimura, K. Kumagai, E. Bauer, G. Rogl, P. Rogl	\$^{127}Al- and \$^{195}Mo-NMR Study on Noncentrosymmetric Superconductor Mo₃Al₂C

11P-B020	B1	B0573	K. Magishi, T. Saito, K. Koyama, N. Matsumoto and S. Nagata	NMR Study of Layered Transition Metal Ditetelluride (Ir,Pt)Te₂
11P-B021	B1	B0604	H. C. Xu, Y. Zhang, B. Zhou, L. X. Yang, D. L. Feng*	Angular Resolved Photoemission Spectroscopy Study on layered pnictide-oxide BaTi₂As₂O
11P-B022	B1	B0606	H. C. Xu, Y. Zhang, B. Zhou, L. X. Yang, D. L. Feng*	Angular Resolved Photoemission Spectroscopy Study on layered pnictide-oxide BaTi₂As₂O
11P-B023	B1	B0613	J. I. Gorina, G. A. Kaljuzhnaja, M. V. Golubkov, V. V. Rodin, N. N. Sentjurina, S. G.	Growth, structure and some superconducting properties of FeSe crystals
11P-B024	B1	B0630	J. Wosnitza, O. Ignatchik, S. Blackburn, B. Prevost, A.D. Bianchi, M. Cote, G.	Fermi Surfaces of the Iron-Pnictides LaFe\$₂P\$₂ and CeFe\$₂P\$₂
11P-B025	B1	B0671	K. Rogacki, P. J. W. Moll, N. D. Zhigadlo, S. Katrych, J. Karpinski, and B. Batlogg	Critical currents anisotropy in REFeAs(O,F) (RE = Sm, Nd) single crystals
11P-B026	B1	B0836	N.G. Margiani, I.R. Metskhvarishvili, T.D. Medoidze, N.A. Papunashvili, D.I.	Superconducting Properties of Boron-doped Eu-123 HTSs
11P-B027	B1	B0838	N.G. Margiani, I.R. Metskhvarishvili, T.D. Medoidze, N.A. Papunashvili, D.I.	Phase Evolution and Superconducting Properties of Boron-doped (Bi,Pb)-2223 HTSs
11P-B028	B1	B0935	J. Karpinski, N.D. Zhigadlo, S. Katrych, Z. Bukowski, P.J.W. Moll, R. Puzniak, K. Rogacki,	Doping and substitutions in LnFeAsO single crystals grown at high pressure: influence on superconducting properties and structure
11P-B029	B1	B0942	K. Ookuma, M. Ebata, T. Tomita, H. Takahashi, T. Hanna, Y. Muraba, S.	High-pressure studies for hydrogen substituted CaFeAsF1?xH_x
11P-B030	B1	B0983	N.D. Zhigadlo, S. Katrych, Z. Bukowski, P.J.W. Moll, K. Rogacki, J. Karpinski,	High-pressure crystal growth of LnFeAsO (Ln=rare earth)
11P-B031	B1	B1164	F. Dahlem, K. Hoummada, T. Kociniewski, D. Mangelinck, D.	Probing the local properties of superconducting silicon
11P-B032	B1	B1212	A. S. Vasenko, S. Kawabata, A. A. Golubov, M. Yu. Kupriyanov, C. Lacroix,	Current-voltage characteristics of SIFS Josephson junctions
11P-B033	B1	B1216	A. Sugimoto, R.Ukita, T. Ekino and S. Yamanaka	STM/STS Observation on Layered Nitride Superconductor \$\alpha\$-(H₂N-(CH₂)₁₀-NH₂)_xTiCl

11P-B034	B1	B1247	Liling Sun and Zhongxian Zhao	Pressure tuning of superconductivity of $AxFe_2-ySe_2$ ($A=K$ and Rb) single crystals
11P-B035	B1	B1252	A. Karimi and M. A. Shahzamanian	Shear Viscosity of the Superconductor of Sr_2RuO_4 in the Normal State
11P-B036	B1	B1256	G. Leon, M.J. Calderon and E. Bascones	Anisotropy in the magnetic state of undoped iron pnictides
11P-B037	B1	B1269	M.I. Tsindlekht, I. Felner, M. Zhang, A. F. Wang and X. H. Chen	Superconducting Critical Fields in $K_{(0.8)}Fe_{2.2}Se_2$
11P-B038	B1	B1300	Wenjian Lu, Lijun Li, Xiangde Zhu, and Yuping Sun	Superconductivity induced by Fe doping in 1T- TaS_2 single crystals
11P-B039	B1	B1322	Wenhe Jiao, Jinke Bao, Chunmu Feng, Zhu'an Xu, and Guanghan Cao	Evolution of superconductivity and ferromagnetism in $Eu(Fe_1-xRu_x)_2As_2$
11P-B040	B1	B1366	J. T. Ye, Y. J. Zhang, Y. Matsuhashi, and Y. Iwasa	Gate-Induced Superconductivity in Layered- Material-Based Electric Double Layer Transistors
11P-B041	B1	B1378	Q. Q. Liu, X. C. Wang, Z. Deng, Y. X. Lv1, J. L. Zhu, S. J. Zhang, Z. Y. Lu, C. Q. Jin	“111” iron pnictide superconductors: pressure enhanced superconductivity
11P-B042	B1	B1396	G. D. Gu, Zhijun Xu, Guangyong Xu, J. Tranquada, Su Jung Han, Q. Li, Hongbo	Crystal growth and superconductivity of Fe- base materials
11P-B043	B1	B1444	Kosmas Prassides	Fullerene Superconductivity 20 Years on
11P-B044	B1	B0961	M.E.Yakinci 1,2, E.Ortakoglu 1,2, M.A.Aksan 1,2, Y.Balci 1,2, S.Altin 1,2 and	Growth of Y-123 Thick Film with Modified Ultrasonic Spray Pyrolysis method and effects of post-annealing on the critical current density
11P-C001	C1	C0055	E. Fertman, A. Beznosov, V. Desnenko, S. Dolya, M. Kajnakova, and A.	Static and Dynamic Low Temperature Magnetic Properties of the $(Nd_{0.9}Y_{0.1})_{2/3}Ca_{1/3}MnO_3$
11P-C002	C1	C0074	T. Yokoo, S. Itoh, F. Trouw, A. Llobet- Megias, J. Taylor and J. Akimitsu	Magnetic Excitation of Possible Spin-Peierls System $TiOBr$
11P-C003	C1	C0081	Ivica Zivkovic	Low temperature magnetization of a new spin- ice system $CdEr_2Se_4$

11P-C004	C1	C0110	H. Manaka and Y. Miura	Electron Spin Resonance in Triangular Spin Tubes
11P-C005	C1	C0157	P. Farkasovsky and H. Cencarikova	Simple model of magnetization processes in rare-earth tetraborides
11P-C006	C1	C0158	P. Farkasovsky and H. Cencarikova	Simple model of magnetization processes in rare-earth tetraborides
11P-C007	C1	C0178	T.T.A. Lummen, C. Strohm, F. Parmigiani, M. Malvestuto, and P.H.M. van Loosdrecht	Geometrically frustrated CuFeO₂
11P-C008	C1	C0179	V.I. Nizhankovskii	Magnetostriction of Tb₂(MoO₄)₃ and MnF₂ in high magnetic field
11P-C009	C1	C0201	Y. Nakanishi, F. Shichinomiya, M. Koseki, G. Koseki, M. Nakamura, M. Kosaka,	Ultrasonics in the two-dimensional dimer spin system YbAl₃C₃
11P-C010	C1	C0208	M. Hiroi, H. Ko, S. Nakashima, I. Shigeta, M. Ito, H. Manaka, and N. Terada	Spin-Glass and Antiferromagnetic Transitions in Ru_{2-x}FexCrSi
11P-C011	C1	C0214	Z. Y. Zhao, X. G. Liu, Z. He, X. M. Wang, C. Fan, W. P. Ke, Q. J. Li, and X. F. Sun	Heat Transport of Quasi-One-Dimensional Ising-Like Antiferromagnet BaCo₂V₂O₈ in the Longitudinal and Transverse Fields
11P-C012	C1	C0240	N. Mufti, T. Dellmann, H.-H. Klau?, T. Woike, T.T.M. Palstra, H. Rosner, and C. Geibel	Antiferromagnetism, structural instability, frustration, and quantum critical point in intermetallic AFe₄X₂ systems
11P-C013	C1	C0257	Q. J. Li, X. M. Wang, W. P. Ke, X. G. Liu, C. Fan, Z. Y. Zhao and X. F. Sun	Huge magnetothermal conductivity in a spin liquid material Tb₂Ti₂O₇
11P-C014	C1	C0261	Uchima Kiyoharu	Transport properties of Y_{1-x}Nd_xCo₂
11P-C015	C1	C0266	Y. Matiks, B. Boris, E. Benckiser, A. Frano, T. Prokscha, E. Morenzoni, G. Cristiani,	Dimensionality-Controlled Collective Charge and Spin Order in Nickel-Oxide Superlattices
11P-C016	C1	C0269	Y. Furukawa, E. Micotti, A. Lascialfari, F. Borsa, P. Kogerler	Spin freezing in geometrically frustrated magnetic molecule Fe₃₀
11P-C017	C1	C0270	Yoko Miura and Hirotaka Manaka	Studies of Crystal Structure and Spin State in Diluted Triangular Spin Tube KCr_{1-x}Al_xF₄

11P-C018	C1	C0271	P. Ribeiro, P. D. Sacramento, K. Penc	Finite energy spectral function of an anisotropic 2D system of coupled Hubbard chains
11P-C019	C1	C0289	X. G. Liu, X. M. Wang, W. P. Ke, W. Tao, X. Zhao and X. F. Sun	Thermal conductivity of pure and Zn-doped LiCu₂O₂ single crystals
11P-C020	C1	C0294	S. Mühlbauer, E. Pomjakushina, S. Gvasaliya, S. Zhao, and A. Zheludev	Novel Phase of the Dzyaloshinsky-Moriya Spiral Magnet Ba₂CuGeO₇
11P-C021	C1	C0297	L. Yin, C. Huan, J. S. Xia, N. S. Sullivan, V. S. Zapf, A. Paduan-Filho, R. Yu and	Investigation of the magnetic susceptibility of the disordered BEC system NiCl_{0.85}Br_{0.15}-4SC(NH₂)₂
11P-C022	C1	C0299	Yu-Zhong Zhang	Possible origin of dual character of the electrons in iron-pnictides
11P-C023	C1	C0350	L. Didukh, Yu. Skorenkyy, O. Kramar and Yu. Dovhopaty	Analytical Approach for Investigation of Generalized Hubbard Model with Correlated Hopping and Low-Temperature
11P-C024	C1	C0360	L. Balicas, S. Nakatsuji, Y. Machida, and S. Onoda	Anisotropic hysteretic Hall-effect and magnetic control of chiral domains in the chiral spin states of Pr₂Ir₂O₇
11P-C025	C1	C0372	Zhi-chao Guo Hong-li Suo Yan-ling Cheng Zhi-yong Liu Lin Ma Min Liu	Is superconductor magnetic characteristic associated with unpaired itinerant electrons?
11P-C026	C1	C0374	D. X. Li, S. Nimori, S. Ohta, Y. Yamamura and Y. Shikama	Random spin freezing in single crystalline Ce₂CuSi₃
11P-C027	C1	C0377	Chomsin S Widodo, Muneake Fujii	Temperature Dependence of Magnetization at Zero Applied Magnetic Field in Nearly Two Dimensional Ferromagnets
11P-C028	C1	C0395	C. Fan, Y. Y. Lv, X. M. Wang, W. P. Ke, X. G. Liu, Z. Y. Zhao and X. F. Sun	Heat transport study of Dy₂Ti₂O₇ single crystals in a [110] magnetic field
11P-C029	C1	C0453	E. Cizmar, M. Orendac, A. Orendacova, A. Feher, S.-D. Jiang, and S. Gao	Thermodynamic and magnetic properties of triangular spin cluster system Cu₃(C₁₂H₉N₂O)₃(OH)(NO₃)₂·CH₃CN
11P-C030	C1	C0454	M.S.Tagirov, E.M.Alakshin, A.S.Alexandrov, A.V.Egorov,	Low temperature magnetism of PrF₃ single crystal, micro- and nanopowders
11P-C031	C1	C0457	A. Wisniewski, V. Markovich, I. Fita, R. Puzniak, P. Iwanowski	Size effect on magnetic properties of (La,Ca)MnO₃ nanoparticles

11P-C032	C1	C0464	Erik Wulf, Sebastian Muhlbauer, Tatiana Yankova, Vasiliy Glazkov, Dan	Bond randomness in the frustrated spin ladder $\text{Cu}_2(\text{Cl}_{1-x}\text{Br}_x)_4$
11P-C033	C1	C0506	K. Kimura, Y. Ohta, Y. Machida, S. Takajo, K. Matsubayashi, Y. Uwatoko, Y. Shimura,	Low Temperature Magnetism in the Metallic Pyrochlore $\text{Pr}_2\text{Ir}_2\text{O}_7$
11P-C034	C1	C0512	W. P. Ke, X. F. Sun	Heat Transport in the Quasi-one-Dimensional Alternating Spin Chain Material $(\text{CH}_3)_2\text{NH}_2\text{CuCl}_3$
11P-C035	C1	C0515	Zheng-Xin Liu, Yi Zhou and Tai-Kai Ng	Fermionic representation and mean
11P-C036	C1	C0518	K. Igarashi, Y. Shimizu, E. Satomi, Y. Kobayashi, T. Takami and M. Itoh	Absence of Magnetic Order in Ising Honeycomb-Lattice $\text{Ba}_3\text{Co}_2\text{O}_6(\text{CO}_3)_0.7$
11P-C037	C1	C0519	W. P. Ke, X. M. Wang, C. Fan, Z. Y. Zhao, X. G. Liu, L. M. Chen, Q. J. Li, X. Zhao and X. F.	Heat transport study of a layered spin-dimer compound $\text{Ba}_3\text{Mn}_2\text{O}_8$
11P-C038	C1	C0524	P. Vrábel, M. Orendá?, E. ?imá?r, A. Orend á?ová, L. Ru-Yin and S. Gao	Spin glass state in Kagomé antiferromagnet $\text{Co}(\text{NO}_3)_2\text{(bpg)DMF}_4/3$
11P-C039	C1	C0525	H. Kubo, K. Zemyo, T. Hamasaki, M. Hagihala and X. G. Zheng	NMR Study of Geometrically Frustrated Compounds $\text{Mn}_2\text{Br}(\text{OH})_3$
11P-C040	C1	C0527	Toru Sakai and Hiroki Nakano	Novel Field-Induced Quantum Phase Transition of the Kagome-Lattice Antiferromagnet
11P-C041	C1	C0536	Morodomi Hiroki, Inagaki Yuji, Kawae Tatsuya, Asano Takayuki and Ajiro	Low-Temperature Magnetization Study of Spin Gap System $(\text{CH}_3)_2\text{NH}_2\text{CuCl}_3$ with
11P-C042	C1	C0537	Y. Fuji, S. Nishimoto, and Y. Ohta	Ground State Properties of the $S=3/2$ Three-Leg Heisenberg Tube
11P-C043	C1	C0565	X. F. Sun, X. M. Wang, C. Fan, Z. Y. Zhao, W. P. Ke, L. M. Chen, and X. Zhao	Low-Temperature Heat Transport of Spin Gapped Quantum Magnets
11P-C044	C1	C0567	S. Zhao, D. Huvonen, T. Yankova, V. Glazkov, and A. Zheludev	Magnetic properties of disordered quasi-two-dimensional Heisenberg antiferromagnets
11P-C045	C1	C0568	Y. Ohta, T. Toriyama, M. Sakamaki, and T. Konishi	Anomalous electronic states of hollandite-type transition-metal oxides

11P-C046	C1	C0589	A. Orendacova, V. Tkac, K. Tibenska, E. Cizmar, M. Orendac	Spin dynamics in a low-dimensional dipolar magnet CsGd(MoO₄)₂
11P-C047	C1	C0612	B. Wolf, P. T. Cong, N. Kr\"uger, F. Ritter, W. Assmus, M. Lang	Ultrasonic investigations near the \$B\$-induced quantum critical point of the triangular antiferromagnet Cs\$ _{2}\$CuCl\$ _{4}\$
11P-C048	C1	C0627	R. Tarasenko, L. Sedlakova, A. Orendacova, M. Orendac, and A. Feher	Experimental Study of Magnetocaloric Effect in the Two-Dimensional Quantum System Cu(en)(H₂O)2SO₄
11P-C049	C1	C0634	M. U. Gutowska, J. Wieckowski, A. Szewczyk, A. Wisniewski, R.	Thermal Properties of Quasi-2D Cobaltites
11P-C050	C1	C0681	T. Asano, K. Matsuura, M. Sanda, J. Wang, A. Matsuo, Y. Narumi, K. Kindo	Magnetization Process of S=1/2 Antiferromagnetic Trimer System
11P-C051	C1	C0695	Y. Shimizu, K. Matsudaira, M. Itoh, T. Kajita, M. Ikeda, J. Miyazaki, T. Katsufuji	Orbital Ordering and Spin-Singlet Clusters in Triangular-Based Vanadates
11P-C052	C1	C0714	M. Ito, T. Hisamatsu, T. Rokkaku, I. Shigeta, M. Hiroi	Thermodynamic Properties of Heusler Compounds Ru\$ _{2-x}\$Fe\$ _{x}\$CrSi
11P-C053	C1	C0717	X Xu, CS Widodo, M Fujii	Spin lattice relaxation of proton NMR in Mn formate di-urea single crystal at low temperatures
11P-C054	C1	C0727	M. Ito, T. Ogawa, S. Urakawa, T. Kado	Magnetic and Thermodynamic Properties of Fe\$ _{2}\$Cr\$ _{2}\$Se\$ _{4}
11P-C055	C1	C0736	H. Takeda, Y. Shimizu, M. Itoh, M. Isobe and Y.Ueda	Electronic States of Half-Metallic Chormium Oxides Proved by \$^{13}\$Cr NMR
11P-C056	C1	C0745	Takao Nakama	Effect of pressure on thermopower of EuNi₂Ge₂
11P-C057	C1	C0756	T. Kawamata, M. Sato, K. Naruse, K. Kudo, N. Kobayashi, and Y. Koike	Anisotropic Behavior of Thermal Conductivity in the Bose-Einstein Condensed State of the Bond-Alternating Spin-Chain System
11P-C058	C1	C0762	H.Morodomi, Y. Inagaki, T. Kawae, X.G.Zheng and M. Haghjala	Magnetic dependence of specific heat in clinoatacamite Cu\$ _{2}\$(OH)\$ _{3}\$Cl
11P-C059	C1	C0775	K. Wierschem and P. Sengupta	Dimensional Crossover in Spin-1 Heisenberg Antiferromagnets: a Quantum Monte Carlo Study

11P-C060	C1	C0790	T. Hosaka, S. Hachiuma, H. Kuroe, T. Sekine, M. Hase, K. Oka, T. Ito, H. Eisaki,	Magnetic and Electric Properties in the Distorted Tetrahedral Spin Chain System Cu₃Mo₂O₉
11P-C061	C1	C0799	H. Ishizuka, M. Udagawa, and Y. Motome	Numerical Study of Itinerant Electron Systems Coupled with Classical Degrees of Freedom under Geometrical Frustration
11P-C062	C1	C0815	Masahiko Isobe, Touru Yamauchi, Hiroaki Ueda and Yutaka Ueda	Metal-insulator transition in Hollandite-type K₂V₈O₁₆ and K₂Cr₈O₁₆
11P-C063	C1	C0832	W. Zhang, M. Tomoo, S. Okubo, T. Sakurai, H. Ohta, H. Kikuchi, H. Yoshida, Y. Okamoto,	Low-Temperature Multi-frequency ESR Study of Spin 1/2 Kagome lattice Antiferromagnetic Materials
11P-C064	C1	C0834	N. Takahashi, M. Tomoo, S. Okubo, T. Sakurai, M. Fujisawa, H. Kikuchi, and H. Ohta	Dzyaloshinsky-Moriya Interaction Estimated by AFMR of Kagome Like Sub-stance Cu₂O(SO₄) Observed at 1.8K
11P-C065	C1	C0839	R. Kajimoto, K. Nakajima, S. Ohira-Kawamura, Y. Inamura, K. Kakurai, M. Arai, T.	Inelastic Neutron Scattering Study of Mg and Al Doped Two-Dimensional Triangular Antiferromagnet CuCrO₂
11P-C066	C1	C0851	H. Shinaoka, Y. Tomita and Y. Motome	Spin-glass Transition in Bond-disordered Heisenberg Antiferromagnets Coupled with Local Lattice Distortions on a Pyrochlore Lattice
11P-C067	C1	C0884	M. Sanda, K. Kubo, T. Asano, H. Wada, D. Morodomi, Y. Inagaki, T. Kawae, J. Wang, A.	Magnetic Ordering of Antiferromagnetic Trimer System 2B₃CuCl₃·2H₂O
11P-C068	C1	C0910	J. Lim, E. Blackburn, S. Roy, K. Seu, J. J. Turner and J. S. Gardner	X-ray Photon Correlation Spectroscopy as a Probe for Magnetisation Dynamics in the Spin Ice, Holmium Titanate
11P-C069	C1	C0929	Shigeki Onoda	Theory of quantum spin ice for realistic magnetic pyrochlore oxides
11P-C070	C1	C0946	Shunsuke Furukawa, Masahiro Sato, Shigeki Onoda	Vector spin chirality order and dynamical magnetoelectric effects in frustrated spin-1/2 chain systems
11P-C071	C1	C0948	Nobuhiro Shirasaki	Pressure Dependence of Electrical Properties in the Layered Triangular Antiferromagnet FeGa₂S₄
11P-C072	C1	C0949	T. Yamasaki, S. Okubo, H. Ohta, T. Sakurai, S. Ikeda, H. Oshima, M. Takahashi, S. Hara, K.	Possible new temperature phase observed in GeCo₂O₄ spinel by high field ESR
11P-C073	C1	C1011	R. Nakamura, J. Tozawa, M. Akaki, D. Akahoshi, K. Itatani, and H. Kuwahara	Anisotropic magneto-transport properties of layered perovskite Sr₃Fe_{2-x}CoxO_{7-δ} crystals

11P-C074	C1	C1021	M. Jeong, F. Bert, P. Mendels	Spin dynamcis of a quantum-spin-liquid $\text{ZnCu}_3(\text{OH})_6\text{Cl}_2$ probed by NMR
11P-C075	C1	C1022	E.Vavilova, A.Alfonsov, V.Kataev, A.Podlesnyak, E.Pomjakushina,	Collective spin states in lightly doped LaCoO_3
11P-C076	C1	C1024	C. R. Wang ,Y. L. Jhan and Y. Y. Chen	The magnetic properties of Ce_3Pt_4 nanoparticles
11P-C077	C1	C1027	M. Botko, M. Kajnakova, E. Cizmar, Yu. Eliyashevskyy, V. Starodub, and A. Feher	Antiferromagnetic Ordering in Genuine Organic Anion-Radical Salt ($\text{N-Me-2,6-di-Me-Pz}(\text{TCNQ})_2$) at Very Low Temperatures
11P-C078	C1	C1036	T. Harada, T. Matsushita, N. Wada, and Y. Hosokoshi	One-Dimensional Short-Range Ordering of Bond-Alternating Antiferromagnetic Chains in F_5PNN
11P-C079	C1	C1055	E.Vavilova, M.Yehia, R.Klingeler, V.Kataev, T.Taetz, U.Loev, A.Moeller, B.Buechner	Finite size effects in the honeycomb lattice compound $\text{InCu}_{2/3}\text{V}_{1/3}\text{O}_3$
11P-C080	C1	C1061	A. I. Smirnov, L. E. Svistov, M. Hagiwara, T. Fujita, H.Yamaguchi, S. Kimura, K. Omura,	High-Field Magnetic Phase of the $S=1/2$ Frustrated Chain Antiferromagnet LiCuVO_4
11P-C081	C1	C1062	Zhe Qu, Renwen Li, Wei Tong, Langsheng Ling, Lei Zhang and Yuheng Zhang	Micromagnetism and Spin Dynamics in Geometry Frustrated Magnets CuCrO_2 and $\text{CaBaCo}_4\text{O}_7$
11P-C082	C1	C1092	M. Prester, D. Drobac, I. Zivkovic and H. Berger	Dynamic Minor and Major Hysteresis Loops of New Ferromagnetic Oxi-halide System $\text{Co}_7(\text{TeO}_3)_4\text{Br}_6$
11P-C083	C1	C1151	A. Antonakos, E. Liarokapis, S. Wang, and K. Conder	Low temperature Raman study of the spin ladder compound BiCu_2PO_6
11P-C084	C1	C1177	T. Inomata, M. Matsukawa, Y. Nakanishi, S. Kobayashi, S. Nimori,	Effect of pressure on magnetization and magnetostriction jumps in the manganite $(\text{Eu,Gd})_{0.58}\text{Sr}_{0.42}\text{MnO}_3$
11P-C085	C1	C1184	S. Nishimoto, S.-L. Drechsler, R.O. Kuzian, J. Richter and J. van den Brink	The effect of interchain coupling on multipolar phases in quasi-1D quantum helimagnets
11P-C086	C1	C1191	T. Ono, K. Matan, Y. Nambu, T. J. Sato and H. Tanaka	Ground State and Magnetic Excitations of $S=1/2$ Kagome Antiferromagnets
11P-C087	C1	C1195	Shenggao Xu, Yunlei Sun, Hui Xing, Chunmu Feng, Zhu'an Xu, Guanghan Cao	Evolution from spin-density wave to spin glass and ferromagnetism in $\text{Ba}(\text{Fe}_{1-x}\text{Cr}_x/2\text{Ni}_x/2)\text{As}_2$

11P-C088	C1	C1198	N. Amaya, N. Obata, H. Yamaguchi, T. Ono and Y. Hosokoshi	Crystal dependence of the magnetic properties of an antiferromagnetic alternating chain compound F5PNN
11P-C089	C1	C1199	K. Iwase, H. Yamaguchi, H. Nojiri, A. Matsuo, K. Kindo and Y. Hosokoshi	The crystal structure and magnetic properties of an organic verdazyl biradical.
11P-C090	C1	C1264	V. Janis	Replica-symmetry breaking in zero-temperature mean-field spin-glass models
11P-C091	C1	C1282	Masashi Hase, Vladimir Yu. Pomjakushin, Sikolenko Vadim, Lukas Keller, Andreas	Negative magnetization of Li\$2\$Ni\$2\$Mo\$3\$O\$12\$ including two spin subsystems, distorted honeycomb lattice
11P-C092	C1	C1286	Authors(T. Muto, K. Kobayashi, T. Goto, A. Oosawa, S. Yoshii, T. Sasaki, N. Kobayashi,	11B-NMR study on Shastry-Sutherland system TbB4
11P-C093	C1	C1287	K. Misoka, K. Doi, T. Hamasaki, H. Kuroe, T. Goto, T. Sekine, T. Sasaki, M. Hase, K.	Cu-NMR study on dimer-chain complex quantum spin system Cu3Mo2O9
11P-C094	C1	C1288	X.G. Zheng, M. Fujihala, M. Hagihala, H. Morodomi, T. kawae	Novel Magnetic Order and Quantum Spin Fluctuations in d-Electron Magnetic Compounds of Hydroxyhalogenides M2(OH)3X
11P-C095	C1	C1291	T.H. Han, J.S. Helton, A. Prodi, C. Mazzoli, P. Muller, D. K. Singh, J.A. Rodrigues,	Inelastic neutron scattering study of S=1/2 kagome lattice single crystals
11P-C096	C1	C1311	M. Hagiwara, Y. Idutsu, Z. Honda and S. Yamamoto	Magnetic Properties of the S=2 Heisenberg Antiferromagnetic Chain Compound MnCl\$3\$(bpy)
11P-C097	C1	C1312	S.A. Zvyagin, M. Ozerov, J. Wosnitza, E. Cizmar, R. Feyerherm, S.R. Manmana, and F.	Field-Induced Gap in Quantum Spin-1/2 Chains in Strong Magnetic Fields
11P-C098	C1	C1316	Zhe Wang, M. Schmidt, A. Günther, S. Schaille, N. Pascher, F. Mayr, Y. Goncharov, D. L.	Orbital fluctuations and orbital order below the Jahn-Teller transition in Sr3Cr2O8
11P-C099	C1	C1342	J.-J. Wen, Y. Nambu, J. Rodriguez, C. Stock, S. Nakatsuji, S. Onoda, Y. Maeno, C. Broholm	Competing Interactions and Continuum Excitations in the Spin-1 Triangular Lattice Antiferromagnet NiGa\$2\$S\$4\$
11P-C100	C1	C1351	P. Li, S.-Q. Shen	Majorana Fermion Representation of Gapless Spin Edge
11P-C101	C1	C1363	S. Itoh	Two-Dimensional Antiferromagnetic Fractons in Rb\$2\$Mn\$c\$Mg\$1-c\$F\$4\$ with \$c\$ close to the percolation concentration

11P-C102	C1	C1364	D.V. Efremov, G. Khaliullin	Decay of helical magnons and spectral weight transfer in ferrates
11P-C103	C1	C1365	Ru Chen, Hyejin Ju, Leon Balents	Field-anisotropy phase diagrams of some frustrated magnets
11P-C104	C1	C1371	Y. Matsumoto, A. Terai	Monte Carlo Study of Spin-Peierls Transition in Quasi-One-Dimensional Heisenberg Model with Finite-Frequency Phonons
11P-C105	C1	C1397	Y. J. Yan	Magnetic properties in the doped spin-1/2 honeycomb-lattice compound In₃Cu₂VO₉
11P-C106	C1	C1413	A. Zheludev	Disorder in quantum magnets: from Random Singlet to Bose Glass.
11P-D001	D1	D0024	O.V.Kirichenko, I.V.Kozlov, V.G.Peschansky	Quantum oscillations of the surface impedance of a layered conductor
11P-D002	D1	D0126	Ling Hao, David Cox and John Gallop	Development of ultra-low noise nanoSQUIDs using FIB for quantum measurement
11P-D003	D1	D0226	I.C.Hoi, C.M. Wilson, G. Johansson, T. Palomaki, B. Peropadre and Per	Strong Interaction Between a Single Artificial Atom and Propagating Microwave Photons
11P-D004	D1	D0249	T. Lindstrom, J. Burnett, M. Oxborrow, Y. Sekine, Y. Harada and A. Ya. Tzalenchuk	Direct characterization of noise processes in superconducting microresonators
11P-D005	D1	D0256	Lingzhen Guo, M. Marthaler, Stephan Andre, and Gerd Schoen	Temperature Dependence of Driven Duffing Oscillators
11P-D006	D1	D0277	V. Bubanja	Effects of dissipative electromagnetic environment on transport properties of hybrid single-electron transistor in Coulomb blockade
11P-D007	D1	D0293	T. Aref, V. Maisi, M. Gustafsson, P. Delsing and J. Pekola	Observation of Andreev Tunneling Effects in Current Pumping with SINIS turnstiles
11P-D008	D1	D0295	S. Gasparinetti, Y. Yoon, P. Solinas, M. Mäkinen and J. P. Pekola	Breakdown of Adiabaticity and Role of the Environment in a Cooper-Pair Pump
11P-D009	D1	D0303	S.V. Lotkhov, A. Kemppinen, O.-P. Saira, J.P. Pekola, and A.B. Zorin	Superconductor-normal metal single-electron trap in a combined on-chip RC-environment

11P-D010	D1	D0306	Dongchan Jeong, Jae-Hyun Choi, Gil-Ho Lee, Sanghyun Jo, Yong-Joo Doh, and Hu-Jong	Observation of Supercurrent in PbIn-Graphene-PbIn Josephson Junction
11P-D011	D1	D0345	H. Moreira, Q. Yu, B. Bresson, B. Nadal, N. Lequeux, B. Dubertret, A. Zimmers and H.	Electron co-tunneling transport in gold nanocrystals arrays
11P-D012	D1	D0352	Y. Kanai, K Nakayama, R. S. Deacon, A. Oiwa, K. Shibata, K. Hirakawa, and S.	Phase measurement in strong Kondo regime in a self assembled InAs dot superconducting quantum interference device
11P-D013	D1	D0419	F. Godschalk, F. Hassler and Yu.V. Nazarov	Proposal for an optical laser producing light at half the Josephson frequency
11P-D014	D1	D0429	M. A. Laakso, T. T. Heikkila, and Y. V. Nazarov	Statistics of temperature fluctuations in superconductor-normal metal tunnel structures
11P-D015	D1	D0450	M. Marthaler, D. Golubev, Y. Utsumi, G. Sch?n	Statistics of voltage fluctuations in resistively shunted Josephson junctions
11P-D016	D1	D0451	M. Marthaler, Y. Utsumi, D. Golubev, A. Shnirman, G. Sch?n	Lasing without Inversion in Circuit Quantum Electrodynamics
11P-D017	D1	D0462	K. Kadowaki, T. Kashiwagi, H. Asai, M. Tsujimoto, M. Tachiki, K. Delfanazari and R.	Terahertz Wave Emission from Intrinsic Josephson Junctions in Bi₂Sr₂CaCu₂O_{8+d}
11P-D018	D1	D0489	Gil-Ho Lee, Dongchan Jeong, Jae-Hyun Choi, Yong-Joo Doh, and Hu-Jong Lee	Electrically Tunable Quantum States in Graphene-based Josephson Junctions
11P-D019	D1	D0505	Akira Oguri, and Yoichi Tanaka	Andreev reflection and Josephson current through a Kondo Y-junction
11P-D020	D1	D0534	Shi-Kun He, Wei-Jun Zhang, Xiang-Gang Qiu	Interstitial vortex in superconducting film with honeycomb array
11P-D021	D1	D0535	Mikko M?tt?nen	Superadiabatic Approximations for Cooper Pair Pumping
11P-D022	D1	D0545	Roland Schaefer, Christoph Kaiser and Michael Siegel	From thermal to quantum: A detailed look at escape rates in Josephson junctions
11P-D023	D1	D0555	J. Wei and V. Chandrasekhar	Local and nonlocal conductance enhancement due to Cooper pair splitting

11P-D024	D1	D0576	Wei-Cheng Chien, Saxon Liou, Kuan-Yu Lin and Watson Kuo	Microwave scattering on single one-dimensional array of Josephson junctions as a point defect in standing wave regime
11P-D025	D1	D0608	W.J.Zhang, S.K. He, X.G. Qiu, X. Li, S.Y. Yang, W.H. Cao, S.P. Zhao, Z.C. Wen, X.F.	Josephson quantum interference in anisotropic superconducting antidot lattices
11P-D026	D1	D0669	J. T. Peltonen, P. Virtanen, M. Meschke, J. V. Koski, T. T. Heikkil?, and J. P.	Thermal Conductance by the Inverse Proximity Effect in a Superconductor
11P-D027	D1	D0789	J. H. Cole, M. Marthaler	Temporal dynamics within linear arrays of Josephson junctions in the Coulomb blockade regime
11P-D028	D1	D0845	S. Chaudhuri and I. J. Maasilta	Cooling and Thermometric Performance of Non-ideal SINIS Tunnel Junction Devices
11P-D029	D1	D0866	Q. Fan, L. X. Yang, Q. Q. Ge, and D. L. Feng	Setup of laser-based angular resolved photoemission spectroscopy
11P-D030	D1	D0897	M. Gustafsson, T. Bauch, J. Lublin, G. Johansson, J. Clarke, P. Delsing	Comparing Charge Offset and Charge Noise for a Single Electron Transistor
11P-D031	D1	D0903	A.M. Hriscu, Y. V. Nazarov	Quantum Phase-slip Devices
11P-D032	D1	D0912	D. Gunnarsson, M. Sillanp??, J. Pirkkalainen and M. Prunnila	Wafer-scale Fabrication of High Quality Josephson Tunnel Junction Phase Qubits.
11P-D033	D1	D0921	M. Silveri, K.S. Kumar, J. Li, J.-M. Pirkkalainen, J. Tuorila, M. A. Sillanp??, P. J.	Theoretical Description of Motional Averaging in a Superconducting Qubit
11P-D034	D1	D0953	H. Shimada, C. Ishida and Y. Mizugaki	Current Induction in Strongly Coupled Arrays of Small Josephson Junctions
11P-D035	D1	D0955	A.Yamanaka, Y.Amakai , K.Matsumoto, N.Momono, H.Takano, S.Murayama	Temperature dependence of the electrical resistivity and the magnetization in RuSr_{2-x}CaxGdCu₂O₈(x=0,0.1,0.3,2.0)
11P-D036	D1	D0970	M. A. Sillanp??, J. Li, K. Cicak, F. Altomare, J. I. Park, R. W. Simmonds, G. S. Paraoanu, and P.	Dynamic Autler-Townes effect, decoherence, and dark states in a phase qubit
11P-D037	D1	D1000	P. Virtanen, F.S. Bergeret, J.C. Cuevas and T.T. Heikkila	Microwave induced effects in diffusive SNS junctions

11P-D038	D1	D1043	J. Li and G. S. Paraoanu	Decay and generation of entanglement in coupled, driven systems with bipartite decoherence
11P-D039	D1	D1047	J. Li, M. Silveri, K. S. Kumar, J.-M. Pirkkalainen, J. Tuorila, M. A. Sillanpaa, P. J.	Experimental demonstration of motional averaging in a transmon
11P-D040	D1	D1060	M. Gustafsson, P.V. Santos, P. Delsing	Coupling propagating acoustic waves to quantum circuits
11P-D041	D1	D1107	M. Sillanpaa, F. Massel, T. Heikkila, P. Hakonen, J. Pirkkalainen, and S. U.	Micromechanical resonator cooled down close to the motional ground state, and electromechanically induced microwave
11P-D042	D1	D1128	B. Tanatar, S. H. Abedinpour, A. L. Subasi	Coulomb drag in double layer graphene systems
11P-D043	D1	D1160	Shuchao Meng, Luke Yaraskavitch, Andrew Sachrajda and Jan Kycia	Switching Current of a Superconducting Single Electron Transistor in a Tunable Dissipative Environment
11P-D044	D1	D1225	A. Halfar, M. Bazrafshan, A . Fleischmann, C. Enss	Novel Non-Contact Measurement of the Specific Heat of Insulating Glasses at Low Temperatures
11P-D045	D1	D1227	D. Zhang, S. Schmult, V. Venkatachalam, W. Dietsche, A. Yacoby, K. von Klitzing and J. H.	Energy gap evolution of the $\nu_{\text{tot}}=1$ quantum Hall state in an electron-electron bilayer system measured
11P-D046	D1	D1232	A.Yamanaka, Y.Amakai, N.Momono,H.Takano,S.Murayama	Temperature dependence of the electrical resistivity and the magnetization in RuSr_{2-x}CaxGdCu₂O₈(x=0,0.1,0.3,2.0)
11P-D047	D1	D1234	A.Yamanaka, Y.Amakai, K.Matsumoto, N.Momono, H.Takano,	Temperature dependence of the electrical resistivity and the magnetization in RuSr_{2-x}CaxGdCu₂O₈
11P-D048	D1	D1237	V.L. Gurtovoi and V.A. Tulin	A strategy for development of superconducting qubits with large decoherence time
11P-D049	D1	D1272	P. J. Jones, J. A. M. Huhtam?ki, K. Y. Tan and M. M?tt?nen	Single-photon heat conduction in electrical circuits
11P-D050	D1	D1356	D. Gustafsson, T. Bauch, F. Lombardi	All YBCO Transmon for Low Energy Quasiparticle Spectroscopy
11P-D051	D1	D1358	N. Antler, K. W. Murch, R. Vijay, S. Weber, E. M. Levenson-Falk and I. Siddiqi	Readout and Control of Spin Systems with Superconducting Circuits

11P-D052	D1	D1386	M. Mori, S. Hikino, S. Takahashi, and S. Maekawa	Dynamics of Josephson-phase coupled with spin waves
11P-D053	D1	D1404	M. H. Ansari and F. K. Wilhelm	Critical current noise in Josephson junction from interacting trap states
11P-D054	D1	D1440	Xiaobo Zhu, Shiro Saito, Alexander Kemp, Kosuke Kakuyanagi, Shin-ichi Karimoto,	Coupling an ensemble to a superconducting qubit
11P-D055	D1	D1466	Andreas Wallraff	Generating and Detecting Propagating Photons in Superconducting Circuits
11P-D056	D1	D1489	Z.H. Peng, Y.X. Liu, and J.S. Tsai	Fast generation of multi-particle entanglement state with flux qubits in tunable coupled cavities
11P-E001	E1	E1120	J. Sulkko, M.A. Sillanp\"a, P. H\"akkinen L. Lechner, M. Helle, A. Fefferman,	Strong Gate Coupling of High-Q Nanomechanical Resonators
11P-E002	E1	E1144	X. Song, M. A. Sillanp\"a and P. J. Hakonen	Approaching the quantum limit of thermal motion on a graphene mechanical resonator
11P-E003	E1	E1468	Meifen Wang, Huan Yang, Feipeng Ning and Zian Zhu	Development of a Zero Boil-off Helium Cryostat for superconducting magnets

Friday Aug.12

Time Slot	Category	ABSN	Name	Title
Half Plenary Session(12H1)				
12H1-1			Eunseong Kim	
12H1-2		A0478	Robert Hallock	Temperature Dependence of 4He Diffusion through Common Epoxies
12H1-3			Cheng Chin	
Half Plenary Session(12H2)				
12H2-1		C1299	Naoto Nagaosa	Emergent electromagnetism in solids - Spin-orbit interaction as a gauge field
12H2-2		C1152	Leon Balents	Quantum spin liquids in quantum spin ices
12H2-3		C1370	Steve Bramwell	Monopoles and Magnetivity in Spin Ice

Parallel Session(12m-B₁) Novel Phenomena in Superconductivity

12m-B ₁ 1		B1241	Norman Birge	Spin-Triplet Supercurrent in Ferromagnetic Josephson Junctions
12m-B ₁ 2		B1477	Rafi Budakian	Probing the Physics of the Fractional Vortex State in Mesoscopic Rings of Sr₂RuO₄
12m-B ₁ 3		B0674	Yosi Yeshurun	Large oscillations of the magnetoresistance in nano-patterned La_{1.84}Sr_{0.16}CuO₄
12m-B ₁ 4		B0072	Dirk Manske	Consequences of broken time-reversal symmetry in triplet Josephson junctions
12m-B ₁ 5		B0173	Julie Bert	Direct imaging of coexistence of ferromagnetism and superconductivity in

Parallel Session(12m-B₂) New Superconducting Materials

12m-B ₂ 1		B1369	Yoshihiro Kubozono	Structures and physical properties of new types of organic superconductors, Axipicene,
12m-B ₂ 2			Xian-Hui Chen	Phase diagram in high-T_c iron pnictide and chalcogenide superconductors
12m-B ₂ 3		B1494	C. W. Chu	A possible unusual superconducting state up to 49 K in single crystalline R-doped CaFe₂As₂
12m-B ₂ 4			M. K. Wu	
12m-B ₂ 5		B1484	V.V. Moshchalkov	Vortex Matter in Type-1.5 Superconductors

Parallel Session(12m-C) Low Dimensional and Frustrated Magnetism II

12m-C1		C0962	R. K. Kremer	The spin-1/2 frustrated helicoidal afm multiferroic system LiCuVO₄: Recent Results
12m-C2		C0107	A. Zheludev	Low Temperature Dynamics of Magnons in a Spin-1/2 Ladder Compound
12m-C3		C0856	A. I. Smirnov	Low Energy Dynamics of Spin-Liquid and Ordered Phases of S=1/2 Antiferromagnet
12m-C4		C0991	S. Okubo	Spin Dynamics of Frustrated Honeycomb Lattice Antiferromagnet

12m-C5		C0649	Hsiu-Hau Lin	Graphene Nanoribbon Turns Magnetic
Parallel Session(12m-D) Superconducting Devices/Qubits II				
12m-D1		D0197	Mika Sillanpää	Stark effect and generalized Bloch-Siegert shift in a strongly driven two-level system
12m-D2		D1362	Valerii Vinokour	Quantum Turbulence and Localization of Disordered Bosons
12m-D3		D0850	Olli-Pentti Saira	Quasiparticle transport measurements in attoampere scale in metallic devices
12m-D4		E1491	Per Delsing	Demonstration of a single-photon router in the microwave regime
12m-D5		D1044	Han Keijzers	Vibrating Suspended Carbon Nanotube Josephson Junctions
Parallel Session(12m-A) Quantum Gases I				
12m-A1			Ruichao Ma	
12m-A2		A1441	Yoshiro Takahashi	Quantum Simulation Using Two-electron Atoms
12m-A3			Xuzong Chen	
12m-A4		A1347	Yuki Kawaguchi	Pattern Formation Dynamics in a Spinor Dipolar Bose-Einstein Condensate
12m-A5		A1412	Andrew Truscott	Higher Order Correlations in Quantum Gases
Parallel Session(12a-A₁) Supersolid II				
12m-A ₁ 1			Minoru Kubota	
12m-A ₁ 2		A1159	Norbert Mulders	The Crystal Structure of Solid Helium-4 in Vycor
12m-A ₁ 3		A0278	Zhigang Cheng	Heat Capacity of Solid ⁴He in Aerogel
12m-A ₁ 4		A0458	Dukyoung Kim	Solid helium in long path length torsional oscillators
Parallel Session(12a-B) Pseudogap Phase in Cuprates				
12a-B1		B1483	Martin Greven	Novel Magnetism and the Phase Diagram of the Cuprates
12a-B2		B1220	Hugo Keller	From cuprate to iron-based superconductors – some key elements of high-temperature
12a-B3		B1303	Alain Sacuto	Superconducting gap and pseudo gap in hole doped cuprates
12a-B4		B1443	Eun Kim	Electronic Liquid Crystal Correlations in the Pseudogap States of High T_c Superconductors
12a-B5		B1421	Marc-Henri Julien	Magnetic-field-induced stripe order in YBa₂Cu₃O_x
Parallel Session(12a-C) Novel Magnetic Phases				
12a-C1		C1414	Gang Su	Emergence of novel states in low-dimensional quantum magnets

12a-C2		C1408	Virginie Simonet	Slow dynamics in ordered Fe-oxalates kagome antiferromagnets
12a-C3		C1431	Satoru Nakatsuji	Quantum criticality without tuning in the intermediate valence material β-YbAlB₄
12a-C4		C0791	Suguru Ueda	Spin and charge ordering in heterostructures of strongly correlated electron systems
12a-C5		C1073	Holger Ulbrich	Stripe-type order of spin, orbitals and charges in single-layered manganites
12a-C6		C0702	Mingxuan Fu	Single Crystal NMR Study of Frustrated Spin-liquid in S = 1/2 Kagome Lattice ZnCu₃(OD)₆C₁₂

Parallel Session(12a-D) Superconducting Devices/Qubits III

12a-D1		D1165	Konstantin Kechedzhi	Origin of 1/f magnetic noise in superconducting circuits
12a-D2		D0902	Alina Hriscu	Quantum Phase-slip Devices
12a-D3		D1123	Pertti Hakonen	Dynamical Casimir effect in a Josephson metamaterial
12a-D4		D1417	Hu-Jong Lee	Spin-relaxation in graphene: by covalently bonded adsorbates via EY mechanism

Parallel Session(12a-A₂)

12m-A ₂ 1		D0875	Liang Liu	Annealing and Doping Effects of 1D Cuprates Investigated by Thermal Conductivity and
12m-A ₂ 2		A0063	J. Tempere	Preformed pairs and quasicondensation in imbalanced Fermi gases in 2D
12m-A ₂ 3			Tian-Cai Zhang	
12m-A ₂ 4			Shih-Chuan Gou	
12m-A ₂ 5		A0694	Congjun Wu	Hidden symmetries and exotic quantum magnetism of large-spin alkali and alkaline-

Poster Session

12P-A001	A1	A0014	Kwang-Hua Chu	Possible Effects of He-3 Impurities and Shearing on the Formation of Locally Amorphous Supersolid He-4 driven by a
12P-A002	A1	A0022	Jeroen P. A. Devreese, S. N. Klimin, M. Wouters and J. Tempere	Resonant enhancement of the FFLO state in 3D by an optical potential
12P-A003	A1	A0067	Enrico Arrigoni, Michael Knap, and Wolfgang von der Linden	Strongly-correlated lattice bosons in the superfluid phase: a selfenergy-functional cluster approach
12P-A004	A1	A0071	P. Schlottmann and A. A. Zvyagin	Fermi Gas with Attractive Potential and Arbitrary Spin in Highly Elongated Trap
12P-A005	A1	A0077	T. A. Zaleski and T. K. Kope?	Effects of restricted geometry on Bose-Einstein condensation in optical lattices

12P-A006	A1	A0103	Xue Ju-Kui	Coherent dynamics of quantum superfluid gases in optical lattices
12P-A007	A1	A0202	Takashi Kimura	{Gutzwiller study for phase diagram of extended Hubbard models
12P-A008	A1	A0212	Sei-ichiro Suga and Kensuke Inaba	Color Superfluid of Three-Component Fermionic Atoms with Repulsive Interaction in Optical Lattices
12P-A009	A1	A0243	Kenichi Kasamatsu, Akira Kato, Yuki Nakano and Tetsuo Matsui	Dynamical properties of bosons in an optical lattice with a synthetic magnetic
12P-A010	A1	A0259	M. Bruderer and W. Belzig	Mesoscopic Transport of Ultracold Atoms in Optical Lattices
12P-A011	A1	A0317	Daisuke Yamamoto, Ippei Danshita and Carlos A. R. S'a de Melo	Anomalous Hysteretic Behavior in a System of Dipolar Bose Gases
12P-A012	A1	A0338	Achim Rosch	Dynamics of ultracold fermions in optical lattices: negative absolute temperatures and constant forces
12P-A013	A1	A0378	Shingo Kobayashi, Yuki Kawaguchi, Michikazu Kobayashi, Muneto	Stability of topological excitations under the phase transition in spinor BECs
12P-A014	A1	A0501	Ying Hu and Zhaoxin Liang	Visualization of Dimensional Effects in Collective Excitations of Optically Trapped Quasi-Two-Dimensional Bose Gases
12P-A015	A1	A0531	D. Inotani, R. Watanabe, M. Sigrist, Y. Ohashi	Pseudogap Phenomena of an Ultracold Fermi Gas with a \$P\$-wave Feshbach Resonance
12P-A016	A1	A0600	A. Kotani, D. Hirashima	Collective excitations in correlated two-dimensional fermion systems
12P-A017	A1	A0701	J. Chen and Q. Lin	Partially coherent matter wave soliton solutions Multimode theory
12P-A018	A1	A0768	V. Ramesh Kumar, Lin Wen, W.M. Liu	Controlled Split-Recombination of 2D Matter-Wave Solitons in Time-Dependent Trap
12P-A019	A1	A0798	A. Masaki and H. Mori	Localization of Bose-Fermi Mixtures in One-Dimensional Incommensurate Lattices

12P-A020	A1	A0822	Qijin Chen	Effects of particle-hole channel and BCS-BEC crossover on an optical lattice
12P-A021	A1	A0852	Ya-fan Duan,Jianfang Sun,Bo-nan Jiang,Xu Zhen,Tao Hong,Yu-zhu Wang	The Quantum Simulation Setup of Rb87 Bose-Einstein Condensates and Numerical Analysis of Disorder Induced Dynamic-Equilibrium
12P-A022	A1	A0874	Ya-fan Duan,Jianfang Sun,Bo-nan Jiang,Zhen Xu,Tao Hong and Yu-zhu	The Quantum Simulation Setup of Rb87 Bose-Einstein Condensates and Numerical Analysis of Disorder Induced Dynamic-Equilibrium
12P-A023	A1	A0880	Yafan Duan, Jianfang Sun, Bonan Jiang, Xu Zhen, Tao Hong, and Yuzhu	The quantum simulation setup of 87Rb Bose-Einstein condensates and numerical analysis of disorder induced dynamic-equilibrium
12P-A024	A1	A0890	Bao-Sen Shi*, Dong-Sheng Ding, Zhi-Yuan Zhou, Wen Huang, Xu-Bo Zou	Experimental image transfer and frequency conversion based on an atom ensemble
12P-A025	A1	A0901	Jun'ichi Ozaki, Masaki Tezuka, and Norio Kawakami	One-dimensional collision dynamics of fermion clusters
12P-A026	A1	A0959	C. M. Jian, J. Zhang, F. Ye, H. Zhai	Bosons in Hofstadter Model: mesoscopic phenomenon and effective theory for superfluid
12P-A027	A1	A0978	Yafan Duan, Jianfang Sun, Bonan Jiang, Zhen Xu, Tao Hong and Yuzhu	The quantum simulation setup of 87Rb Bose-Einstein condensates and numerical analysis of disorder induced dynamic-equilibrium
12P-A028	A1	A1034	J. Kajala, F. Massel, and P. T?rm?	Expansion dynamics in the one-dimensional Fermi-Hubbard model
12P-A029	A1	A1085	Hongli. Liu, Shiqi. Yin, Zhen. Xu and Tao. Hong	Progress of making the MOT for neutral mercury atoms
12P-A030	A1	A1098	Xinyu Luo, Qiang Cao, Xiaorui Wang and Ruquan Wang	Ultra low cost single chamber BEC apparatus with good optical access
12P-A031	A1	A1161	P.W. Pleary, T.W. Hijmans and J.T.M. Walraven	Manipulation of a Bose-Einstein condensate by a time-averaged orbiting potential using phase jumps of the rotating field
12P-A032	A1	A1210	Xuguang Yue, Zhongkai Wang, Yueyang Zhai, Xinxing Liu, Xiaoji	Manipulating external states of a condensate for rapid lattice loading
12P-A033	A1	A1214	Xuguang Yue, Wei Xiong, Zhongkai Wang, Xiaoji Zhou and Xuzong Chen	Manipulating the momentum state of a condensate by sequences of standing wave pulses

12P-A034	A1	A1215	Xinxin Liu, Xiaoji Zhou , Thibault Vogt, Bo Lu, Xueguang Yue, Xuzong Chen	Exploring multi-band excitations of interacting Bose gases in a 1D optical lattice by coherent scattering
12P-A035	A1	A1233	Chen Shu	Properties of super-Tonks-Girardeau gases
12P-A036	A1	A1250	Xiaorui.Wang Xinzhou.Tan Lu.Yang,Hongwei.Xiong Baolong.lu	Finite temperature effect in phase transition to superfluidity for Bose-Einstein condensates in a 1-D optical lattice
12P-A037	A1	A1259	Jing Zhang (张靖), Peng-Jun Wang (王鹏军), Zheng-Kun Fu (付正坤), Shi-jie	Feshbach resonances in ultracold mixture of 87Rb and 40K
12P-A038	A1	A1262	Yafan Duan, Jianfang Sun, Bonan Jiang, Xu Zhen, Tao Hong, and Yuzhu	The quantum simulation setup of 87Rb Bose-Einstein condensates and numerical analysis of disorder induced dynamic-equilibrium
12P-A039	A1	A1274	F. Heidrich-Meisner, A. Feiguin, U. Schollwoeck, W. Zwerger	FFLO physics in spin-polarized Fermi gases in one dimension
12P-A040	A1	A1280	T. Vogt, B. Lu, X. Liu, X. Xu, X. Zhou, and Xuzong Chen	Mode competition in superradiant scattering of matter waves
12P-A041	A1	A1285	Test	Test
12P-A042	A1	A1331	L. Munday, M. Kumar, M. Poole	Drag Forces at mK Temperatures of Multiple Resonating Wires, Including Frequency Dependency
12P-A043	A1	A1387	S. Yamada, M. Machida	Single-particle excitation spectrum in 1D ultracold fermionic optical lattices
12P-A044	A1	A1395	Yuzhen Yuan	Quantum computer and quantum gases
12P-A045	A1	A1454	Congjun Wu	Unconventional Bose-Einstein condensations and exotic orbital physics in high bands of optical lattices
12P-A046	A1	A1459	jiang-ming zhang, chao Shen, and wu-ming liu	Strong thermalization of a mesoscopic two-component Bose-Hubbard model
12P-A047	A1	A1460	wu-bao jun and jiang-ming zhang	Schrodinger cat states prepared by Bloch oscillation in a spin-dependent optical lattice

12P-A048	A1	A1461	Qing Sun, Xing-Hua Hu, W. M. Liu, X. C. Xie, and An-Chun Ji	Effect on Cavity Optomechanics of the Interaction Between a Cavity Field and a 1D Interacting Bosonic Gas
12P-A049	A1	A1470	Wen-Zhuo Zhang, Peng Zhang, Ru-Quan Wang, Wu-Ming Liu	Solution and testing of the Abraham-Minkowski controversy in light-atom interacting system
12P-A050	A2	A0143	T.N. Antsygina, K.A. Chishko, A.A. Lisunov, V.A. Maidanov, V.Yu.	Fluctuation effects in 3He-4He solid mixtures near the phase separation temperature
12P-A051	A2	A0216	B. Liu, L. Yin	Antiferromagnetism and superfluidity of a dipolar Fermi gas in a 2D optical lattice
12P-A052	A2	A0387	Ying Liang, Huai-ming Guo	Effect of dominant three-body interaction in two-dimensional square lattice
12P-A053	A2	A0513	T. Kawakami, T. Mizushima and K. Machida	Textures of Spin-Orbit Coupled F=2 Spinor Bose Einstein Condensates
12P-A054	A2	A0532	Takashi Kashimura, Shunji Tsuchiya and Yoji Ohashi	\$\pi\$-phase and Spontaneous Supercurrent induced by Pseudo-ferromagnetic Junction in a Spin-polarized Superfluid Fermi Gas
12P-A055	A2	A0595	T. Yoshida and Y. Yanase	Crossover from Fulde-Ferrell state to Larkin-Ovchinnikov state in cold fermion gases
12P-A056	A2	A0611	R. Watanabe, S. Tsuchiya and Y. Ohashi	Inhomogeneous Pseudogap Phenomenon in the BCS-BEC Crossover Regime of a Trapped Superfluid Fermi Gas
12P-A057	A2	A0625	A. Kauch, K. Byczuk, and D. Vollhardt	Mott-insulator and superfluid phases of correlated bosons in the bosonic dynamical mean-field theory with the strong coupling
12P-A058	A2	A0628	Emmi Ruokokoski, Mikko M?tt?nen	Monopoles and Dipoles in Spinor Bose-Enstein Condensates
12P-A059	A2	A0700	C. Tao and Q. Gu	Ferromagnetism of spinor atomic condensates in the double
12P-A060	A2	A0825	Endo Shimpei, Naidon Pascal, and Ueda Masahito	Efimov and Non-Efimov Three-Body Bound States for 2+1 Particles
12P-A061	A2	A0905	S. Vasiliev, J. Ahokas, S. Novotny, S. Sheludyakov, O. Vainio, D. Zvezdov	Magnons in Spin-Polarized Atomic Hydrogen Gas

12P-A062	A2	A0960	C.-H. Hsueh, S.-W. Su, S.C. Gou	Fragmentation and Stillbirth of Condensation in the Rapid Evaporative Cooling of a Dual Species Bose Mixture
12P-A063	A2	A1013	M. O. J. Heikkinen, F. Massel, J. Kajala, M. J. Leskinen, G. S. Paraoanu, and P.	Spin-asymmetric Josephson effect in ultracold Fermi gases
12P-A064	A2	A1091	Zheyu Shi	Resonances Induced by Dipolar Scattering
12P-A065	A2	A1136	R. E. Zillich, D. Hufnagl, A. Macia, F. Mazzanti, and J. Boronat	Two-dimensional dipolar Bose gas with tilted polarization
12P-A066	A2	A1145	R. Holler, H. M. B?hm, E. Krotscheck and M. Panholzer	Microscopic Dynamics of He-3 in Two and Three Dimensions
12P-A067	A2	A1183	P. Naidon, M. Ueda	Efimov trimers in ultracold Lithium 6
12P-A068	A2	A1207	Hui Zhai	Spin-orbit Coupled Boson Superfluid
12P-A069	A2	A1242	Yu Shi	aAmixture of two species of spinor Bose gases with interspecies spin exchange
12P-A070	A2	A1334	A. Pikovski, M. Klawunn, A. Recati, G. Shlyapnikov, and L. Santos	Ultra-cold Polar Fermionic Molecules in Bilayers
12P-A071	A2	A1384	B. Capogrosso-Sansone and A.B.Kuklov	Superfluidity of flexible chains of dipolar molecules in layered optical lattices
12P-A072	A2	A1462	Deng-Shan Wang, Shu-Wei Song, Bo Xiong and W. M. Liu	Quantized vortices in a rotating Bose-Einstein condensate with spatiotemporally modulated interaction
12P-A073	A2	A1493	SALOMON CHRISTOPHE	From ultracold Fermi Gases to Neutron Stars
12P-B001	B2	B0017	G. Koren and T. Kirzhner	Observation of two Andreev-like energy scales in \$La_{2-x}Sr_xCuO_4\$ superconductor/normal-metal/superconductor
12P-B002	B2	B0031	F. H. L. Essler, A. A. Nersesyan and A. M. Tsvelik	Dr.

12P-B003	B2	B0076	K. Le Hur, C.H. Chung, I. Paul	Designing heterostructures with higher temperature superconductivity
12P-B004	B2	B0135	E.D. Gutliansky	Acoustic analog of Hall effect in superconductive films
12P-B005	B2	B0140	Mayraluna L. Lao, Roland V. Sarmago	A Different Perspective on the AC Magnetic Susceptibility of $\text{Bi}_{1.7}(\text{Pb}_{0.3})\text{Sr}_2\text{Ca}_2\text{Cu}_3\text{O}_{10+x}$ Superconductor Modelled using a Mechanism
12P-B006	B2	B0162	E. Martinez, B. Ruiz, and R. Escudero	Coexistence of Superconductivity and Magnetism in Intermetallic NiBi_3
12P-B007	B2	B0165	D.O. Ledenyova, V.O. Ledenyovb, and O.P. Ledenyovc	On the Oxygen and its Vacancies Diffusion in Proximity to Abricosov Magnetic
12P-B008	B2	B0176	B. Rosenstein, I. Shapiro and B. Ya. Shapiro	Current carrying vortex crystals
12P-B009	B2	B0189	V. Sandu and I. Ivan	On the scaling of pinning force in ceramic MgB_2
12P-B010	B2	B0190	G.E. Volovik	Topological Matter, Flat Bands and Room Temperature Superconductivity
12P-B011	B2	B0194	Mintu Mondal, Sanjeev Kumar, Anand Kamlapure, John Jesudasan,	Evolution of Kosterlitz-Thouless-Berezinskii (KTB) Transition in Ultra-Thin NbN Films
12P-B012	B2	B0217	S.I. Bondarenko, V.P. Koverya, A.V. Krevsun	The critical state of a superconducting ring caused by a current.
12P-B013	B2	B0223	P. D. Kulkarni, U. V. Vaidya, S. S. Banerjee, C. V. Tomy, G.	Novel Facets of Crossover from Surface Superconductivity to Vortex State
12P-B014	B2	B0227	E.F.C. Driessens, H.L. Hortensius, N. Verheyen, K.K. Berggren, T. Zijlstra,	The Superconducting Transition in Highly Resistive NbTiN Nanowires
12P-B015	B2	B0231	H.J. Gardner, A. Kumar, L. Yu, M.P. Warusawithana, L. Wang, O. Vafek,	Enhancement of Superconductivity by a Parallel Magnetic Field in Two Dimensional Superconductors
12P-B016	B2	B0237	Jens Mueller, Jens Brandenburg, John A. Schlueter	Universal critical slowing down of the electron dynamics near the Mott transition in the organic superconductors κ-(BEDT-TTF)$_2$X

12P-B017	B2	B0247	Xiao-Fen Li and Jean-Claude Grivel	Temperature dependence of power-law index in $(Nd_xSm_xGd_{1-2x})Ba_2Cu_3O_{7-\delta}$ films
12P-B018	B2	B0252	A. Buzdin , A. V. Samokhvalov, and A. S. Mel'nikov	Vortex molecules in thin films of layered superconductors
12P-B019	B2	B0273	A. Maniv , T. Maniv , V. Zhuravlev ,B. Bergk , J. Wosnitza , P. C. Canfield , J. E.	Order-disorder transition and quantum magnetic oscillations in the vortex state of strong type-II superconductors
12P-B020	B2	B0298	R.C.Ramos, Steven Carabello and Joseph Lambert	Measurement of Sub-structure in the Dual Energy Gap of Magnesium Diboride below 1 Kelvin
12P-B021	B2	B0339	M.D.Croitoru, M.Houzet, A.Buzdin	In-plane magnetic field anisotropy in FFLO state in layered superconductors
12P-B022	B2	B0354	D. C. Peets, G. Eguchi, M. Kriener, S. Harada, Sk. Md. Shamsuzzaman, Y.	Li₂(Pd_{1-x}Pt_x)₃B Magnetic Phase Diagram and Superconducting Parameters
12P-B023	B2	B0370	Jian Wang and Moses H. W. Chan	Proximity effect in crystalline nanowires and topological insulators
12P-B024	B2	B0385	Taro Kanao, Masao Ogata	Spatial Modulation Patterns in Two-Dimensional Fulde-Ferrell-Larkin- Ovchinnikov Superconductivity
12P-B025	B2	B0400	I. V. Boylo, I. B. Krasnyuk, R. M. Taranets	Vortex penetration into type-II superconductors with pinning centers
12P-B026	B2	B0404	M. Uehara, K. Kozawa, M. Ohashi, Y. Suganuma, S. Tadera, T. Yamazaki	Ni-site Doping Effect of New Antiperovskite Superconductor ZnNNi₃
12P-B027	B2	B0406	M. Nunez-Regueiro	The Universal behavior of Superconducting Quantum Critical Points
12P-B028	B2	B0414	M. Tsujimoto, T. Yamamoto, K. Delfanazari, R. Nakayama, N. Orita,	THz-wave Emission from the Inner I-V Branches of the Intrinsic Josephson Junctions in Bi₂Sr₂CaCu₂O_{8+δ}
12P-B029	B2	B0430	Kouji Segawa, M. Kriener, Zhi Ren, S. Sasaki and Yoichi Ando	Physical properties of the bulk-superconducting Cu_xBi₂Se₃
12P-B030	B2	B0432	Y. Ota, M. Machida and T. Koyama	Longitudinal Collective Excitations in Intrinsic Josephson Junction Stacks with Two Tunneling Channels

12P-B031	B2	B0444	Swee K. Goh, L. E. Klintberg, P. L. Alireza, J. Yang, B. Chen, K. Yoshimura	High Pressure Studies of $(Sr,Ca)_3IrSn_{13}$ Single Crystals
12P-B032	B2	B0456	E. Morenzoni, H. Saadaoui, W. Dong, M. Horisberger, E. Kirk, W.A.	Observation of enhanced nuclear spin-lattice relaxation by superconducting fluctuations in thin films by depth resolved beta-NMR
12P-B033	B2	B0494	H. L. Liu, L. Y. Kuo, B. C. Chang, and H. C. Ku	Optical Studies of Weak-Ferromagnetic Superconductors
12P-B034	B2	B0507	R. Ishiguro, M. Yakabe, T. Nakamura, E. Watanabe, D. Tsuya,	Fabrication of the SQUID with Nb/Ru/Sr₂RuO₄ junction
12P-B035	B2	B0558	I. Guillamon, H. Suderow, S. Vieira, J. Sese, R. Cordoba, J.M. De Teresa and	Superconducting vortex imaging through scanning tunneling microscopy and spectroscopy at very low temperatures
12P-B036	B2	B0592	J. Michelsen, R. Grein	Properties of Hetero-structures involving Superconducting and Semiconducting Elements with Strong Spin-Orbit Coupling
12P-B037	B2	B0593	K. Yu. Arutyunov and J. S. Lehtinen	Quantum Phase Slip Phenomena in Superconducting Nanostructures
12P-B038	B2	B0596	K. Yu. Arutyunov, H.-P. Auraneva, and A. S. Vasenko	Experimental Study of Spatially Resolved Charge and Energy Imbalance in a Superconductor
12P-B039	B2	B0599	H. Nobukane, A. Tokuno, T. Matsuyama, and S. Tanda	Majorana-Weyl fermions in (2+1)-dimensional superconductors
12P-B040	B2	B0610	V. V. Baranov and V. V. Kabanov	The bifurcation phenomena in the resistive state of the narrow superconducting channels.
12P-B041	B2	B0614	A. Maldonado, H. Suderow and S. Vieira	Direct Observation of Superconducting Vortices under an Applied Supercurrent
12P-B042	B2	B0618	Yoichi Higashi, Yuki Nagai, Masahiko Machida and Nobuhiko Hayashi	Phase-Sensitive Quasiparticle Scattering inside a Vortex Core in Unconventional Superconductors
12P-B043	B2	B0632	F. Couedo, O. Crauste, L. Berge, Y. Dolgorouky, C. Marrache-Kikuchi,	Superconductor-Insulator Transitions in Pure Polycrystalline Nb Thin Films
12P-B044	B2	B0636	O. Crauste, F. Couedo, L. Berge, C. Marrache-Kikuchi and L. Dumoulin	Superconductor-Insulator Transition in Amorphous Nb_xSi_{1-x} Thin Films. Comparison between Thickness, Density of States and

12P-B045	B2	B0639	S. Saini and S.-J. Kim	Appearance of Quantum Fluctuations in Submicron Intrinsic Josephson Junctions of Bi₂Sr₂CaCu₂O_{8+delta} Single Crystal Whiskers
12P-B046	B2	B0667	C. Y. Cheng, C. L. Chan, C. L. Huang, Y. P. Chin, C. H. Chen, M. W. Chu, J.	Pressure Dependent Anomalous Phase Transition in Ternary Superconductor Bi₂Rh₃Se₂
12P-B047	B2	B0675	K. Miyoshi, E. Mutou, K. Fujiwara and J. Takeuchi	Pressure Dependence of Superconductivity in FeSe Studied by DC Magnetic Measurements
12P-B048	B2	B0676	K. Miyoshi, S. Ogawa, E. Kojima and J. Takeuchi	DC Magnetization Measurements of LiFeAs under High Pressure
12P-B049	B2	B0680	M Fogelstrom	Vortex-core structure in d-wave superconductors with a subdominant triplet pairing
12P-B050	B2	B0703	J. H. Miller, Jr., A. I. Wijesinghe, Z. Tang, and A. M. Guloy	Quantum Nucleation of Josephson Vortices in Superconducting Grain Boundary Junctions
12P-B051	B2	B0704	Jian-Ping Lv, Qing-Hu Chen	Percolation transition in Josephson-junction arrays
12P-B052	B2	B0705	M. Ichioka, K. Machida, and J.A. Sauls	Vortex Structure in Chiral p-wave Superconductors Studied by Eilenberger Theory
12P-B053	B2	B0715	Y. Tanabe, K. Huynh, T. Urata, R. Nouchi, N. Mitoma, S. Heguri, J. Xu, G. Mu and K.	Ru Doping Effect on the Dirac Cone State and the Possible Coexistence of the Dirac Cone state and the Superconductivity in Ba(Fe_{1-x}Co_x)₂As₂
12P-B054	B2	B0720	K. Yamaki, M. Tsujimoto, T. Yamamoto, T. Kashiwagi, H.	Magnetic field effects and dynamical control of terahertz electromagnetic wave emission from high-T_c superconducting Bi₂Sr₂CaCu₂O_{8+d}
12P-B055	B2	B0728	N. Kokubo, T. Yoshimura, and B. Shinozaki	Vortex-Lattice Orientation in the Flux-Flow State of
12P-B056	B2	B0730	N. Kokubo, H. Tamochi, B. Shinozaki, T. Nishizaki, and N.	Reorientation of a Moving Vortex Lattice in Amorphous Mo_{1-x}Gex Superconducting Films
12P-B057	B2	B0746	Y. Imai, D. Nakamura, F. Nabeshima, T. Katase, H.	THz conductivity measurements of Ba(Fe_{1-x}Co_x)₂As₂ and FeSe_{1-x}Te_x films
12P-B058	B2	B0772	R.Cao, Lance Horng, T. C. Wu, J. C. Lin, J. C. Wu, T. J. Yang	A Multi-Vortex State Related Pinning Phenomena in Nb Thin Films with Square Pinning Arrays

12P-B059	B2	B0779	T. Nojima, K. Ueno, S. Yonezawa, M. Kawasaki, Y. Maeno and Y. Iwasa	Upper Critical Fields of Electric-Field-Induced Superconductivity in SrTiO₃
12P-B060	B2	B0804	S. Uji, A. Harada, K. Enomoto, Y. Takahide, M. Kimata, T. Yakabe, K.	Single Vortex Flow in a Mesoscopic Superconducting Al Disk
12P-B061	B2	B0807	T. J. Yang, R. Cao, Lance Horng, T. C. Wu, C. M. Chen	Simulations for Superconducting Thin Films with Honeycomb Pinning Arrays
12P-B062	B2	B0848	Ece Uykur, Kiyohisa Tanaka, Takahiko Masui, Shigeki Miyasaka and	Overdoping effect on the in-plane charge dynamics in (Y,Ca)Ba₂Cu₃O_{7-d}
12P-B063	B2	B0858	J. Jiang, C. He, and D. L. Feng	Strain detwinning of NaFeAs single crystals: Resistivity and magnetic susceptibility study
12P-B064	B2	B0882	Yuke Li, Jun Tong, Xiao Lin, Qian Tao, Guanghan Cao, Zhu'an Xu	Phase diagram of the SmFe_{1-x}CoxAsO (0≤x≤1) system
12P-B065	B2	B0898	K. Delfanazaria, M. Tsujimotoa, T. Kashiwagia, R. Nakayamaa, T.	THz emission from a triangular mesa structure of Bi-2212 IJJs
12P-B066	B2	B0904	H. Minami, T. Koike, N. Orita, T. Kashiwagi, M. Tsujimoto, T.	Coupling to External Structures: Boundary Conditions for the Bi2212-based Superconducting THz Emitter
12P-B067	B2	B0919	F. Tafuri, A. Barone, F. Beltram, F. Carillo, F. Lombardi, L. Longobardi, D.	Frontiers Problems of the Josephson Effect in High T_c: From unconventional superconductivity to Mesoscopics and
12P-B068	B2	B0923	Taketomo Nakamura, T. Sumi, S. Yonezawa, T. Terashima, M.	Magnetic field effect in a topological superconducting junction Pb/Ru/S\$ 2\$RuO\$ 4\$
12P-B069	B2	B0937	S. Katano and H. Nakagawa	Novel superconductivity of the noncentrosymmetric compounds La\$T\$C\$ \{2\}(\$T\$=Ni, Pd and Pt)
12P-B070	B2	B0987	Shanyu Liu, Wentao Zhang, Haiyun Liu, Lin Zhao, Xiaowen Jia, Daixiang Mou,	New Fermi Surface Sheets Revealed in Sr₂RuO₄ Revealed by High Resolution Angle-Resolved Photoemission Spectroscopy
12P-B071	B2	B0992	M. Nishida, Y. Aoki and T. Fujii	Relativistic dynamics of domain wall in one-dimensional SQUID array
12P-B072	B2	B0998	S. M. Anton, J. S. Birenbaum, S. R. O' Kelley, A. F. Dove, G. A. Olson, Z. R.	Low Frequency Flux Noise in dc-SQUIDs: Dependence on Temperature and SQUID Geometry

12P-B073	B2	B1019	K. Deguchi, Y. Takano	Alcoholic beverages induce superconductivity in FeTe_{1+x}S_x
12P-B074	B2	B1023	M.R. Eskildsen, C. Rastovski, C.D. Dewhurst, D.C. Peets, H. Takatsu, Y.	Observation of a Fractured Vortex Lattice Phase in Sr₂RuO₄ with H parallel a
12P-B075	B2	B1046	P. D. Kulkarni, J. G. Rodrigo, H. Suderow, S. Vieira, M. R. Baklanov, T.	Scanning tunneling spectroscopy in ultra thin TiN films
12P-B076	B2	B1066	Itsuhiro Kakeya, Takaaki Mizuno, Hitoshi Kambara, and Minoru Suzuki	Macroscopic Quantum Tunneling and Thermal Activation Switchings
12P-B077	B2	B1086	N. Momono, S. Kurabayashi, R. Shiroshita, Y. Amakai, S.	Stripe order and superconductivity in the mechanical milled La_{1.6-x}Nd_{0.4}S_xCuO₄
12P-B078	B2	B1099	Wenhai Wu, Haidong Liu, Zhiyuan Wei, and Isabel Schultz	Long-Range Superconducting Proximity Effect in Template-Fabricated Single-Crystal Nanowires
12P-B079	B2	B1106	L.N.Zherikhina, A.M.Tskhovrebov, L.A.Klinkova, D.A.Balaev,	Ba_{0.6}K_{0.4}BiO₃ single crystal as a multiple Josephson system: new coherent effect
12P-B080	B2	B1117	M. Zgirski, L. Bretheau, Q. Le Masne, H. Pothier, D. Esteve and C. Urbina	Evidence for long-lived quasiparticles trapped in superconducting point contacts
12P-B081	B2	B1135	A. L. Karuzskii, A. V. Perestoroinin, N. A. Volchkov and L. N. Zherikhina	Anomalous Skin Effect in a Drude-type Model Incorporating the Spatial Dispersion for Systems with Conductivity of Metal
12P-B082	B2	B1139	Nobuyuki Kurita, Motoi Kimata, Kota Kodama, Atsushi Harada, Megumi	Anomalous Normal State Properties of the Pressure-Induced Superconductor EuFe₂As₂
12P-B083	B2	B1150	Philip Adams	Zeeman Limited Superconductivity and Incoherent Cooper Pairing
12P-B084	B2	B1181	Y.Y. Peng, J.Q. Meng, L. Zhao, W.T. Zhang, H.Y. Liua, C.T. Chen, Z.Y. Xu,	Doping Evolution of Mass Renormalization Effects in Bi₂₂₀₁ Superconductors
12P-B085	B2	B1192	Y. Liu and C. T. Lin	Upper critical field, second magnetization peak and irreversibility line in BaFe₂(As_{1-x}P_x)₂ single crystals
12P-B086	B2	B1193	E. Farber and N. Bachar	Overdoped YBaCuO thin films in THz range

12P-B087	B2	B1200	Kh. R. Rostami	A Method for the Analysis of Physical Processes on the Interface between Meissner and Vortex Domains in HTSCs
12P-B088	B2	B1205	L. H. Greene, H. Z. Arham, C. R. Hunt, W. K. Park, J. Gillett, S. Sebastian Z. J.	Detection of Novel Electronic Order Above the Structural Transition in Underdoped Ba(Fe_{1-x}Cox)2As₂ and Fe_{1-y}Te with Point Contact
12P-B089	B2	B1208	Y. Asano, A.A.Golubov, Ya. V. Fominov, Y. Tanaka	Testing odd-frequency Cooper pairing by microwave surface impedance
12P-B090	B2	B1209	Won-Gi Lee, Kisung Kwak, Joonkyu Rhee, Jaeun Yoo, and Dojun Youm	Correlations between critical current density profiles and microstructures in various superconducting coated conductors
12P-B091	B2	B1244	G. Garbarino, R. Weht, A. Sow, P. Toulemonde, P. Bouvier, M.	Pressure Effects on the Crystal Structure and Electronic Properties of the 1111 Iron Superconductors
12P-B092	B2	B1265	V.A. Gasparov, L. Drigo, A. Audouard, D.L. Sun, C.T. Lin, S.L. Bud'ko, S.	Electron transport and anisotropy of the upper critical magnetic field in Ba_{0.68}K_{0.32}Fe₂As₂ and Ba(Fe_{0.92}Co_{0.08})₂As₂ single crystals
12P-B093	B2	B1268	Jorge Berger	Fluctuation Current in Superconducting Loops
12P-B094	B2	B1292	Jie Yong, K. Il'in, M. Siegel and T. R. Lemberger	Superfluid Density Study of Two-Dimensional NbN Films near the Superconductor-Insulator Transition
12P-B095	B2	B1296	W. T. Guo, G. Xu, T. Dong, B. F. Hu, B. Cheng, P. Zheng, Y. G. Shi, and N. L.	Peculiar metallic properties of LaSb: a combined study of optical spectroscopy and band structure calculations
12P-B096	B2	B1353	A.F. Fang, T. Dong, Y. G. Shi, and N. L. Wang	Optical Spectroscopy Study on SrPt₂As₂ Single Crystal
12P-B097	B2	B1374	R.C. Ramos, Joseph G. Lambert, Steven A. Carabello and Jerome T. Mlack	Demonstration of Microwave Resonant Activation in large MgB₂-based thin film Josephson junctions
12P-B098	B2	B1376	K. Jin, B. X. Wu, B. Y. Zhu, B. Xu, L. X. Cao, B. R. Zhao, A. Volodin, J.	Sign reversal of the Hall resistance in the mixed-state of electron doped superconducting thin films
12P-B099	B2	B1398	J. J. Ying, X. F. Wang, T. Wu, Z. J. Xiang, R. H. Liu, Y. J. Yan, A. F. Wang, M.	Distinct electronic nematicities between electron and hole
12P-B100	B2	B1426	G.A.Gogadze, A.A.Lyogenkaya, S.N.Dolya	Reentrant effect in a mesoscopic cylindrical structure of a superconductor coated with a normal metal layer

12P-B101	B2	B1452	Suk Bum Chung and Steven A. Kivelson	Entropy driven formation of a half-quantum vortex lattice
12P-B102	B2	B1486	Y. Iwasa	Electric Field Induced Interface Superconductivity
12P-B103	B2	B1497	T.-L. Xia and T.-S. Zhao	Superconductiviy in Rh-doped CaFeAsF
12P-B104	B2	B0552	T.Tomita, H. Takahashi, H. Takahashi, H. Okada, Y. Mizuguchi,	Superconducting Transitions and Crystal Structure for FeSe\$ \{1-x\}Sr\$ \{x\} (\$x=0.1, 0.2, and 0.3) under Pressure.
12P-B105	B2	B0018	O.V. Dobrovolskiy, M. Huth and V.A. Shklovskij	Odd Magnetoresistive Response in Nanostructured Nb Thin Films
12P-B106	B2	B0019	Valerij A. Shklovskij	Nonadiabatic Ratchet Effect in Superconducting Films With a Tilted Cosine Pinning Potential
12P-B107	B2	B0886	M. Kato, Y. Niwa	Microscopic Investigation of Vortex-Vortex Interaction in Conventional Superconductors
12P-B108	B3	B0138	Saleh Hasan Naqib and R. S. Islam	Probing the interplay among superconductivity, pseudogap, and stripe correlations by Zn substitution in high-Tc cuprates
12P-B109	B3	B0139	Shinji Kawasaki, C. T. Lin, P. L. Kuhns, A.P. Reyes and Guo-qing Zheng	Cu-NMR Study of Bi\$ 2\$Sr\$ \{2-x\}La\$ x\$CuO\$ \{6+\delta\} Superconductor in Very High Magnetic Fields
12P-B110	B3	B0326	X. T. Wu and R. Ikeda	Pseudogap in strongly disordered conventional superconductors
12P-B111	B3	B0373	H. Kamimura and H. Ushio	Occurrence of Fermi Pockets without the Pseudogap Hypothesis and
12P-B112	B3	B0407	Tess L. Williams, Elizabeth J. Main, Ilija Zeljkovic, Michael Boyer, Doug	STM imaging of broken symmetry states in cuprate superconductors
12P-B113	B3	B0440	E. Morenzoni, B. M. Wojek, A. Suter, T. Prokscha, G. Logvenov, I. Bozovic	The Meissner effect in a strongly underdoped cuprate well above its critical temperature
12P-B114	B3	B0654	T. Domanski	Manifestation of superconducting correlations above the critical temperature

12P-B115	B3	B0664	Han-Yong Choi and Seung Hwan Hong	Dynamically induced Fermi arcs and pockets: A model for
12P-B116	B3	B0751	Minoru Suzuki, Takashi Hamatani, Kenkichi Anagawa, and Takao	A Model and Calculation of Evolving Tunneling Spectra for the Superconducting Gap and Pseudogap in
12P-B117	B3	B0828	Y.-J. Chen, P. J. Lin, C. H. Pan, J.-Y. Lin, C. W. Luo, K. H. Wu, B. Rosenstein, J. Y.	Superconducting Fluctuation and Electric Transport Properties Revealed from the Phase Diagram of Ca-doped Cuprates
12P-B118	B3	B0854	Qijin Chen, K. Levin, Chih-Chun Chien, and Yan He	Unifying Fermi arcs and protected nodes in cuprate superconductors01
12P-B119	B3	B0867	M. Miyazaki, R. Kadono, M. Hiraishi, A. koda, K. M. Kojima, Y. Fukunaga,	Pseudogap state of (Bi,Pb)2201 studied by muon Knight shift
12P-B120	B3	B0964	Hitoshi Kambara, Itsuhiro Kakeya, and Minoru Suzuki	Intrinsic Tunneling Spectroscopy for Pb-Substituted BSCCO
12P-B121	B3	B1009	Xiaoqing Zhou, B. Morgan, W. A. Hutmama, J. R. Waldram, D. Peets,	Logarithmic flux-flow resistivity across the cuprate phase diagram
12P-B122	B3	B1065	I. Kakeya, K. Sumida, S. Shinada, Y. Takamarau, M. Suzuki, K. Suga, and	Doping Evolution of Normal State Transport Properties in BiPb2201 Cleaved Thin Crystals
12P-B123	B3	B1105	T. Fujii and A. Asamitsu	Pressure Dependence of Nernst Effect for La_{2-x-y}Nd_ySr_xCuO₄
12P-B124	B3	B1125	D. Munzar and J. Marek	Magnetic-field dependence of the c-axis infrared response of underdoped YBa₂Cu₃O_{7-delta}) interpreted in terms of the multilayer
12P-B125	B3	B1153	M. M. Yee, E. Main, T. Williams, A. Soumyanarayanan, I. Zeljkovic, M. Boyer,	STM Imaging of Spatial Variations in the Charge-Ordered states of BSCO
12P-B126	B3	B1293	Jie Yong, Andrew McCray, T.R. Lemberger, Muntaser Naamneh, Amit	Two-dimensional quantum critical point in underdoped Bi₂Sr₂Ca₂Cu₂O_{8+x} revealed by superfluid density measurements
12P-B127	B3	B1301	K. Fujita, J. P. Hinton, J. D. Koralek, E. -A. Kim, M. J. Lawler, H. Eisaki, S.	Electronic Symmetry of the Cuprate Pseudogap States from SI-STM
12P-B128	B3	B1346	J. K. Ren, Y. F. Ren, Ye Tian, H. F. Yu, D. N. Zheng, S. P. Zhao, and C. T. Li	Intrinsic tunneling study of Bi₂Sr_{1.6}La_{0.4}CuO₆

12P-B129	B3	B1478	Y. Chen	Theoretical investigation of superconductivity and antiferromagnetism in tri-layer cuprate superconductors
12P-C001	C2	C0029	A. A. Saberi	Two-dimensional Criticality in a Three-dimensional Spin Ising Model
12P-C002	C2	C0058	Naoya Arakawa and Masao Ogata	Theoretical Study of Electronic States in Ca_{2-x}S_xRuO₄
12P-C003	C2	C0097	S. Ebisu, K. Koyama, T. Horikoshi, M. Kokita and S. Nagata	Extremely broad hysteresis in the magnetization process of alpha-Dy₂S₃ single crystal induced by high field cooling
12P-C004	C2	C0183	Shi-Dong Liang and Guang-Yao Huang	Persistent current and quantum phase transition in mesoscopic Rashba rings
12P-C005	C2	C0198	Yu.Goryunov, A. Levchenko, A.{Nateprov	Unusual Magnetism of the Eu Based Compounds - EuB_{6-x}C_x, EuZn₂As₂): the Low Temperature
12P-C006	C2	C0209	M. Hiroi, I. Yano, K. Sezaki, I. Shigeta, M. Ito, H. Manaka, and N. Terada	Substitution Effect on the Magnetic Transitions of Fe₂MnSi
12P-C007	C2	C0232	Liuqi Yu, Xiaohang Zhang, S. von Molná r, L. Wang, W.B. Wu and P. Xiong	Hall effect in La_{0.67}Ca_{0.33}MnO₃ thin films with anisotropic strain
12P-C008	C2	C0244	B. W. Zhi, Z. Huang, L. F. Wang, X. L. Tan, P. F. Chen, and W. B. Wu	Controlling phase separation in La_{0.67}Ca_{0.33}MnO₃ thin films via oxygen deficiencies
12P-C009	C2	C0245	L. F. Wang, Z. Huang, B. W. Zhi, and W. B. Wu	Anisotropic transport in phase-separated La_{0.67}Ca_{0.33}MnO₃/NdGaO₃(100) film
12P-C010	C2	C0280	M. Sasaki1, A. Ohnishi1, T. Kikuchi1, M. Kitaura1, Ki-Seok	Interplay between the Kondo effect and randomness in M_xTiSe₂ (M = Co, Ni, and Fe) single crystals
12P-C011	C2	C0301	A.A. Dubrovskiy, O. N. Martyanov, D.A. Balaev, K.A. Shaykhutdinov, S.S.	Magnetic properties of monophase e-Fe₂O₃ nanoparticles system.
12P-C012	C2	C0311	D.C. Ling, P.C. Hsu, and C.L. Lee	Correlation between A-site Randomness and Magnetic Phase Transition in Pr_{0.5}Ba_{0.5}MnO₃
12P-C013	C2	C0375	D. X. Li, S. Nimori and Y. Shikama	Magnetic ordering and magnetocaloric effect in PrPdIn and NdPdIn

12P-C014	C2	C0383	Y.Kawasaki, S.Takase, Y.Kishimoto, I.Yamada, K.Shiro,	NMR study of successive magnetic transitions in A-site-ordered perovskite LaMn₃Cr₄O₁₂
12P-C015	C2	C0403	T. Tolinski, A. Kowalczyk, M. Falkowski, K. Synoradzki, A.	Magnetic structure and magnetocaloric effect in NdNiAl₄
12P-C016	C2	C0417	M. Matsumura, T. Inagaki, H. Kato, T. Nishioka, H. Tanida and M. Sera	²⁷Al-NQR Study on Novel Phase Transition in CeOs₂Al₁₀
12P-C017	C2	C0445	Y. Sun, Y. F. Guo, W. Yi, X. X. Wang, J. J. Li, S. B. Zhang, C. I. Sathish, A. A. Belik,	The lattice and magnetic and electronic properties of the antiperovskite Mn₃XN (X=Zn, In, Sn) prepared under high pressure
12P-C018	C2	C0495	I. Umehara, S. Mizoguchi, G. H. Hu , Y. Uwatoko, K. Matsubayashi, S.	Disappearance of Metal-Insulator Transition in Pr_{0.5}Ca_{0.5}MnO₃ under Pressure
12P-C019	C2	C0516	A. Shimokata, S. Yamada, Y. Shimizu and M. Itoh	Spin-State Transition in \$R\$CoO\$ \cdot 3\\$ (\$R\$ = La, Pr, and Nd): Single-Crystal \$^{159}\$Co NMR Measurements
12P-C020	C2	C0520	K. Tsutsui, T. Tohyama, W. Koshibae, and S. Maekawa	Theoretical Study of Resonant Inelastic X-ray Scattering Spectrum in Nickelates
12P-C021	C2	C0587	T. Okuda, S. Oozono, T. Hokazono, K. Uto, Y. Fujii, S. Seki, Y.	Substitution effect on the Magnetic State of Delafossite CuCrO₂ Having a Spin-3/2 Antiferromagnetic Triangular Sublattice
12P-C022	C2	C0648	A. Yazdani, P. Amin Javaheri	Quantum Phase Transition at Critical Magnetic Field
12P-C023	C2	C0711	Q. Zhang and S. Yunoki	Magnetic Properties and Improper Ferroelectricity in LaFeO₃/LaCrO₃ Superlattices
12P-C024	C2	C0712	Q. Zhang, G. H. Chen, X. G. Gong and S. Yunoki	d0 Ferromagnetic Surface in HfO₂
12P-C025	C2	C0774	H. Kuroe, N. Takami, M. Niwa, T. Sekine, Matsumoto, F. Yamada, H. Tanaka	Longitudinal Magnetic Excitation in KCuCl₃ Studied by Raman Scattering under Hydrostatic Pressures
12P-C026	C2	C0795	M. Isobe, H. Okabe, E. Takayama- Muromachi, A. Koda, S. Takeshita, M.	Spin-Orbit Mott State in the Novel Quasi-2D Antiferromagnet Ba₂IrO₄
12P-C027	C2	C0821	R. Fukuta, K. Hemmi, S. Miyasaka, S. Tajima, D. Kawana, K. Ikeuchi, Y.	R-site randomness effect on spin/orbital order in perovskite RVO₃

12P-C028	C2	C0906	M. Isobe, T. Kawashima, M. Arai, E. Takayama-Muromachi, and A.	Transport Properties of the Novel Quasi-1D Cobalt Oxide (Ca,Na)Co₂O₄
12P-C029	C2	C0966	R. K. Kremer, J. M. Law, C. Hoch, R. Glaum, M.-H. Whangbo, J. Kang,	Spin-Peierls transition in TiPO₄
12P-C030	C2	C0971	J. Li, Z. W. Wu, S. L. Li, Y. G. Yang, X. S. Sun, and D. N. Zheng	A field-induced IM-type transition observed in low-energy H₂₊ ion implanted epitaxial La₂/3Ca₁/3MnO₃ thin films
12P-C031	C2	C0972	J. Li, Y. Zhang, L. M. Cui, N. L. Guo, Y. R. Jin, H. Y. Tian, and D. N. Zheng	The anisotropic magnetoresistance and planar Hall effect in tetragonal La₂/3Ca₁/3MnO₃ thin films
12P-C032	C2	C0981	N. Sanada, T. Yoshioka, R. Watanuki and K. Suzuki	Elastic Constants of NdCu₂Ge₂
12P-C033	C2	C0999	Y. Araki and M. Ohashi	Itinerant-electron metamagnetism of magnetocaloric material RCo₂ and their borides
12P-C034	C2	C1001	A. Zaleski, W Strek, and P. Gluchowski	The effect of grain size of GaN nanocrystallites subjected to high pressing has been manifested in a strong deformation of grains of
12P-C035	C2	C1174	Shile Zhang, Shun Tan, Li Pi, Changjin Zhang, Yuheng Zhang	The role of Ru⁵⁺ in increasing T_c of Cr-doped SrRuO₃ system
12P-C036	C2	C1235	H. Yamaguchi, M. Tada, K. Iwase, T. Shimokawa, H. Nakano, H. Nojiri, A.	Magnetic Phase Transition in the Verdazyl Biradical Crystal p-BIP-V2
12P-C037	C2	C1261	J.S. Lu, Y.Y. Chien, and M.D. Lan	Magnetic and Transport properties of Cr_{1-x}Ti_xN_δ solid solution nitrides
12P-C038	C2	C1344	T. Ohgoe, T. Suzuki and N. Kawashima	Supersolid Mechanism of Dipolar Bosons and Double Peak Structure in Momentum Distribution
12P-C039	C2	C0788	Y.Takenaka and N.Kawakami	Variational Monte Carlo Study of Two-Dimensional Multi-Orbital Hubbard Model on Square Lattice
12P-D001	D9	D1496	Jinxin Zhong	Tuning Electronic Transport Properties of Two-dimensional Quantum Films
12P-D002	D9	D0036	S B Ota, S Ota	A new model of GaAlAs semiconductor diode

12P-D003	D9	D0658	K. Gloos, J. Huupponen and E. Tuuli	Phonon-drag induced suppression of the Andreev hole current in superconducting niobium contacts
12P-D004	D9	D0659	E. Tuuli, K. Gloos	Normal reflection at superconductor - normal metal interfaces due to Fermi surface mismatch
12P-D005	D9	D0582	T. H. Kao, S. Mukherjee, Y. H. Lin, C. C. Chou and H. D. Yang	Size-dependent Anomalous Dielectric Behavior in La\$2\$O\$3\$:SiO\$2\$ Nano-glass Composite System
12P-D006	D9	D1176	A. Aparecido-Ferreira, G.M Ribeiro, E.S. Alves, and J.F. Sampaio	Determination of a soft gap in the density of states of a granular carbon
12P-D007	D9	D0274	V.V. Marchenkov, A.Yu. Volkov, O.N. Kapitonova, H.W. Weber	Electrical and galvanomagnetic properties of AuAl2+6%Cu intermetallic compounds at low temperatures
12P-D008	D9	D0470	A.M. Goldman and Yen Hsiang Lin	Magnetic Field Tuned Quantum Phase Transition in the Insulating Regime of Ultrathin Amorphous Bi Films
12P-D009	D9	D1319	Y. Yamane and M. Itoh	From Ward Identity to Exact Transport Equation: Complement to Eliashberg's Derivation of Landau-Silin Equation and
12P-D010	D9	D0318	K. Nakano, R. Eder, Y. Ohta	Exact wave functions and excitation spectra of the one-dimensional double-exchange model with one mobile electron
12P-D011	D9	D1175	K. Yamada, B. Shinozaki, K. Yano and H. Nakamura	The temperature dependence of hall mobility of the oxide thin film In\$2\$O\$3\$-ZnO
12P-D012	D9	D0914	K. Kuga, Y. Karaki, Y. Matsumoto and S. Nakatsuji	Quantum Phase Transition Induced by Chemical Substitution in the valence fluctuating system \$\alpha\$-YbAlB4
12P-D013	D9	D0153	K. Shunkeyev, L. Myasnikova, A. Barmina, Sh. Sagimbaeva	Effect of intrinsic luminescence of alkali halide amplification by low temperature deformation
12P-D014	D9	D0279	V.V. Marchenkov, E.P. Platonov, and H.W. Weber	Size effect and the quadratic temperature dependence of the transverse magnetoresistivity in "size-effect" tungsten
12P-D015	D9	D1056	H. Katsura, Y. Onose, T. Ideue, Y. Shiomi, N. Nagaosa, and Y. Tokura	Thermal Hall Effect in Ferromagnetic Insulators
12P-D016	D9	D1357	Yuki Yamaki	Dopant-dependence on charge/orbital ordering in layered manganite La0.5Sr1.5MnO4

12P-D017	D9	D0729	Neng-Fu Shih, B. R. Chen, B. C. Yao, H. Z. Chen, and C. H. Lin	Transparency Conducting AZO Films by Using DC Sputtering and RF Sputtering
12P-D018	D9	D1273	F. Heidrich-Meisner, A. Feiguin, I. Gonzalez, K. Al-Hassanieh, M.	Steady-state transport: From quantum dots to extended structures with electronic correlations
12P-D019	D9	D0341	A. Zimmers, B. Wu, H. Aubin, R. Gosh, Y. Liu and R. Lopez	Electric-field-driven phase transition in vanadium dioxide
12P-D020	D9	D0842	K. Taguchi and G. Tatara	Theory of inverse Faraday effect in disordered metal in the THz regime
12P-D021	D9	D0657	K. Gloos and E. Tuuli	Break-junction experiments on the zero-bias anomaly of non-magnetic and ferromagnetically ordered metals
12P-D022	D9	D1480	S. Sakhi	Self-dual Josephson junction arrays: quantum dissipation and the quantum Hall effect
12P-D023	D9	D1010	R. Yoshii, M. Eto and I. Affleck	Decoherence in Aharonov-Bohm Ring with Embedded Quantum Dot in Kondo Regime
12P-D024	D9	D0938	K. Makisea, B. Shinozaki, T. Asano, K. Yano, and H. Nakamura	Activation like behavior on the temperature dependence of the carrier density in In₂O₃-ZnO films
12P-D025	D9	D0557	T. Toriyama, T. Konishi, Y. Ohta	Hollandite ruthenate K₂Ru₈O₁₆ as a new Tomonaga-Luttinger-liquid system
12P-D026	D9	D0651	V. Janis and V. Pokorný	Quantum transport in strongly disordered crystals: Electrical conductivity with large negative vertex corrections
12P-D027	D9	D0013	N.V. Khotkevych, Yu.A. Kolesnichenko and J.M. van Ruitenbeek	Aharonov-Bohm-type Oscillations in a System of Two Tunnel Point-Contacts in the Presence of a Single Scatterer: Determination of the
12P-E001	E2	E0594	H. Motzkau, S.-O. Katterwe, A. Rydh, and V.M. Krasnov	Transformation from a Triangular to a Rectangular Fluxon Lattice in Bi-2212 Intrinsic Josephson Junctions
12P-E002	E2	E0833	Y.R. Jin, N. Wang, , H. Deng, J. Li, Y.L. Wu, Y. Tian, and D.N. Zheng	Effect of field gradient and disturbance on the ultra-low field NMR signal detecting using a high-T_c dc-SQUID
12P-E003	E2	E1007	Mikko Kiviranta and Leif Grönberg	SQUID development for multiplexed cryogenic detectors

12P-E004	E2	E1155	V.S. Chernichenko, A.I. Bidenko, N.V. Tribulev, N.I. Krobka	Comparative analysis of optical-physical schemes of gyroscopes based on macroscopic quantum effects of superfluid helium isotopes
12P-E005	E2	E1166	J. R. O'Brien, A. Strydom, W. G. Coors	Low Temperature Analysis of Nickel Nano Particles by SQUID Based AC Susceptibility
12P-E006	E2	E1197	Chiu-Hsien Wu, Fong-Jyun Jhan, and Jen-Tzong Jeng	Josephson effects of High-Tc YBCO variable- thickness bridges
12P-E007	E2	E1349	G. M. Xue, H. F. Yu, Y. F. Ren, Ye Tian, and S. P. Zhao	Fabrication of rhenium Josephson junctions
12P-E008	E2	E0152	D. Sergeyev, K. Shunkeev	Four electrons transport of a supercurrent in Josephson junction and anharmonic dependence by a current-phase

Evening Session (12E) Chair: Zhongxuan Zhao

12E-1		B1446	Peter Kes	Kamerlingh Onnes's Notebooks and the Discovery of Superconductivity
12E-2		B1485	Georg Bednorz	High Tc Superconductivity in copper oxides - from retrospective to outlook
12E-3		B1314	Frank Steglich	Heavy-Fermion Superconductivity Mediated by Antiferromagnetic Spin Fluctuations
12E-4		B0645	Douglas Scalapino	A Common Thread: the pairing mechanism in the unconventional superconductors

Saturday Aug.13

Time Slot	Category	ABSN	Name	Title
Half Plenary Session(13H1)				
13H1-1			Andrew Cleland	
13H1-2			Seigo Tarucha	
13H1-3			Andreas Wallraff	
Half Plenary Session(13H2)				
13H2-1			Kosmas Prassides	
13H2-2			Yoshihiro Iwasa	Electric Field Induced Interface Superconductivity
13H2-3			Xing-Jiang Zhou	
Parallel Session(13m-A) Superfluid He-3 in Aerogel				
13m-A1		A0778	Osamu Ishikawa	The Proximity Effect at the Interface between Superfluid 3He-B and Aerogel of 97.5%
13m-A2		A0908	Vladimir Dmitriev	Structure of A-like Phase of 3He in Anisotropic Aerogel
13m-A3		A0434	Pierre Hunger	New Types of Magnon BEC in Superfluid 3He in Aerogel
13m-A4		A1474	Jeevak Parpia	Phase diagram of superfluid 3He in 10% uniaxially compressed aerogel
13m-A5		A0397	Hiromitsu Takeuchi	Drag Force on a High Porosity Aerogel in Liquid3He
Parallel Session(13m-B₁) Recent Discovery and Properties of AFex Se2 (A=K, Rb, Cs, Tl)				
13m-B ₁ 1		B1471	Xiao-Long Chen	Superconductivity in iron selenide K0.8Fe2Se2
13m-B ₁ 2		B0493	Dong Lai Feng	Electronic structure of iron chalcogenides
13m-B ₁ 3		B1432	Wei Bao	Neutron Scattering Study on the Newest 245 Family of Fe-based Superconductors
12m-B ₁ 4		B0931	Zhong-Yi Lu	Electronic structures and magnetic orders of iron- pnictides or chalcogenides
12m-B ₁ 5		B1451	Qimiao Si	Electron Correlations and Superconductivity in Iron Pnictides and Selenides
Parallel Session(13m-C) Quantum Criticality and Novel Phases I				
13m-C1			Collin Broholm	
13m-C2		C0324	Guangming Zhang	Landau forbidden continuous quantum phase transition between two topologically valence
13m-C3		C1162	Oliver Stockert	Superconductivity and magnetism in CeCu2Si2
13m-C4		C1345	Andy Schmidt	Imaging Heavy Fermion Hybridization in URu2Si2

13m-C5		C0204	Kazunari Yamaura	Continuous metal-insulator transition at 410 K of the 5d oxide NaOsQ3
Parallel Session(13m-D) Single Spin Devices / Qubits				
13m-D1		D1134	Kuan-Yen Tan	Single-shot readout of an electron spin in silicon
13m-D2		D1189	Katja Nowack	Single-shot correlations and two-qubit gate of electron spins in a double quantum dot
13m-D3		D1224	Christian Enss	Investigation of the dephasing of tunneling systems in glasses using two-pulse polarisation
13m-D4		D1202	Shingo Katsumoto	Magnetization dependent rectification in (Ga,Mn)As magnetic tunnel junctions
Parallel Session(13m-B₂) Heavy Fermion Superconductivity				
13m-B ₂ 1			Meigan Aronson	
13m-B ₂ 2		B0743	Hui-Qiu Yuan	Nodal gap structure in weak-coupling non-centrosymmetric
13m-B ₂ 3		B1239	Honda Fuminori	Pressure-induced novel superconductivity and heavy electron state in rare earth compounds
13m-B ₂ 4		B1447	Stefan Kirchner	Tracing the Kondo Lattice in YbRh₂Si₂
13m-B ₂ 5		B1456	Milan P. Allan	Intra-band Quasiparticle Interference and Direct Determination of the Anisotropic
Parallel Session(13a-A) Vortices and Quantum Turbulence				
13a-A1		B0393	Wei Guo	Effect of copper-site spin polarization on the pair state in the high T_csuperconductors
13a-A2		A0442	Vladimir Eltsov	Turbulent and Laminar Dynamics of Superfluid ³He-B at Low Temperatures
13a-A3			P.V.E. McClintock	
13a-A4			Andrei Golov	Turbulence in superfluid 4He in the T=0 limit, generated and probed by injected ions
13a-A5			Enrico Fonda	
Parallel Session(13a-B) Theory for Fe-based Superconductors				
13a-B1		B1430	Zlatko Tesanovic	Nature of Correlations and Spin-Orbital Symmetry in Iron-Based Superconductors
13a-B2		B1419	J. P. Hu	A Unified Paradigms of High Temperature Superconductors
13a-B3		B0699	Takami Tohyama	Spin and Charge Excitations in the Antiferromagnetic Metallic Phase of Iron
13a-B4		B0268	Hiroshi Kontani	Superconductivity and structure transition in iron based superconductors: analysis based on
13a-B5		B1416	Yunkyu Bang	Volovik Effects of the ±S-wave state in the Iron-based Superconductors
Parallel Session(13a-C) Quantum Criticality and Novel Phases II				
13a-C1		C0035	Vladimir Mineev	

13a-C2		C0686	Nic Shannon	Quantum Ice
13a-C3		C0887	Michael Lang	Magnetic cooling through quantum criticality
13a-C4		C1178	Zhihuai Zhu	Spin-Polarization Control at the Surface of a Topological Insulator
13a-C5		C1170	Georgios Varelogian	Patterns of Coexisting Condensates Forming Domes Preventing the Quantum Critical Point
Parallel Session(13a-D) Single Spin Devices / Spin Transport				
13a-D1		D0514	Kohei Ohnishi	Non-local Spin Current Injection into a Superconductor
13a-D2		D0111	Shiu-Ming Huang	Rashba spin-orbit interaction in vertical In0.05Ga0.95As/GaAs quantum dots
13a-D3		D0283	Till Benter	InAs spin-filter cascades in magnetic fields
13a-D4		D0810	Akihito Takeuchi	Magnetic Monopole Generated by Spin Damping with Spin-Orbit Coupling
Parallel Session(13a-E) THz and Nanomechanical Technologies				
13a-E1		E1422	Joel Ullom	Development of Transition-Edge Sensor Arrays at NIST
13a-E2		E1211	Biaobing Jin	Development of Transition-Edge Sensor Arrays at NIST
13a-E3		E0276	Dongming Mei	Cryogenic Large Liquid Xenon Detector for Dark Matter Searches
13a-E4		E0114	E. Collin	Low temperature nanomechanical probes: from linear to nonlinear regimes
13a-E5		E1025	Francesco Massel	Microwave amplification in nanomechanical systems
Poster Session				
13P-A001	A4	A0117	R. G. Bennett, N. Zhelev, E. Smith, J. Pollanen, W. Halperin, J. Parpia	Phase diagram of superfluid 3He in uniaxially compressed aerogel
13P-A002	A4	A0123	N. Zhelev, R. Bennett, E. Smith, J. Pollanen, S. Higashitani, P.	Torsion pendulum measurements of normal 3He in axially compressed aerogel
13P-A003	A4	A0358	I.A. Fomin and E.V. Surovtsev	Aerogel as a non-ideal gas of impurities in superfluid 3He
13P-A004	A4	A0479	J. I. A. Li, J. Pollanen, C. A. Collett, W. J. Gannon and W. P.	Identification of He-3 Superfluid B-phase Order Parameter Structure in Aerogel
13P-A005	A4	A0713	J. Pollanen, J.I.A. Li, C.A. Collett, W.J. Gannon, W.P. Halperin	Anisotropy Stabilized Equal-Spin Pairing State of He-3 in Radially Compressed Aerogel

13P-A006	A4	A0915	R.Sh. Askhadullin, V.V. Dmitriev, D.A. Krasnikhin, P.N. Martynov, A.A.	NMR Studies of Superfluid 3He in "Ordered" Aerogel
13P-A007	A4	A0925	V.V. Dmitriev, D.A. Krasnikhin, A.A. Senin, A.N. Yudin	NMR properties of 3He-A in biaxially anisotropic aerogel
13P-A008	A4	A0930	R.Sh. Askhadullin, V.V. Dmitriev, D.A. Krasnikhin, P.N. Martynov,	Measurements of Spin Diffusion in Liquid 3He in "Ordered" Aerogel
13P-A009	A4	A1063	Y. Tanaka, R. Kado, S. Feat, R. Toda, R. Ito, M. Kanemoto, O. Ishikawa, and Y.	NMR/MRI Study of Superfluid ${}^3\text{He}$ in Aerogel
13P-A010	A5	A0020	N. Suramishvili, A. Baggaley, Y.A. Sergeev, and C.F. Barenghi	Numerical simulations of the interaction between thermal quasiparticles and a three-dimensional vortex tangle in superfluid ${}^3\text{He}$
13P-A011	A5	A0054	Wei Guo, Sidney B. Cahn, James A. Nikkel, Williams F. Vinen, and Daniel	Flow Visualization in Superfluid 4He Using Metastable Helium Molecules as Tracers
13P-A012	A5	A0062	S.K. Nemirovskii and E.B.S onin	Equilibrium rotation of a vortex bundle terminating on a lateral wall
13P-A013	A5	A0083	I.Gritsenko, V. Chagovets, A. Zadorozhko, and G. Sheshin	Acoustic Radiation Modes of Quartz Tuning Fork in the Ballistic Regime of the Scattering of Thermal Excitations
13P-A014	A5	A0084	Luiza P. Kondaurova	Numerical Study on the Free Decay of Vortex Tangle at Zero Temperature
13P-A015	A5	A0106	G.Sheshin, V. Chagovets, I. Gritsenko, and A. Zadorozhko	The Mechanism of Acoustic Dissipation of an Oscillating Quartz Tuning Fork Immersed in He II
13P-A016	A5	A0109	A. Zadorozhko, V.Chagovets, I. Gritsenko and G. Sheshin	Additional Dissipation Mechanism of the First Sound in the Development of Quantum Turbulence
13P-A017	A5	A0128	P. M. Walmsley, P. A. Tompsett and A. I. Golov	Vortex Interactions in Superfluid 4He in the Zero Temperature Limit
13P-A018	A5	A0141	V.B. Efimov, Deepak Garg, M. Giltrow, P.V.E. McClintock, L.	Quantum turbulence and the free decay of grid oscillations in He-II
13P-A019	A5	A0149	Shevchenko Sergii	Vortices and vortex rings as a source of electrical activity of superfluid systems

13P-A020	A5	A0156	Davide Proment, Carlo F. Barenghi, and Miguel Onorato	Diffusion and ballistic expansion of a two-dimensional quantum vortex bundle
13P-A021	A5	A0169	J. J. Hosio, V.B. Eltsov, R. de Graaf, M. Krusius, J. M?kinen, and D.	Propagation of Quasiparticles in a Cluster of Vortices in Superfluid 3He-B
13P-A022	A5	A0220	M. La Mantia, T.V. Chagovets, M. Rotter, and L. Skrbek	Visualisation of Liquid 4He Flows
13P-A023	A5	A0233	S. Babuin, M. Stammeier, M. Rotter, L. Skrbek	Two Types of Quantum Turbulence: Mechanically versus Thermally Driven 4He Superflow in a Channel
13P-A024	A5	A0248	Deepak Garg, V.B. Efimov, M. Giltrow, P.V.E. McClintock, L. Skrbek and W.F.	Damping of quartz forks in superfluid He-4 in the zero-temperature limit
13P-A025	A5	A0267	E. B. Sonin	Dynamics of twisted vortex bundles and laminar propagation of vortex front
13P-A026	A5	A0285	P.A. Tompsett, P.M. Walmsley and A.I. Golov	Simulations of the Charge Transport by Quantum Turbulence in ${}^4\text{He}$ at $T \rightarrow 0$
13P-A027	A5	A0330	A.N. Ganshin, V.B. Efimov, G.V. Kolmakov, L.P. Mezhov-Deglin, and	Professor
13P-A028	A5	A0349	Pekko Kuopanportti, Jukka A. M. Huhtam?ki and Mikko M?tt?nen	Size and Dynamics of Vortex Dipoles in Dilute Bose-Einstein Condensates
13P-A029	A5	A0389	H. Yano, A. Nishijima, S. Yamamoto, T. Ogawa, Y. Nago, K.	Generation and Detection of Vortex Rings in Superfluid ${}^4\text{He}$ at Very Low Temperature
13P-A030	A5	A0503	S. Yamamoto, M. Tsubota and W. F. Vinen	Time-development of energy spectra in the simulation of quantum turbulence
13P-A031	A5	A0645	V.B. Eltsov, R. de Graaf, J.J. Hosio, P.J. Heikkinen, M. Krusius, R.	Vortex Front in Rotating 3He-B in the Zero-Temperature Limit
13P-A032	A5	A0661	R. Hanninen	Kelvin Spectrum for a Harmonically Driven Vortex at Low Temperatures
13P-A033	A5	A0662	R. Hanninen and N. Hietala	Spin-Down of the Superfluid Component of 3He-B in Different Geometries

13P-A034	A5	A0683	Andrew Forrester and Gary A. Williams	Vortex Loops and the Superfluid Phase Transition in d Dimensions
13P-A035	A5	A0719	Y. Mineda, M. Tsubota, Y. A. Sergeev, C. F. Barenghi, and W. F.	The coupled dynamics of micron-size particles and quantized vortices
13P-A036	A5	A0783	E. Gordon	Catalysis of Impurity Coalescence by Quantized Vortices in Superfluid Helium
13P-A037	A5	A0806	Efimov B.Victor	When does acoustic turbulence begin?
13P-A038	A5	A0913	S. Ishino, H. Takeuchi, M. Tsubota	Vortex nucleation and transition to binary quantum turbulence in two-component Bose--Einstein condensates
13P-A039	A5	A0958	T. Kusumura, M. Tsubota, and H. Takeuchi	Formation of Quantum Turbulence from Dark Solitons in Atomic Bose-Einstein Condensates
13P-A040	A5	A0994	D. E. Zmeev, F. Pakpour, P. M. Walmsley, A. I. Golov, W. Guo, D.	Capture of He2* Molecules by Vortex Lines in Superfluid 4He at T < 0.2 K
13P-A041	A5	A1083	L.V. Abdurakhimov, M.Yu. Brazhnikov, I.A. Remizov, A.A. Levchenko	Capillary Turbulence on the Surface of Quantum Liquids
13P-A042	A5	A1088	S.-W. Su, I.-K. Liu, and S.-C. Gou	Nucleation of 1/3-vortices in a rotating and rapid quenched F=2 spinor Bose-Einstein codensate in the cyclic state
13P-A043	A5	A1094	V. Tsepelin, D.I. Bradley, A.M. Guenault, S.N. Fisher, R.P. Haley,	Power spectrum and higher-order structure functions of quantum turbulence in superfluid 3He-B
13P-A044	A5	A1119	L. Merahi, M.Abidat	Large eddy simulations analysis of coupling force effect on the evolution of energy spectrum in superfluid
13P-A045	A5	A1143	I.A. Remizov, L.V. Abdurakhimov, M.Yu. Brazhnikov, and A.A. Levchenko	Structure functions of capillary wave turbulence on the surface of He-II.
13P-A046	A5	A1333	C. Yuce; Z. Oztas	Berry's Phase for Ultracold Atoms in an Accelerated Optical Lattice
13P-A047	A8	A0965	M. Khademi Dehkordi, M. A. Shahzamanian, M. R. Abolhasani and	The Calculation of Transport Coefficients of Ultra Cold Normal Dipolar Bose Gas

13P-A048	A8	A0980	A.Ohma, T. Matsushita, M. Hieda and N. Wada	Three-Dimensional Superfluid Transition of \$^4\$He Films Formed in 3D Nanopores of HMM-2
13P-A049	A8	A1479	Chang-Qin Wu, Hui-Min Chen, Hui Zhao, and Hai-Qing Lin	Phase Diagram of a Half-filled Two-dimensional Ionic Hubbard Model
13P-A050	A8	A1182	F. de Pasquale and G. L. Giorgi	Quantum phase diffusion of a Bose system: beyond the Hartree-Fock-Bogoliubov approximation
13P-A051	A8	A1278	S.K.Mehdi, N.Daoudi, S.Kessal	The Mean Energy in the Canonical and Grand Canonical Ensemble
13P-A052	A8	A0982	O. Kirichek, T. R. Charlton, C. J. Kinane, R. M. Dagliesh, A.	Neutron transparency measurements in cryogenic \$^3\$He vapour
13P-A053	A8	A0172	E. Zaremba, Z. Wu	Dissipative Dynamics of a Harmonically Confined Bose-Einstein Condensate
13P-A054	A8	A0435	Ambarish Ghosh and Humphrey J. Maris	Optical Properties of Electron Bubbles in the 1P State
13P-A055	A8	A0108	K.A. Nasyedkin and V.E. Syvokon	Influence of Damaging Electric Fields on Melting of the 2D Electron Crystal
13P-A056	A8	A0105	V.E. Syvokon and K.A. Nasyedkin	Comparison of the Non-Linear Phase Transitions in 2D Electron System and 2D Helium Film
13P-A057	A8	A0254	Maika Takita, F.R. Bradbury, S.A. Lyon, Kevin Eng, T.M. Gurrieri, K.J.	Extremely Efficient Clocked Electron Transport on Superfluid Helium
13P-A058	A8	A0046	A.I. Krivchikov, O.A. Korolyuk, I.V. Sharapova, L.C. Pardo, M.D. Ruiz-	Universal behavior of the heat transport properties of molecular glassy crystals
13P-A059	A8	A1368	S. Janecek, E. Krotscheck, M. Liebrecht, R. E. Zillich	Metal Clusters in a Helium Matrix
13P-A060	A8	A0171	K. Nemchenko, S. Rogova	Unusual Resonances in Superfluid \$^4\$He - metal Double-layer System
13P-A061	A8	A1138	I. Taminiau, J. Scherschligt, D. Hussey, D.L. Jacobson, D.G.	\$^3\$He-\$^4\$He liquid mixtures investigated by neutron imaging technique at low temperatures

13P-A062	A8	A1004	R. E. Zillich, G. Guillon, and A. Viel	Rovibrational Excitation and Relaxation of Molecules in ${}^4\text{He}$ Nanodroplets
13P-A063	A8	A1236	L.P. Mezhov-Deglin, V.B. Efimov, G.V. Kolmakov, V.V. Nesvizhevsky	A Tool for Production of Ultra Cold Neutrons in Superfluid He-II
13P-A064	A8	A1017	M. Watanabe and K. Kono	Low Energy Electron Source for Low Temperature
13P-A065	A8	A1406	Andrij Rovenchak and Solomija Buk	Evolution of the Temperature Parameter in Texts
13P-A066	A8	A1473	W. Wei, Z. Xie, G.M. Seidel, H.J. Maris	Studies of Fast Negative Ions in Superfluid Helium
13P-A067	A8	A0474	J. Rysti, J. Tuoriniemi, A. Salmela and A. Sebedash	Melting Pressure of ${}^3\text{He}$-${}^4\text{He}$ Mixtures
13P-A068	A8	A1140	J. Scherschligt, I. Taminiau, D. Hussey, D.L. Jacobson, D.G.	Neutron imaging study of the phase separation of ${}^3\text{He}$-${}^4\text{He}$ liquid mixtures at low temperatures
13P-A069	A8	A0191	F.Ancilotto, M.Barra nco, J.Navarro and M.Pi	Localization of electrons in liquid para-hydrogen from Density Functional calculations
13P-A070	A8	A1453	Andrew N Cleland	Mechanical resonators in the quantum regime
13P-A071	A8	A0347	Souris F, Grucker J, Dupont-Roc J and Jacquier Ph	Observation of metastable hcp solid helium
13P-A072	A8	A1093	MJ Patton, CJ Mellor, AD Armour and JR Owers-Bradley	A Fibre Interferometer for Low Temperature Measurements of High-Stress Silicon Nitride Nano-mechanical Devices
13P-A073	A8	A1137	A. Sokolovsky, N. Gusevik	Hydrodynamics of Superfluid Bose Liquid as Hydrodynamics of One-component System
13P-A074	A8	A1337	E. Baudin, S.W. Morgan, H. Desvaux, P.-J. Nacher and G.	Multiple Spin Echoes and Instabilities in Hyperpolarized ${}^3\text{He}$-${}^4\text{He}$ Solutions
13P-A075	A8	A0028	W. Casteels, J. Tempere and J. T. Devreese	Polaronic Groundstate Properties of an Impurity in a Bose-Einstein Condensate

13P-A076	A8	A0064	S. N. Burmistrov	Energy Dissipation Effects in the Dynamics of a Josephson Junction Between Two Binary Bose-Condensed Mixtures
13P-A077	A8	A0392	S. Park and Y. Kwon	Higher Order Propagators for Path-integral Monte Carlo Study: Application to Quantum Quadrupolar Rotors
13P-A078	A8	A0066	Ye.O. Vekhov , N.P. Mikhin and Yu.A. Freiman	Thermodynamic Grounds for the bcc-hcp Transition in Solid Helium Isotopes
13P-A079	A8	A0363	V.V. Khmelenko, D.H. Hawthorne and D.M. Lee	Spin waves and moving domain walls in dilute spin polarized ${}^3\text{He}$-${}^4\text{He}$ mixtures
13P-A080	A8	A0197	Justin K. Perron and Francis M. Gasparini	Giant Proximity Effect in Superfluid Helium-4
13P-A081	A8	A0082	Hongwei Xiong and Biao Wu	Universal behavior of quantum chaotic gas
13P-A082	A8	A1295	Mucio A. Continentino	Interplay of quantum and classical fluctuations near quantum critical points
13P-A083	A8	A0313	T. Takahashi, R. Nomura, and Y. Okuda	Generation and Annihilation of ${}^4\text{He}$ Negative Crystals
13P-A084	A8	A0314	T. Takahashi, R. Nomura, and Y. Okuda	Equilibrium Shape of ${}^4\text{He}$ crystal under mGE
13P-A085	A8	A0362	V.V. Khmelenko, I.N. Krushinskaya, R.E. Boltnev, I.B. Bykhalo, and D.M.	Spectroscopic studies of impurity-helium condensates containing stabilized N and O atoms
13P-A086	A8	A0112	I.A. Degtyaryov and S.S. Sokolov	The Features of Liquid ${}^3\text{He}$ - ${}^4\text{He}$ Mixture Phase Diagram in Narrow Geometry
13P-A087	A8	A0761	H. Kobayashi, J. Taniguchi, M. Suzuki, K. Miura, and I. Arakawa	Mechanical Response of Noble Gas Films to an Oscillating Substrate
13P-A088	A8	A0144	Yuri Freiman, Serge Tretyak and Balazs Hetenyi	The Pomeranchuk Effect and Broken Symmetry Phase (BSP) Transitions in Solid Hydrogens under Pressure
13P-A089	A8	A0892	Tomoki Minoguchi, Davide E. Galli, Maurizio Rossi and Akira Yoshimori	A non-perturbative approach to freezing of superfluid He-4 in density functional theory

13P-A090	A8	A0881	J. Tuoriniemi, J. Rysti, and A. Salmela	Mode Analysis for an Immersed Quartz Tuning Fork Coupled to Acoustic Resonances of the Medium in a Cylindrical Cavity
13P-A091	A8	A0522	S.Watabe, Y.Kato and Y.Ohashi	Anomalous Tunneling of Spin Wave in Polar State of Spin-1 BEC
13P-A092	A8	A0509	K. Nagai, Y. Nagato and S. Higashitani	Low Temperature Properties of the Mermin-Ho Texture of Superfluid 3He in a Cylinder
13P-A093	A8	A0752	C.Kato, S.Sasamoto, Y.Kimura, K.Obara, H.Yano, O.Ishikawa	Fourth Sound Resonance of Superfluid \$^3\$He in Slab Geometry
13P-A094	A8	A0473	C.A. Collett, J. Pollanen, W.J. Gannon, J.I.A. Li, W.P. Halperin	Moderate Magnetic Field Transverse Acoustics Experiments in Superfluid \$^3\$He-B
13P-A095	A8	A0538	A. Yamaguchi, H. Tanaka, M. Wada, G. Motoyama, A. Sumiyama, Y. Aoki,	Development of a \$^3\$He-hydraulic actuator for spin pump in superfluid \$^3\$He-A\$ \$
13P-A096	A8	A0988	Shokouh Haghdani and M. A. Shahzamanian	Energy of Stable Half-Quantum Vortex in Equal-Spin -Pairing
13P-A097	A8	A1064	J. Hitomi, R. Ito, T. Kakuda, M. Kanemoto, and Y. Sasaki	Quest for Randomly Networked Superfluidity of \$^3\$He in Porous Glass
13P-A098	A8	A1255	Shokouh Haghdani and M. A. Shahzamanian	Spin Diffusion Coefficient of the A Phase of Liquid 3He at Low Temperature and Stable Half Quantum Vortex
13P-A099	A8	A0721	K. Matsumoto, K. Ohmori, S. Abe, K. Kanamori and K. Nakanishi	Ultrasound Propagation in Dense Aerogels Filled with Liquid 4He
13P-A100	A8	A0125	A.S. Rybalko, V.A. Tikhiy, A.S. Neoneta, K.R.Zhekov	Observation of electric response in He II under excitation of second sound waves.
13P-A101	A8	A1289	Fabien Souris, Jules Grucker, Jacques Dupont-Roc and Philippe	Imaging Focused Ultrasound Pulses in Superfluid \$^4\$He
13P-A102	A8	A0767	K. Mikami, T. Kobayashi, J. Taniguchi, M. Suzuki and K.	Anomalous Suppression of Superfluidity for \$^4\$He in Gelsil Glass
13P-A103	A8	A0327	L. Skrbek and V.S. L'vov	Viscosity of Liquid 4He and Quantum of Circulation: Why and How Are They Related?

13P-A104	A8	A0095	A.V. Smorodin, V.A. Nikolaenko, and S.S. Sokolov	Mobility of the surface electron in quasi-zero-dimensional system
13P-A105	A8	A0096	A.V. Smorodin and V.A. Nikolaenko	The analysis of nanoroughnes substrates with use of levitating electron over a superfluid helium film
13P-A106	A8	A0104	V.A. Nikolaenko, A.V. Smorodin, and S.S. Sokolov	Possible Formation of Autolocalized State of Quasi-One-Dimensional Surface Electrons in Dense Helium Vapor
13P-A107	A8	A1149	A. Sokolovsky, N. Bannikova	Dynamics of Condensate as a Subsystem of Superfluid Bose Gas
13P-A108	A8	A0133	K. A. Chishko, T. N. Antsygina, I. I. Poltavsky, M. I. Poltavskaya	Magnetization of \$^3\$He films in ferromagnetic regime: Cluster size effects
13P-A109	A8	A0812	Yuki Endo and Nikuni Tetsuro	Properties of the Trapped Dipolar Ultracold gases at Finite Temperatures
13P-A110	A8	A0853	D. Hufnagl, R. Kaltseis, V. Apaja and R. E. Zillich	Roton-Roton Crossover in Strongly Correlated Dipolar Bose-Einstein Condensates
13P-A111	A8	A0742	K. Obara, Y. Kimura, A. Fukui, C. Kato, Y. Nago, H. Yano, O. Ishikawa,	Anomalous Sound Absorption of Finite Amplitude Sound in Liquid 4He
13P-B001	B6	B0329	L.X. Cao, B. Xu, B.Y. Zhu, Y. Han, W.Y. Li, B.R. Zhao, G.F. Chen, Z.X.	Structural and physical properties of iron chalcogenide thin
13P-B002	B6	B0455	Weiqiang Yu, L. Ma, G. F. Ji, J. Zhang, J. B. He, D. M. Wang, T. -L. Xia, G. F.	NMR Study of Pairing Symmetry and Spin Fluctuations in KyFe2-xSe2 and (Tl,Rb)yFe2-xSe2 Superconductors
13P-B003	B6	B0483	Y. Zhang, L. X. Yang, M. Xu, Z. R. Ye, F. Chen, C. He, H. C. Xu, J. Jiang,	angle-resolved photoemission studies on AxFe2Se2 (A=K, Cs)
13P-B004	B6	B0498	Rong Yu, Pallab Goswami, Jian-Xin Zhu, Predrag Nikolic, and Qimiao	Mott Transition, Magnetism, and Pairing Symmetry of (Tl,K)yFexSe2
13P-B005	B6	B0738	Long Ma, G. Ji, J. Dai, J. B. He, D. M. Wang, G. F. Chen, W. Bao, and	High-temperature NMR Evidence of Pseudogap Opening in Superconducting Ti0.47Rb0.34Fe1.63Se2
13P-B006	B6	B0835	A. M. Zhang, K. Liu, J. H. Xiao, J. B. He, D. M. Wang, G. F. Chen, B. Normand,	Raman scattering study on the new FeSe superconductors

13P-B007	B6	B0855	D.X. Mou, L. Zhao, S.Y. Liu, L. Yu, X.W. Jia, J.F. He, Y.Y. Peng, and Xingjiang	Distinct Fermi Surface Topology and Isotropic Gap Symmetry in $A_xFe_{2-y}Se_2$ Superconductor
13P-B008	B6	B0877	S.-C. Wang, Z.-H. Liu, P. Richard, Y. Li, N. Xu, G.-F. Chen and H. Ding	Orbital character of electron bands in $A_xFe_{2-y}Se_2$
13P-B009	B6	B0968	A. M. Zhang, K. Liu, J. H. Xiao, J. B. He, D. M. Wang, G. F. Chen, B.	Effect of iron content and potassium substitution in $A0.8Fe1.6Se_2$ ($A=Ti, K, Rb$)
13P-B010	B6	B1045	L. Li, Z. R. Yang, Z. T. Zhang, W. Tong, C. J. Zhang, S. Tan, and Y. H. Zhang	Coexistence of superconductivity and magnetism in $K0.8Fe_2Se_1.4S_0.4$
13P-B011	B6	B1082	Yuke Li, Chenyi Shen, Qian Tao, Guanghan Cao, and Zhu'an Xu	Effect of non-magnetic Zn impurity in iron chalcogenide $K0.8Fe_2-dSe_2$
13P-B012	B6	B1254	J.Guo, X.J. Chen and L.L. Sun	Pressure-Driven Quantum Criticality in An Iron-Selenide Superconductor
13P-B013	B6	B1307	R. H. Yuan, T. Dong, G. F. Chen, J. B. He, D. M. Wang, and N. L.	Observation of a small superconducting energy gap in $K0.7Fe_1.8Se_2$ by optical spectroscopy
13P-B014	B6	B1355	Z. G. Chen, R. H. Yuan, T. Dong, G. Xu, Y. G. Shi, P. Zheng, J. L. Luo, J.	Optical study of the new iron selenide $K0.83Fe_1.53Se_2$ single crystals
13P-B015	B6	B1399	Aifeng Wang, Meng Zhang, Jianjun Ying, Yajun Yan, Ronghua Liu,	Transport properties and phase diagram in $K_xFe_2-ySe_2$ superconductors
13P-B016	B7	B0262	J. K. Dong, H. Zhang, X. Qiu, B. Y. Pan, Y. F. Dai, T. Y. Guan, S. Y. Zhou,	Field-induced quantum critical point and nodal superconductivity in the heavy-fermion superconductor Ce_2PdIn_8
13P-B017	B7	B0376	Bin Liu	Local electronic structure around an impurity in superconductor without an inversion center
13P-B018	B7	B0496	K. Oshiba and T. Hotta	Isotope Effect in Rattling-Induced Superconductor
13P-B019	B7	B0570	K. Kumagai, H. Shishido, T. Shibauchi, Y. Matsuda	NMR Study of the FFLO State and Magnetism in $CeCoIn_5$
13P-B020	B7	B0602	D. Maruyama, M. Sigrist and Y. Yanase	Superconductivity without Local Inversion Symmetry: Multi-layer Systems

13P-B021	B7	B0670	Richard A. Klemm, Christopher Loerscher, Jingchuan Zhang	Upper critical field of p-wave ferromagnetic superconductors with orthorhombic symmetry
13P-B022	B7	B0722	W. J. Gannon, W. P. Halperin, J. A. Sauls, K. Schlesinger, M. R.	Small Angle Neutron Scattering and the Vortex Lattice of UPt3
13P-B023	B7	B0732	K. M. Suzuki, Y. Tsutsumi, M. Ichioka, and K. Machida	Field evolution of the FFLO state studied by the microscopic Eilenberger method
13P-B024	B7	B0797	N. Tateiwa, T. D. Matsuda, Y. Onuki, Y. Haga, and Z. Fisk	Scaling relation found in anomalous electrical transport and superconductivity of heavy fermion superconductor URu\$2\$Si\$2\$
13P-B025	B7	B0813	F. Ronning, E.D. Bauer, M. Altarawneh, N. Harrison, J.-X. Zhu,	Anisotropy in the electronic structure of superconducting 115's
13P-B026	B7	B0847	M. Shiotsuki, G. Motoyama, Y. Oda, A. Yamaguchi, A. Sumiyama, T.	Specific Heat Study of the Non-centrosymmetric Superconductor LaPt3Si in Magnetic Fields
13P-B027	B7	B0894	N. Aso, M. Takahashi, H. Yoshizawa, H. Iida, N. Kimura and H.	Neutron Diffraction in the Pressure-Induced Superconducting Antiferromagnet CeIrSi3
13P-B028	B7	B1070	Yi-feng Yang, E. D. Bauer, C. Capan, R. R. Urbano, C. F. Miclea, H. Sakai, F.	Electronic inhomogeneity and pair breaking in heavy fermion superconductors
13P-B029	B7	B1100	R. Ikeda, Y. Hatakeyama, K. Hosoya, and K. Aoyama	Coexistence of antiferromagnetism and d-wave superconductivity induced by paramagnetic pair-breaking
13P-C001	C3	C0051	Keshav N. Shrivastava	Aharonov-Bohm Effect in a Semiconducting Ring With Finite Spin and Angular Momentum
13P-C002	C3	C0052	Keshav N. Shrivastava	Electrons in a Magnetic Field: Special Spin in the de Haas-van Alphen Effect
13P-C003	C3	C0192	Ke-Wei Sun and Qing-Hu Chen	Ground-state behaviors of quantum compass model in an external field
13P-C004	C3	C0196	Nicolae A Enaki	Nonlinear Interaction of Quasi-Particle with Thermostat and the Problem of Second Order Phase Transitions in Cooperative Phenomena
13P-C005	C3	C0251	H. Suzuki, H. Kaneko, Y. Yun, N. Shumsun, A. Savinkov, H. Xing,	Low Temperature X-ray Diffraction Study on Phase Transition

13P-C006	C3	C0260	A. Ralko, F. Trouselet and D. Poilblanc	Quantum Melting of Spin-Ice as a New Route for Supersolidity
13P-C007	C3	C0282	O. Kramar, Yu. Skorenkyy, L. Didukh, and S. Dubyk	Ground-State Ferromagnetism in a model with Anderson-Hubbard centers
13P-C008	C3	C0321	L.A. Sibley, E. Pugh, G.G. Lonzarich, N. Kimura, S.	High Pressure Measurements on the Itinerant Ferromagnet ZrZn₂
13P-C009	C3	C0342	A. Schilling and H. Grundmann	Josephson E
13P-C010	C3	C0343	Dan Huvonen, Shuangyi Zhao, Erik Wulf, Tatiana Yankova, Vasily	Experimental Observations of Magnetic Bose Glass
13P-C011	C3	C0379	Yuki Nakano, Takumi Ishima, Naohiro Kobayashi, Kazuhiko	Phase Structure of the t-J Model of Hard-Core Bosons in Three-Dimensions at Finite Temperatures
13P-C012	C3	C0469	S. Kettemann, E. Mucciolo, K. Slevin	Multifractal Quantum Spin Phases at Kondo-Anderson Transitions
13P-C013	C3	C0476	D. Tayurskii, N. Beysengulov	Non-extensive thermodynamics for the Ginzburg-Landau theory of phase transitions in the strong-correlated systems
13P-C014	C3	C0504	T. Kaneko, T. Toriyama, T. Konishi, and Y. Ohta	Electronic structure of Ta₂NiSe₅ as a candidate for excitonic insulators
13P-C015	C3	C0529	T. Sakai, M. Sato, K. Okunishi, K. Okamoto and C. Itoi	Exotic Quantum Phase Transitions in the Spin Nanotubes
13P-C016	C3	C0549	Yu-Ren Lai, Da-Wei Wang, Juhn-Jong Lin	Two-impurity Kondo Effect in Al/AIO_x/Y Tunnel
13P-C017	C3	C0581	A. Langari, M. Kargarian, R. Jafari and A. T. Rezakhani	Renormalization of quantum information measures: an approach to quantum criticality
13P-C018	C3	C0647	E. M. Alakshin, Yu. M. Bunkov, R.R. Gazizulin, A. V. Klochkov, V. V.	Atomic type magnon Bose-Einstein condensation in antiferromagnet.
13P-C019	C3	C0697	T. Jinno, S. Aoyama, Y. Shimizu, M. Itoh, Y. Ueda	\$3d\$ Electron Quadrupole Moments in Vanadium Oxides

13P-C020	C3	C0740	Zhi Li, John S. Tse and Toshiaki Iitaka	Spin Density Wave in Chromium under High Pressure
13P-C021	C3	C0754	H. Yoshioka	Collapse of Charge Ordering Due to Disorder in Quasi One-Dimensional Electron Systems
13P-C022	C3	C0781	H. Okabe, N. Takeshita, M. Isobe, E. Takayama-Muromachi, T.	Transport properties in spin-orbit Mott insulator Ba₂IrO₄ under high pressure
13P-C023	C3	C0786	H. Okabe, M. Isobe, E. Takayama-Muromachi, A. Koda, S. Takeshita,	Magnetic ordering in spin-orbit Mott insulator Ba₂IrO₄ probed by mSR
13P-C024	C3	C0831	V. Glushkov, A. Bogach, A. Kuznetsov, I. Sannikov, M.	Magnetic phase separation in Eu_{1-x}Ca_xB₆
13P-C025	C3	C0860	S. Hayami, M. Udagawa, and Y. Motome	Partial Disorder in the Periodic Anderson model on a triangular lattice
13P-C026	C3	C0863	S. Hayami, M. Udagawa and Y. Motome	Partial Disorder in the periodic Anderson Model on a Triangular Lattice
13P-C027	C3	C0879	T. Shirakawa, H. Watanabe, and S. Yunoki	Theoretical study of J_{eff}=1/2 Mott insulator in Ir oxides: cooperation of a strong spin-orbit coupling and local electron correlations
13P-C028	C3	C0926	S. Abe, F. Sasaki, T. Oonishi, D. Inoue, and K. Matsumoto	High Sensitive Capacitive Dilatometer for Investigation of Quantum Critical Phenomena near Absolute Zero
13P-C029	C3	C0995	S. Nakamura, K. Matsui, T. Matsui, and Hiroshi Fukuyama	New Heat-Capacity Measurements of the Possible Order-Disorder Transition in the 4/7-phase of 2D Helium
13P-C030	C3	C1186	Y. Mori, Y. Nishio, K. Kajita, S. Aonuma, and R. Kato	Deuterium degrees of Freedom of Selectively deuterated (DMe-DCNQI)₂Cu Systems
13P-C031	C3	C1187	T. Tanaka, A. Sugawara, N. Tajima, K. Kajita, R. Kato and Y. Nishio	Novel phase transition in spin frustrated Et₂Me₂Sb[Pd(dmit)₂]₂ System
13P-C032	C3	C1190	B. Lake, S. Notbohm, D.A. Tennant, T.G. Perring, P. Ribeiro,	Neutron scattering Studies of Spin-Ladders
13P-C033	C3	C1206	L.H. Greene, W.K. Park, P.H. Tobash, F. Ronning, E.D. Bauer, J.L. Sarrao,	Measurement of the Fano resonance and hybridization gap in URu₂Si₂ with point-contact spectroscopy

13P-C034	C3	C1218	T. Cichorek, L. Bochenek, A. Czulucki, M. Schmidt, G.	Quantum impurities and resultant two-channel Kondo problem in ZrAs_{1.58}Se_{0.39}
13P-C035	C3	C1231	Cui Jian, Jun-Peng Cao, Heng Fan	Quantum Phases and Entanglement Renyi Entropy
13P-C036	C3	C1238	Ninghua Tong and Yanhua Hou	Scaling Analysis in the Numerical Renormalization Group Study of the Sub-Ohmic Spin-Boson Model
13P-C037	C3	C1323	Jihong Qin, Xiaoling Jian and Qiang Gu	Ferromagnetic Phase Transition in Charged Spin-1 Bose Gases
13P-C038	C3	C1339	D. Sun, W. Wu, A. McCollam, S. A. Grigera, R. S. Perry, A. P. Mackenzie,	Investigations of Quantum Critical Metamagnetism in Sr₃Ru₂O₇ with Hydrostatic Pressure
13P-C039	C3	C1379	D.L. Quintero-Castro, B. Lake, E.M. Wheeler, A.T.M.N. Islam, T.	Magnetic excitations of the quantum dimer antiferromagnet Sr₃Cr₂O₈
13P-C040	C3	C1385	S. E. Rowley, G. G. Lonzarich, and S. S. Saxena	Attractive interactions between critical fluctuation modes near ferroelectric and ferromagnetic quantum phase transitions
13P-C041	C3	C1402	S. Haines, S. Saxena	Pressure Tuned Magnetic Quantum Phase Transitions
13P-C042	C3	C1455	B. Normand, P. Merchant, Ch. Ruegg, K. W. Kramer, M. Boehm,	Following elementary excitations to finite temperatures at the pressure-induced quantum phase transition in TiCuCl₃
13P-C043	C5	C0057	R. Konno	Pressure Effects on Ferromagnetic Superconductors
13P-C044	C5	C0070	P. Schlottmann	Lifshitz Transition with Interactions in High Magnetic Fields: Application to CeIn₃
13P-C045	C5	C0308	K. Yano, K. Nishimura, Y. Isikawa, T. Ito and K. Sato	Collapse-Like Decrease of RKKY Interaction and Kondo Effect in Heavy Fermion Compounds (Ce_{1-x}Gd_x)Ni_(0.03 < x < 0.20)
13P-C046	C5	C0325	V.V. Marchenkov, N.V. Mushnikov, T.V. Kuznetsova, E.G. Gerasimov,	Electrical and magnetic properties as well as crystal and electronic structure of non-stoichiometric DyNi₂Mn_x compounds
13P-C047	C5	C0353	J. R. Wensley, E. Pugh, G. G. Lonzarich	High Pressure Resistivity Measurements on the Heavy Fermion System CeAl₂

13P-C048	C5	C0401	A. Kowalczyk, M. Falkowski, and T. Tolinski	Transport properties of La_{1-x}Ce_xCu₄Al alloys
13P-C049	C5	C0431	T. Inagaki, M. Matsumura, M. Mizoo, Y. Kawamura, H. Kato	Co-NQR Study on Successive Magnetic Phase under Pressure in Non-centrosymmetric CeCoGe₃
13P-C050	C5	C0471	Marc Scheffler, Julia P. Ostertag, Katrin Steinberg, Martin Dressel, and	Drude response of slow and fast electrons in heavy-fermion compound UNi₂Al₃
13P-C051	C5	C0510	A. Yamada, K. Seki, R. Eder and Y. Ohta	Mott transition in the Hubbard model on the anisotropic kagome lattice: Variational cluster approach
13P-C052	C5	C0550	N. Sluchanko, A. Azarevich, A. Bogach, V. Glushkov, S.	Vibrational and AF-instabilities and metal-insulator transition in Tm_{1-x}Y_xB₁₂
13P-C053	C5	C0616	D. Kaczorowski, A. Lipatov, A. Gribanov, and Yu. Seropgin	Novel ferromagnetic Kondo lattices Ce₃RhSi₃ and Ce₃IrSi₃
13P-C054	C5	C0760	K. Higuchi and M. Higuchi	A proposal of the kinetic energy functional for the pair density functional theory
13P-C055	C5	C0785	Y. Sato, Y. Nakamura, H. Morodomi, N. Hasuo, Y. Inagaki,	Susceptibility measurements in Pr_xLa_{1-x}InAg₂ with Γ doublet ground state
13P-C056	C5	C0792	T. Maehira and Y. Tatetsu	Electronic structures of Plutonium compounds with the NaCl-type monochalcogenides structure
13P-C057	C5	C0805	Y. Tatetsu and T. Maehira	Electronic property of ThSn₃ in comparison with uranium and transuranium compounds
13P-C058	C5	C0811	T. Yamashita, T. Shiraishi, K. Matsubayashi, Y. Uwatoko and S.	Pressure Effects on Electrical Resistivity of Heavy-Fermion Antiferromagnet Ce₂PdGa₁₂
13P-C059	C5	C0830	T. Yamashita and S. Ohara	Non-Fermi Liquid Behavior on Heavy-Fermion System Ce₂Pt₆Ga₁₅
13P-C060	C5	C0891	V.A. Ivanshin, E. Gataullin, A. Sukhanov	Low Temperature Electron Spin Resonance Of Dense Intermetallics
13P-C061	C5	C0896	M. Hikasa, Y. Kawamura, T. Nishioka, H. Kato, M. Matsumura, T.	Co substitution effect of Kondo semiconductor CeFe₂Al₁₀

13P-C062	C5	C0979	Y. Oogane, Y. Kawamura, T. Nishioka, H. Kato, M. Matsumura, Y.	Equal volume dilution effect of CeRu₂A10
13P-C063	C5	C1038	A.Bogach, N.Sluchanko, V.Glushkov, S.Demishev,	Magnetization of Tm_{1-x}YbxB₁₂ in pulsed and steady magnetic fields
13P-C064	C5	C1110	A.N. Tarasov	Phase Transitions of Dense Neutron Matter with Generalized Skyrme Interaction to Superfluid States with Triplet Pairing in Strong
13P-C065	C5	C1112	Gertrud Zwicknagl	Ground states, quantum phase transitions and electron spectroscopies in 5f-systems
13P-C066	C5	C1114	A.N. Tarasov	Dense Superfluid Neutron Matter with Generalized Skyrme Interaction and Spin-Triplet Pairing without Ferromagnetic
13P-C067	C5	C1245	A. M. Strydom	Low-temperature physical properties of heavy-fermion CeRh₂Sn₂
13P-D001	D2	D0211	Chao Zheng, Liang Hao, Gui-Lu Long	Observation of Fast Evolution in PT-Symmetry System
13P-D002	D2	D0250	P.-Q. Jin, M. Marthaler, A. Shnirman, and G. Schoen	Probing the Nuclear Spin Environment in a Quantum Dot-Resonator System
13P-D003	D2	D0716	Ya Wang, Xing Rong, Pengbo Feng, Wanjie Xu, Bo Chong, Ji-Hu	Preservation of Bipartite Pseudoentanglement in Solids Using Dynamical Decoupling
13P-D004	D2	D1179	J. Kushihara, R. Okuyama, and M. Eto	Coherent and Incoherent Current Drag in Coupled Quantum Dots
13P-D005	D2	D1380	S. Tarucha	Spin Qubits and Qubit Gates with Quantum Dots
13P-D006	D3	D0040	M.Yu. Kagan, K.I. Kugel and V.V. Val'kov	Mesoscopic transport phenomena and nanoscale phase separation in strongly correlated electron systems
13P-D007	D3	D0047	T. Takami, K. Tsuchihashi, R. Kawano, and J.-G. Cheng	Parallel resistor induced by the spin-state crossover
13P-D008	D3	D0099	K. K. Choudhary, Namit Gupta, N. Kaurav and Sumant Katiyal	Quantitative analysis of Spin hall effect in nanostructures

13P-D009	D3	D0148	V.V. Marchenkov, K.A. Fomina, R. Wang, C.P. Yang, E.I. Shreder, E.B.	Effect of thermobaric treatment and severe plastic deformation on the structural and electronic properties of X-Y-Z Heusler alloys (X
13P-D010	D3	D0236	S.A.Obukhov	A New Type of Low Temperature Conductivity in Semiconductors
13P-D011	D3	D0258	M. A. Anisimov, A. V. Bogach, V. V. Glushkov, S. V. Demishev, N. A.	Magnetoresistance of PrB {6} and GdB {6}
13P-D012	D3	D0287	S. W. Kim, Y. Hashimoto, Y. Iye, S. Katsumoto	Novel blockade due to spin-filtering with spin-orbit interaction
13P-D013	D3	D0334	Yusuke Kato, Shohei Watabe and Yoji Ohashi	Anomalous Tunneling of Spin Wave in Heisenberg Ferromagnet
13P-D014	D3	D0390	H.Ma, C.Y.Jiang, J.L.Yu, Y.Liu, Y.H.Chen	Experimental Observation of Temperature Dependence of Circular Photogalvanic Effect in GaAs/Al0.3Ga0.7As Heterostructures
13P-D015	D3	D0521	H. Kobori, A. Hoshino, A. Yamasaki, A. Sugimura, T.	Magneto-Resistance Enhancement due to Self-Hole-Doping in LaMnO₃ produced by Low Temperature Heat Treatment
13P-D016	D3	D0598	T. Yokoyama and M. Eto	Two-Terminal Spin Filter Using Quantum Dot with Spin-Orbit Interaction in Magnetic Field
13P-D017	D3	D0640	A. Yazdania, N. Kamali Sarvestania*	How can SDW change the unstable F.M to stable AF.M in Gd-IMC
13P-D018	D3	D0660	E. Tuuli and K. Gloos	Spin polarization versus lifetime effects at point contacts between superconducting niobium and normal metals
13P-D019	D3	D0688	L.Yu. Tryputen, V.V. Fisun, O.P. Balkashin, Yu.G. Naidyuk, I.K.	Surface Spin-Valve with an Exchange Bias
13P-D020	D3	D0823	F. M. Qu, F. Yang, J. Chen, J. Shen, Y. Ding, J. B. Lu, Y. J. Song, H. X. Yang,	Aharonov-Casher Effect in Bi₂Se₃ Square-ring Interferometers
13P-D021	D3	D0849	H. Kobori, K. Morii, A. Yamasaki, A. Sugimura, T. Taniguchi, T. Horie,	Intensified Magneto-Resistance by Rapid Thermal Annealing in Magnetite (Fe₃O₄) Thin Film on SiO₂ Glass Substrate
13P-D022	D3	D0899	K.A. Shaykhutdinov, S.I. Popkov, S.V. Semenov, D.A. Balaev, A.A.	Low-Temperature Resistance and Magnetoresistance Hysteresis in Polycrystalline (La_{0.5}Eu_{0.5})_{0.7}Pb_{0.3}MnO₃

13P-D023	D3	D0927	N. Taniguchi and T. Nemoto	Spin current manipulation through a Rashba dot by tunable nonequilibrium Fano-Kondo effect
13P-D024	D3	D0933	Ryota Kawai, Hidekatsu Suzuura and Yuh Tomio	Spatial Distribution of Electronic Spins in a Quasi-One-Dimensional Tight-Binding Model with Spin-Dependent Hopping
13P-D025	D3	D1096	M. Urdampilleta, J.-P. Cleuziou, S. Klyatskaya, M. Ruben, W.	Supramolecular spin valve based on terbium nanomagnets and carbon nanotube
13P-D026	D3	D1275	M. Larsson and H. Q. Xu	Gate-induced zero-filament
13P-D027	D3	D1457	H. T. Yuan, K. Morimoto, S. Bahramy, H. Shimotani, R. Arita,	Tunable Rashba Spin Splitting with Liquid Gated Transistors
13P-E001	E3	E0328	L. Grönberg, P. Helistö, A. Luukanen, H. Seppä and J.	Suspended tunnel junction bolometers for THz imaging
13P-E002	E3	E0437	K. Thirunavukkuarasu, M. Langenbach, A. Janssen, H.	Coherent broadband THz spectroscopy in high magnetic fields and low temperatures: a fiber-based setup using photomixers
13P-E003	E3	E0472	Marc Scheffler, Christian Fella and Martin Dressel	Stripline-based resonant microwave spectroscopy at cryogenic temperatures
13P-E004	E3	E1069	Yuta Omukai, Tomonari Kawasaki, Itsuhiro Kakeya, and Minoru	Terahertz Radiation from Bi₂Sr₂CaCu₂O_{8+delta} Intrinsic Josephson Junctions above Critical Current
13P-E005	E3	E1326	Yoshihiko Nonomura	THz wave emission from intrinsic Josephson junctions controlled by surface impedance and in-plane magnetic field: Numerical study
13P-E006	E7	E0122	T. Kawahara, H. Watanabe, M. Emoto, M. Hamabe, S. Yamaguchi, Y.	Current dependence of heat leak on the terminals in the superconducting DC transmission and distribution system of
13P-E007	E7	E1194	K. Matsui, S. Nakamura, T. Matsui, and Hiroshi Fukuyama	Millikelvin LEED apparatus: a feasibility study
13P-E008	E7	E0577	H. Agrawal, F.J. Brown, J.W. Burgoyne, M. Cuthbert, G.	Integrating complex magnets with the cryogen free dilution refrigerator
13P-E009	E7	E1154	J. Zhang	Cryogenic Dark Matter Search Status and Plans

13P-E010	E7	E1217	J. Chen	<u>Prof.</u>
13P-E011	E7	E1228	J. Chen, L. B. Zhang, Q. Y. Zhao, L. Kang, B. B. Jin, W. W. Xu and P. H.	<u>erformance of Superconducting Nanowire Single Photon</u>
13P-E012	E7	E1338	K. Safiullin, E. Baudin, P.-J. Nacher and G. Tastevin	<u>An Active Feedback Scheme for Improved Low Field NMR Detection</u>
13P-E013	E7	E1196	K V Srinivasan	<u>Cryogens production and distribution at TIFR, Mumbai, INDIA</u>

Monday Aug.15

Time Slot	Category	ABSN	Name	Title
Half Plenary Session(15H1)				
12H1-1		A1229	Yuichi Okuda	Surface Andreev Bound State of Superfluid ^3He and Majorana Fermion
12H1-2		A1132	William Halperin	Stability of Impurity Phases of Superfluid ^3He
12H1-3		E1305	Kurt Uhlig	Cryogen-free Dilution Refrigerators
Half Plenary Session(15H2)				
12H2-1		D1442	Joseph Stroscio	Scanning Tunneling Spectroscopy of Dirac Fermions at mK Temperatures
12H2-2			Pengcheng Dai	
12H2-3			Ali Yazdani	
Parallel Session(15m-A) Low Dimensional Systems				
15m-A1		A1458	Hiroshi Fukuyama	Frustrated Nuclear Magnetism of 2D Helium Three
15m-A2		A0228	Luciano Reatto	Novel substrates for Helium adsorption: Graphane and Graphene-Fluoride
15m-A3		A0633	Jan Nyeki	Anomalous "Superfluid" Response with Quantum Criticality of Two-Dimensional ^4He
15m-A4		A1381	E. Krotscheck	Bose and Fermi gases with Lennard-Jones interactions
15m-A5		A1020	M. Hieda	\$^3\text{He}\$ Effect on 2D Superfluidity in \$^3\text{He}\$-\$^4\text{He}\$ Mixture Films on Planar
Parallel Session(15m-B) Theory for Superconductivity (Mottness or mostly Cuprates)				
15m-B1		B0391	Jan Zaanen	Fermionic Quantum criticality and the AdS/CFT correspondence of string theory
15m-B2		B1266	Philip Phillips	Mottness and Holography
15m-B3			Z. Y. Weng	
15m-B4		B0272	Shi-Ping Feng	Doping and Magnetic Field Dependence of Superfluid Density in Cuprate
15m-B5		B0300	P. A. Marchetti	Non-BCS Superconductivity in Cuprates from Attraction of Spin Vortices
Parallel Session(15m-C) Topological Order				
15m-C1			Z. Hasan	Topological Surface States in Topological Insulators and Superconductors : Discovery
15m-C2		D1481	N.P. Ong	Transport experiments on topological insulators
15m-C3		D1411	K. Behnia	Nernst effect in Bismuth and graphite beyond the quantum limit
15m-C4		C0132	C. Franz	Magnetoresistance and Hall Effect in Single-Crystals $\text{Mn}_{1-x}\text{Fe}_x\text{Si}$ and $\text{Mn}_{1-x}\text{Co}_x\text{Si}$

15m-C5		C0175	Xiao-Gang Wen	Complete classification of 1D gapped quantum phases
--------	--	-------	---------------	---

Parallel Session(15m-D) Nanowires / Nanotubes

15m-D1			Gleb Finkelstein	
15m-D2		D1464	Juhn-Jong Lin	Time-dependent universal conductance fluctuations in metal oxide nanowires due to
15m-D3		D0448	Christophe Blanc	Blocking the phonon thermal transport at the nanoscale
15m-D4		D1079	Hongqi Xu	Spin States, Spin Correlations, Supercurrent, and Multiple Andreev Reflections in InSb
15m-D5		D0554	John Owers-Bradley	Non-linear Mode Coupling in Silicon Nitride Beams

Parallel Session(15m-E) Refrigeration

15m-E1		E0556	Simon C. J. Kingsley	Review of Recently Supplied Oxford Instruments UHV/ULT Cryostats
15m-E2		E0603	I. J. Maasilta	Heat Transport in Suspended Membranes and Phononic Crystals at sub- Kelvin
15m-E3		E1490	Chao Wang	Liquid helium solutions with 4 K pulse tube cryocoolers
15m-E4			Martin Davies	
15m-E5				

Parallel Session(15a-A) Electrons on Helium

15m-A1		A0802	Denis Konstantinov	Vanishing conductance states of microwave-excited electrons on a liquid helium surface
15m-A2		A0672	I.A. Todoshchenko	Anisotropy of c-facet of hcp solid 4He
15m-A3		A0782	Masaru Suzuki	Mechanical Response of 4He Films Adsorbed on Single-crystalline Graphite
15m-A4		A0876	Erkki Thuneberg	Pendulum in a Fermi liquid
15m-A5		E1101	A.J. Casey	SQUID Detection of Gold Nanomechanical Resonators

Parallel Session(15a-B) Physical Properties of Fe-based and Cuprate Superconductors II

15a-B1		B1213	Alexander Boris	Complementary Thermodynamic and Optical Studies of Superconductivity - Induced
15a-B2		B0203	T. Terashima	Fermi Surface Studies of Iron-Pnictide Superconductors: BaFe₂As₂ vs. KFe₂As₂
15a-B3		B1424	Igor Zaliznyak	Unconventional temperature-enhanced magnetism in Fe_{1.1}Te
15a-B4		B1425	Guo-Qing Zheng	Spin-orbit coupling, anisotropic magnetic fluctuations and nodeless gap in iron-
15a-B5		B1246	Takashi Imai	NMR investigation of iron-based high T_c superconductors

Parallel Session(15a-C) Multiferroics / Ferroics

15a-C1		C0305	Tsuyoshi Kimura	Magnetism and magnetoelectricity of hexaferrite systems
15a-C2		C1423	Maxim Mostovoy	Dynamical magnetoelectric effects in non-collinear magnets
15a-C3		C0766	Junmin Liu	Spiral spin order induced ferroelectricity in various type-II multiferroics
15a-C4			Premala Chandra	
15a-C5		C0234	B. Lorenz	Giant Magnetoelectric Effect in HoAl₃(BO₃)₄ at Low Temperatures

Parallel Session(15a-D) Topological Insulators

15a-D1		D1415	Zhong Fang	Topological Insulators: non-magnetic vs. magnetic
15a-D2		D1015	Hsueh-Ju Chen	Ultrafast dynamics in Cu_xBi₂Se₃ and Bi₂Se₂ single crystals
15a-D3		D0885	Yingkai Huang	ARPES and STM/S Studies of Cu-doped Bi₂Te₃ and Bi₂Se₃ Based Topological
15a-D4		D0969	Yang Fan	Superconducting Proximity Effect and Conductance Anomalies in Sn-Bi₂Se₃

Parallel Session(15a-E) Sensors

15a-E1		E1435	Masataka Ohkubo	Breakthrough by superconducting particle detector in mass spectrometry
15a-E2		E1223	Andreas Fleischmann	Magnetic Johnson-noise thermometry at milli-Kelvin temperatures and below
15a-E3		E0723	T. Hata	Development of Dry Dilution Refrigerator and Temperature measurement with Quartz
15a-E4		E0777	J. P. Pekola	Real-time observation of discrete Andreev tunneling events - influence on a single-
15a-E5		E1102	M. Rosticher	Detection of Single Electrons or Photons using a Superconducting Nanowire

Poster Session

15P-A001	A6	A0044	M. Ashari, D. Rees, K. Kono, P. Leiderer	Measurements and investigations on Helium-FET
15P-A002	A6	A0049	Yu Ji	NMR Study of HD Adsorbed in a A-type Metal-Organic Framework
15P-A003	A6	A0073	Andrij Rovenchak	Polychronakos fractional statistics with a complex-valued parameter
15P-A004	A6	A0134	T. N. Antsygina, M. I. Poltavskaya, I. I. Poltavsky, K. A. Chishko	Ground-state properties of 2D hard-core bosons in superfluid phase within second-order spin wave theory
15P-A005	A6	A0160	Chalyy Kyrylo	Semi-Phenomenological Approach to C onfined Helium Heat Capacity in Mesopores

15P-A006	A6	A0255	Milton W. Cole, Silvina M. Gatica, Hye-Young Kim and Angela D. Lueking	Gas Adsorption in Novel Environments, Including Effects of Pore Relaxation
15P-A007	A6	A0281	Hyeondeok Shin	Commensurate-Incommensurate Transition in ${}^4\text{He}$ Monolayer Adsorbed on a C₆₀ Fullerene
15P-A008	A6	A0475	D.A. Tayurskii, Y.V. Lysogorskiy	Superfluid Hydrodynamic in Fractal Dimension Space
15P-A009	A6	A0508	K. Seki, S. Yamaki, T. Kaneko, R. Eder and Y. Ohta	A BCS-BEC crossover in the extended Falicov-Kimball model: Variational cluster approach
15P-A010	A6	A0571	M. C. Gordillo, J. Boronat	Phase transitions of H₂ adsorbed on the surface of single carbon nanotubes
15P-A011	A6	A0682	Emin Menacheonian and Gary Williams	Third Sound in Superfluid ${}^4\text{He}$ Films Adsorbed on Packed Multiwall Carbon Nanotubes
15P-A012	A6	A0684	Dragos Victor Anghel	Universality of heat and entropy transport in 1D channels at arbitrary temperatures
15P-A013	A6	A0771	J. Taniguchi and M. Suzuki	Phonon excitation for ${}^4\text{He}$ confined in nanometer-size uniform channel under pressure
15P-A014	A6	A0819	S. Murakawa, Y. Chikazawa, T. Tanaka, R. Higashino, K. Yoshimura, K.	Tortional oscillator measurements for superfluidity of ${}^4\text{He}$ confined in a porous Alumina nanopore array
15P-A015	A6	A0826	S. Murakawa, M. Wasai, K. Akiyama, R. Nomura and Y. Okuda	Suppression of KT transition in ${}^4\text{He}$ film under high pressure ${}^3\text{He}$
15P-A016	A6	A0846	Soomin Shim	${}^4\text{He}$ Adsorption on H₂-preplated C₂₀
15P-A017	A6	A0916	M. Morishita	Solidification of Second Atomic Layer of ${}^4\text{He}$ Film Adsorbed on Graphite
15P-A018	A6	A0918	B. Yager, J. Ny'eki, A. Casey, B.P. Cowan, C.P. Lusher, J. Saunders, D. Drung, T.	DC SQUID NMR Study of Very Dilute ${}^3\text{He}$-${}^4\text{He}$ Mixture Films in Nanopores
15P-A019	A6	A0936	Y. Nakashima, T. Matsushita, M. Hieda, and N. Wada	Phase Diagram of 4He Adsorbed in 1D 2.4 nm Nanopores of FSM

15P-A020	A6	A1029	T. Matsushita, Y. Nakanishi, Y. Nakashima, Y. Minato, M. Hieda, and N.	Possible Finite-Length 1D Superfluidity of ${}^4\text{He}$ Adsorbed in Nanochannels
15P-A021	A6	A1111	M.Savard, G.Dauphinais, G.Gervais	Superfluid Flow and Critical Velocity of Liquid Helium in a Single Nanohole
15P-A022	A6	A1180	D. Sato, K. Naruse, T. Matsui and Hiroshi Fukuyama	Spin-spin Relaxation Time Measurements of 2D ${}^3\text{He}$ on Graphite
15P-A023	A6	A1249	E. Van Cleve, F. Huisman, A. Velasco and P. Taborek	Helium Adsorption and Superfluidity on Lithium and Sodium
15P-A024	A6	A1277	D. Hirashima, A. Kotani and K. Yamashita	Superfluid density in quasi-one dimensional systems
15P-A025	A6	A1315	Xiaolong Deng and Luis Santos	Entanglement spectrum of one-dimensional extended Bose-Hubbard model
15P-A026	A6	A1352	T. Tanaka, S. Murakawa, Y. Chikazawa, Y. Shibayama, K.	Superfluidity of 4He confined in a nanopore array probed by a vibrating wire
15P-A027	A6	A1367	Y. Negishi, Y Iwata, N. Yamanaka, S. Murakawa, Y. Shibayama, and K.	Ultrasound Measurement of Confined 4He near the Quantum Critical Point
15P-A028	A6	A1487	Fei Zhou	What can we learn about near-resonance quantum gases from 2- and 3-atom problems
15P-A029	A6	A1495	M. Hieda, T. Oda, T. Matsushita, and N. Wada	QCM Study on 2D Vortex in Superfluid 4He and 3He-4He Mixture Films
15P-B001	B8	B0068	Z. B. Huang, H. Q. Lin, and E. Arrigoni	Enhancement of d-wave superconducting correlations in the three-band Hubbard model coupled to apical oxygen phonons
15P-B002	B8	B0089	LI Ping-Lin	Superconducting Microcosmic Theory of high-T_c cuprates (I)
15P-B003	B8	B0092	LI Ping-Lin	Superconducting Microcosmic Theory of high-T_c cuprates (II)
15P-B004	B8	B0137	Cesar G. Galvan, Luis A. Perez and Chumin Wang	Bogoliubov-de Gennes analysis of d-wave superconductors through an ARPES-parameterized Hubbard model

15P-B005	B8	B0164	Y. F. Zhang , M. Izumi, Y. J. Li , T. Gao, Y. S. Liu, Y. Xu, P. L. Li	Microstructure and superconducting properties in $\text{GdBa}_2\text{Cu}_3\text{O}_7-\delta$bulk with additives of nano particles
15P-B006	B8	B0167	Partha Goswami	INVESTIGATION OF THE BCS GAP EQUATION FOR d +i d CUPRATE SUPERCONDUCTORS
15P-B007	B8	B0181	Zhihao Geng, Shiping Feng	Electronic Raman response in electron-doped cuprate superconductors
15P-B008	B8	B0195	A.S. Moskvin and A.V. Korolev	Charge transfer instability and phase diagram of a model doped cuprate
15P-B009	B8	B0238	G. Seibold, M. Grilli, and J. Lorenzana	Influence of correlations on transitive electron-phonon couplings in cuprate superconductors
15P-B010	B8	B0275	A. Kulikovskiy, V. Miliaev, and H. Bielska-Lewandowska	Phase Slippage and Josephson Phenomena in Wide Superconducting Films
15P-B011	B8	B0288	Zheyu Huang and Shiping Feng	Doping Dependence of Electromagnetic Response in Electron-Doped Cuprate
15P-B012	B8	B0290	Huai-song Zhao, Zhi Wang and Shi-ping Feng	Quasiparticle Scattering Interference in Electron-Doped Cuprate Superconductors
15P-B013	B8	B0310	K. Miyagawa, Y. Shimizu, F. Kagawa, H. Ooike, H. Taniguchi, K. Kanoda	Superconductivity and pseudogap behavior in organic Mott systems, k-(BEDT-TTF)2X with triangular lattice
15P-B014	B8	B0421	Y. Oka, R. Abe, H. Nobukane, N. Matsunaga, K. Nomura, K. Ichimura	STM Spectroscopy on deuterated \kappa-\rm(BEDT)-\rm(TTF)-\rm{d[n.n]} \{2\}\rm{Cu[N(CN)} \{2\}\rm{Br}
15P-B015	B8	B0533	F. Chen, B. Zhou, Y. Zhang, J. Wei, H. W. Ou, J. F. Zhao, C. He, Q. Q. Ge, M. Arita, K.	Electronic structure of FeTe_{1-x}Se_x
15P-B016	B8	B0652	N. Sluchanko, S. Gavrilkin, K. Mitzin, A. Kuznetsov, I. Sannikov, V.	Superconductivity in ZrB₁₂ with various boron isotope content
15P-B017	B8	B0696	A. Kamlapure, M. Mondal, M. Chand, G. Saraswat, S. Kumar, J. Jesudasan, L.	Observation of Pseudogap state in disordered NbN using scanning tunneling spectroscopy.
15P-B018	B8	B0731	F. Yuan, Z. Huang, X. Wan and Y. Liang	Local Density of States Around Magnetic Impurity in Cuprate

15P-B019	B8	B0733	X. Wan, F. Yuan and Y. Liang	Inhomogeneous d-wave Superconducting State of The Doped Cuprate Superconductors
15P-B020	B8	B0763	H. Sakakibara, H. Usui, K. Kuroki, R. Arita and H. Aoki	Two-orbital view on the origin of the material dependence of T_c in the single-layer cuprates
15P-B021	B8	B0764	T.Kakeshita, H.Fujisaki, N.Kanaya, L.Liu, S.Uchida	Investigation of a Proposed QCP in Overdoped Region at ~ 0.23 in $\text{La}_{2-x-y}\text{Nd}_y\text{Sr}_x\text{CuO}_4$
15P-B022	B8	B0765	M. Xu, Y. Zhang, B. Zhou, and D.L. Feng	Electronic structure of iron pnictides in electron and hole doped BaFe_2As_2
15P-B023	B8	B0793	Hiroshi Watanabe, Tomonori Shirakawa, Seiji Yunoki	Variational Monte Carlo study for superconductivity in multi-orbital systems
15P-B024	B8	B0817	Y. Ono, Y. Yanagi, N. Adachi, K. Hayashi and Y. Yamakawa	S++-wave Superconductivity near the Ferro-orbital QCP in Iron Pnictides
15P-B025	B8	B0843	Q.Q.Ge, Y.Zhang, M. Xu, D.L.Feng	Electronic structure of detwinned BaFe_2As_2
15P-B026	B8	B0859	I. Kanazawa	High-energy Hole-like Excitations and the Evolution Mechanism of Fermi Arc in High-T_c Cuprates
15P-B027	B8	B0864	K. Mitsen, O. Ivanenko	Possible nature of ground state of HTSC
15P-B028	B8	B0868	O. Ivanenko, K. Mitsen	A possible explanation of Fermi arcs and pseudogap
15P-B029	B8	B0996	Nikolai B. Kopnin, Tero T. Heikkila and G.E. Volovik	High-temperature surface superconductivity in topological flat-band systems
15P-B030	B8	B1059	O.V. Dolgov	Superconducting glue: are there limits on T_c?
15P-B031	B8	B1087	L. Jiao, J.L. Zhang, T Shang, F.F. Balakirev, J. Singleton, C. Setty, J.P. Hu, L.J. Li, G.H.	Localized and itinerant dichotomy of electrons in Iron pnictides
15P-B032	B8	B1156	A. Tsukada, K. Saiki and N. Miyakawa	Study of Electronic Phase Diagram of Electron-doped Superconductors by FET

15P-B033	B8	B1204	A. Tsukada, K. Saiki, and N. Miyakawa	Study of Electronic Phase Diagram of Electron-Doped Superconductors by FET
15P-B034	B8	B1281	X. J. Zhou	Laser ARPES on High-Temperature Cuprate Superconductors
15P-B035	B8	B1294	Mucio A. Continentino	Coexistence of superfluid and metallic-like state in two-component fermionic systems
15P-B036	B8	B1302	Sze Kui Ng	Gauge Model of High-T_c Superconductivity
15P-B037	B8	B1377	Sung-Ho Salk and Gwang-Yong Choi	Universal Behaviors and Cross-over from Non-fermi to Fermi Liquid in High Temperature Cuprate Oxides
15P-B038	B9	B0973	M. Bavarsad, G. R. Rashedi and Y. Rahnavard	Nonunitary Spin- Triplet SNS Josephson Junction
15P-B039	B9	B1053	D. Bothner, B. Betz, M. Kemmler, M. Turad, R. Kleiner, and D. Koelle	Abrikosov vortices in Nb thin films with Nb pillar arrays on top
15P-B040	B9	B1270	H.-C. I. Kao,D. C. Ling,H.S.Sheu,J. M. Chen,J. F. Lee and T.S. Chan	Y. C. Chu
15P-B041	B9	B1304	Y. C. Chu,H.-C. I. Kao,D. C. Ling,H.S.Sheu,J. M. Chen,J. F. Lee and	Optimization of the Pr doping in the (Bi1.7Pb0.3)(Sr2-xPrx)CuO6+d superconducting series
15P-B042	B9	B1405	Y. C. Chu, H. - C. I. Kao, D. C. Ling, H.S.Sheu, J. M. Chen, J. F. Lee and T.S.	Optimization of the Pr doping in the (Bi1.7Pb0.3)(Sr2-xPrx)CuO6+δ superconducting
15P-B043	B9	B1067	A. Ohmura, A. Yamamura, M. Einaga, F. Ishikawa, A. Nakayama, Yuh	Pressure-induced superconductivity in Bi\$ {1-x} \$Sb\$ {x} \$ alloy
15P-B044	B9	B0909	Y. Z. Zhang, H. F. Wang, D. P. Li, G. Y. Wang, M. Zu, L. H. Liu, J. Li, D. N. Zheng	Hall effects of overdoped/underdoped of La\$ {2-x} \$Sr\$ {x} \$CuO\$ {4+\delta} \$ multilayers
15P-B045	B9	B0707	M. Hayashi Y. Takane and H. Ebisawa	Numerical Study of Collective Transport in Charge Density Wave Conductors
15P-B046	B9	B0218	K. Kihou, T. Saito, S. Ishida, M. Nakajima, Y. Tomioka, H. Fukazawa, Y. Kohori,	Single crystal growth and physical properties of Ba1?xKxFe2As2

15P-B047	B9	B0309	Y. Kasahara, T. Nishijima, T. Sato, Y. Takeuchi, H. T. Yuan, J. T. Ye, H. Shimotani,	Electrostatically and Electrochemically Induced Superconducting State Realized in Electrochemical Cells
15P-B048	B9	B0641	J. Tomaschko, C. Raisch, V. Leca, T. Chassl'e, R. Kleiner, and D. Koelle	Surface Study of Infinite Layer Superconductor Sr_{1-x}La_xCuO₂ Thin Films: Electric Transport across Planar
15P-B049	B9	B1074	M. Kimata, T. Terashima, N. Kurita, H. Satsukawa, A. Harada, K. Kodama, K.	Cyclotron Resonance in KFe₂As₂
15P-B050	B9	B1039	C. W. Luo, I. H. Wu, T. W. Huang, K. W. Yeh, J.-Y. Lin, K. H. Wu, J. Y. Juang, T. M. Uen	Ultrafast dynamics in the FeSe_{1-x}Tex single crystals studied by femtosecond time-resolved spectroscopy
15P-B051	B9	B0759	M. Higuchi, K. Koide, T. Imanishi and K. Higuchi	Current-Density Functional Theory for Superconductors
15P-B052	B9	B0136	Y. Matsumoto, H. Tanaka, A. Nishida, T. Akune, N. Sakamoto and Ahmed A A.	On the scaling analyses of the flux pinning force density estimated for two types of MgB₂ specimens
15P-B053	B9	B1077	A. Augieri, V. Galluzzi, F. Fabbri, A. Mancini, A. Angrisani Armenio, F. Rizzo, A. Rufoloni,	Study of YBCO-BZO pinning properties grown by PLD and MOD techniques
15P-B054	B9	B0984	Junfeng He, Li Huang, Lin Zhao, Yi Pan, Wentao Zhang, Haiyun Liu, Xiaowen Jia,	ARPES Evidence of Decoupling of Graphene Film from Ruthenium Substrate by Interface Si-Intercalation
15P-B055	B9	B0564	M. Hanawa, A. Ichinose, I. Tsukada, S. Komiya, F. Nabeshima, T. Akiike,	Guiding Principle of Selection of Substrate Material for Iron Chalcogenide Superconducting Thin Films
15P-B056	B9	B0758	S. Pryanichnikov, S. Titova, L.Cherepanova	Effect of Doping Level on the Crystal Structure of HTSC-copounds at Temperature Range 300-100 K
15P-B057	B9	B0219	Y. Sun, Y. Ma, M. R. Chen, J. Y. Yang, H. Li, and J. C. Nie	Thickness dependence of structural and electrical properties of electron-doped Sr_{1-x}La_xCuO₂ infinite-layer thin films grown by
15P-B058	B9	B0755	H. Asai, M. Tachiki T. Kashiwagi, H. Minami, T. Yamamoto and K. Kadowaki	Numerical Study of Radiation Pattern from Intrinsic Josephson Junctions Attached to Finite Size Substrates
15P-B059	B9	B0617	A.S. Malishevskii, V.P. Silin and S.A. Uryupin	Cherenkov Radiation by Josephson Vortex Chain
15P-B060	B9	B0827	D.H. LIN D.J. CUI B. Li J.H. ZHAO B.Q. HU X.Q. WANG	Research on the "cosφ term" riddle in Josephson effect

15P-B061	B9	B0685	C. Holmqvist, W. Belzig, and M. Fogelstr?m	Critical charge and spin Josephson currents through a precessing spin
15P-B062	B9	B0710	M. Hayashi H. Yoshioka and A. Kanda	Supercurrent through Monolayer and Multilayer Graphene
15P-B063	B9	B0749	T. Kashiwagi, K.Deguchi, M.Tsujimoto, T.Koike, N.Orita, K. Delfanazari,	Excitation mode characteristics in Bi2212 rectangular mesa structures
15P-B064	B9	B0941	K. Makisea, H. Terai, T. Yamashita, S. Miki, Z. Wang, Y. Uzawa, S. Ezaki, T. Odou, and B.	Fluctuation conductance and the Berezinskii-Kosterlitz-Thouless transition in two dimensional epitaxial NbTiN ultra-thin films
15P-B065	B9	B0666	S. Tagliati and A. Rydh	Heat capacity measurements of a microgram Pb crystal using ac nanocalorime- try with good absolute accuracy
15P-B066	B9	B0322	Ali A. Babaei-Brojeny, Asghar Sharbaf and Mostafa Molavi	Ac susceptibility of a thin type-II superconducting circular washer with and without a radial transport current
15P-B067	B9	B1388	R. Chaudhury	Mechanism For Superconducting Pairing In Strongly Correlated Layered Systems
15P-B068	B9	B0932	M. Nakajima, S. Ishida, K. Kihou, Y. Tomioka, C. H. Lee, A. Iyo, H. Eisaki, T. Kakeshita, T.	Anisotropic optical spectrum of detwinned Ba(Fe_{1-x}Cox)2As₂
15P-B069	B9	B0090	I. Sochnikov, A. Shaulov, Y. Yeshurun, G. Logvenov and I. Bo?ovi?	Large oscillations of the magnetoresistance in nano-patterned La_{1.84}-\$Sr_{0.16}\$CuO₄
15P-B070	B9	B0091	I. Sochnikov, Y. Shokef, A. Shaulov and Y. Yeshurun	Dichotomic fluxoid quantization effects in a superconducting double network
15P-B071	B9	B1488	M. I. Eremets and I. A. Troyan	Metallic dense hydrogen
15P-B072	B9	B0547	S. Okada, Y. Kamihara, N. Ohkubo, S. Ban, M. Matoba and T. Atou	Physical properties of the novel layered cobalt oxyphosphide Sr₄Sc₂Co₂P₂O₆
15P-B073	B9	B0459	L. Ichkitidze and A. Mironyuk	Weak Magnetic Field Sensor Based on High-Temperature Superconductor Ceramic Material
15P-B074	B9	B0460	L. Ichkitidze and A. Mironyuk	Superconducting Film Flux Transformer for Weak Magnetic Field Sensor

15P-B075	B9	B0241	A. Charnukha, A. N. Yaresko, Y. Matiks, C. T. Lin, B. Keimer, and A. V. Boris	Superconductivity-induced optical anomalies in iron arsenides
15P-B076	B9	B1401	Heesang Kim, H. Chung and Namhee Kim	Density of states and Specific heat in extended s-wave superconductors
15P-B077	B9	B0056	T.Charikova, N.Shelushinina, G.Kharus, O.Petukhova, A.Ivanov	Evolution of the Paring Symmetry by the Doping Change in n-type Superconductors
15P-B078	B9	B0468	A.M. Goldman, Xiang Leng, Javier Garcia-Barriocanal, and Yeonbae Lee	Electrostatic Control of the Evolution from Superconductor to Insulator in Ultrathin Films of Yttrium Barium Copper Oxide
15P-B079	B9	B0561	Lina E. Klintberg, S. K. Goh, Y. Nakai, S. Kasahara, K. Ishida, Y. Ihara, M. L.	Chemical and Physical Pressure Studies of Phosphorous Substituted BaFe₂As₂
15P-B080	B9	B0939	M. Einaga, A. Ohmura, F. Ishikawa, A. Nakayama, Yuh Yamada, and S.	Transport Properties in Bi₂Te₃ under High Pressure up to 8 GPa
15P-B081	B9	B0320	O. Martynova and V. Gasumyants	On the transformation of the normal-state band spectrum of Bi-based HTSC with increasing doping level and number of CuO₂
15P-B082	B9	B1090	V. Gasumyants, O. Martynova, O. Komarova, A. Babichev	The Fermi Level Variation in YBa₂Cu₃O_y Doped by Ca and Pr and Its Influence on the Critical
15P-B083	B9	B0883	Avdeev M., Proshin Yu., Khusainov M. and Tsarevskii S.	Asymmetrical ferromagnet-superconductor trilayers in external magnetic field
15P-B084	B9	B1016	Avdeev M., Proshin Yu., Khusainov M. and Tsarevskii S.	Simulation of spin-valve regime for asymmetrical FS nanostructures in external magnetic field
15P-B085	B9	B0796	M. Miyazaki, T. Adachi, Y. Tanabe, H. Sato, K. Kudo, T. Nishizaki, T. Sasaki, N. Kobayashi,	Inhomogeneity of Superconductivity and Stripe Correlations in the Overdoped Regime of La_{2-x}Sr_xCuO₄ at x ~ 0.21
15P-B086	B9	B0945	K. Tanaka, Y. Sakai, T. Miyake, S. Miyasaka, S. Tajima, M. Tonouchi and T. Sasagawa	Terahertz time-domain spectroscopy on the stripe-orderd La_{1.84-y}Eu_ySr_{0.16}CuO₄
15P-B087	B9	B1258	B. F. Hu, P. Zheng, R. H. Yuan, T. Dong, B. Cheng, Z. G. Chen, and N. L. Wang	Optical Spectroscopy Study on RTe₃(R = La, Ce, Er): Evidence for Multiple Charge-Density-Wave Orders
15P-B088	B9	B1018	N. Eguchi, M. Kodama, F. Ishikawa, A. Nakayama, A. Ohmura, Yuh Yamada,	Powder x-ray diffraction of BaFe₂As₂ under hydrostatic pressure

15P-B089	B9	B1284	H. Yavari, M. Eghbali, E. Afsaneh, and S. Mirzai	Josephson Efct in Superfluid Fermi Atoms at Finite Temperature
15P-B090	B9	B1243	Yue Wang, Zhi-Yong Liu, Cheng-Tian Lin and Hai-Hu Wen	Determination of the superconducting gap in Bi₂Sr_{2-x}LaxCuO_{6+δ} (x ? 0.4) from low-temperature specific heat
15P-B091	B9	B0773	Q. Ding, S. Mohan, T. Taen, Y. Tsuchiya, Y. Nakajima and T. Tamegai	FeSe superconducting tapes with a high critical current density fabricated by diffusion method
15P-B092	B9	B0563	T. Taen, Y. Nakajima, T. Tamegai, S. Okayasu, and M. Sasase	Effects of Swift Xe Irradiation in Ba(Fe_{1-x}Cox)₂As₂ Single Crystals
15P-B093	B9	B0323	S. Harada, Y. Inada, and Guo-qing Zheng	Unconventional Superconducting states in Li₂(Pd_{1-x}Pt_x)₃B with broken inversion symmetry probed by NMR
15P-B094	B9	B0291	D. Kalok, A. Bilusic, I. Schneider, V.M. Vinokur, C. Strunk	Nonlinear Transport at the Superconductor-Insulator Transition in Thin TiN Films
15P-B095	B9	B0619	R. T. Hernández L., M. A. Aguilar-Frutis, C. Falcony	Effect of Fluorine on The Phase Formation of Ti-1223 Films Grown Over Silver Substrates
15P-B096	B9	B0609	J. Fukuyado, K. Narikiyo, M. Akaki, H. Kuwahara, and T. Okuda	Low-Temperaure Thermoelectric Properties for Single Crystals of the Electron-Doped Perovskite Sr_{1-x}CaxTi_{1-y}NbyO₃
15P-B097	B9	B0967	Z.D.Yakinci 2,3, S. Turkoglu 1,2, M.A. Aksan 1,2, Y.Balci 1,2, S.Altin 1,2 and	Fabrication of BSCCO Thick Film with Modified Ultrasonic Spray Pyrolysis (USP) Method and their Transport Properties
15P-B098	B9	B0690	M. Z. Tahar and H. T. Johnson-Steigelman	Growth and Characterization of Superconducting \$In\$ and \$Pb\$ Films
15P-B099	B9	B1253	Chao Zhang,Liling Sun,*Zhaoyu Chen,Xingjiang Zhou,Qi Wu,Wei Yi,	Phase diagram of a pressure-induced superconducting state and its relation to the Hall coefficient of Bi₂Te₃ single crystals
15P-B100	B9	B0411	S. Ishida, M. Nakajima, T. Saito, K. Kihou, C. H. Lee, A. Iyo, H. Eisaki, T. Kakeshita, Y.	In-plane resistivity and superconductivity of iron-pnictide superconductors
15P-B101	B9	B0542	Seiki Komiya, M. Hanawa, I. Tsukada, and A. Maeda	Evolution of the magnetic, thermodynamic, and transport properties of FeSe\$ _x \$Te\$ _{1-x} \$ single crystals with
15P-B102	B9	B0794	T. Sekihara, R. Masutomi, and T. Okamoto	Two-dimensional superconductivity of ultrathin Bi films on cleaved GaAs surfaces

15P-B103	B9	B0340	N. Di Scala, E. Olive, Y. Fly, Y. Lansac, J.C. Soret	Elastic depinning transition of superconductor vortices
15P-B104	B9	B0426	Qing-Hu Chen, Fei Qi, and Wei Zhou	Vortex dynamics in type-II superconductors with columnar defects
15P-B105	B9	B1185	M. Iavarone, A. Scarfato, F. Bobba, M. longobardi, A.M. Cucolo, G. Karapetrov,	Vortex Confinement in Planar Superconducting/Ferromagnet Hybrid Structures
15P-B106	B9	B0922	Y. Tsuchiya, Y. Nakajima, and T. Tamegai	Simulation of vortex penetration into square superconducting network
15P-B107	B9	B0365	G. R. Berdiyorov, M. M. Doria, A. R. de C. Romaguera, E. H. Brandt, F. M. Peeters	Vortex cutting and recombination processes in a mesoscopic superconductor
15P-B108	B9	B0523	S. Okuma, D. Shimamoto and N. Kokubo	Dynamic Ordering and Lattice Orientation of Driven Vortex Matter
15P-B109	B9	B0526	S. Okuma, Y. Tsugawa and Y. Kawamura	Reversible to Irreversible Flow and Absorbing Transitions in Sheared Vortices
15P-B110	B9	B0566	M. Kato, K. Maki	Appearance of magnetization around a pair of half quantum vortices in chiral p-wave superconductors
15P-B111	B9	B0579	H. Sato and S. Okuma	Mode-locking measurements for driven vortices in thick and thin amorphous Mo_xGe_{1-x} Films
15P-B112	B9	B0861	D.E. Fujibayashi and Masaru Kato	Dynamics of Vortices in Nano-Structured Superconductors with Periodic Arrays of Various Antidots
15P-B113	B9	B0951	A. Motohashi and S. Okuma	Plastic Depinning in a Sheared Vortex System with Random Pinning
15P-B114	B9	B0569	S. Mohan, Y. Tsuchiya, Y. Nakajima and T. Tamegai	Magneto-optical Imaging of Flux Turbulence in Ba(Fe_{1-x}Cox)As₂ Crystals
15P-B115	B9	B0086	A. A. Bespalov and A. S. Mel'nikov	Flux-Flow Conductivity in Anisotropic Superconductors with a Cooper Pair Mass-Normal Conductivity Anisotropy Mismatch
15P-B116	B9	B0540	T. Tamegai, T. Taniguchi, T. Taen, Y. Nakajima, T. Nishizaki, T. Naito, N. Kobayashi,	Vortex Phase Diagram of Pristine and Irradiated Co-doped BaFe₂As₂

15P-C001	C4	C0206	Ezawa Motohiko	Giant Skyrmion and Skyrmion Burst in Thin Ferromagnetic Films
15P-C002	C4	C0337	Achim Rosch	Spintorques and skyrmions in chiral magnets
15P-C003	C4	C0388	Pradip Das, Yusuke Suzuki, Masashi Tachiki and Kazuo Kadowaki	Pairing Symmetry and Magnetic Relaxation in Topological Superconductor Cu_xBi₂Se₃
15P-C004	C4	C0583	Shun-Li Yu, X. C. Xie, and Jian-Xin Li	Mott Physics and Topological Phase Transition in Correlated Dirac Fermions
15P-C005	C4	C0584	I. Maruyama, Y. Hatsugai	Z\$ \{Q\}\$ topological invariants of gapped quantum systems for integer \$Q\$
15P-C006	C4	C0650	A. Yazdani, P. Amin Javaheri	Quantum Phase Transition at Critical Magnetic Field
15P-C007	C4	C0776	R. Kondo, T. Yoshinaka, Y. Imai, and A. Maeda	Transport property of compensated topological insulator, Bi₂Se₃
15P-C008	C4	C1297	Jin-Hong Park and Jung Hoon Han	Possible 3D Skyrmion lattice in chiral magnet
15P-C009	C6	C0116	K.T. Lu, T.L. Chou, S.C. Haw, J.M. Lee, S.A. Chen, and J.M. Chen	Substrate-Dependent Bonding Anisotropy of Epitaxial Multiferroic DyMnO₃
15P-C010	C6	C0184	Meihua, Chen and Chong Der Hu	Analysis of electron spin resonance of LiCu₂O₂ at low temperature
15P-C011	C6	C0394	X. M. Wang, C. Fan, Z. Y. Zhao, W. P. Ke, X. G. Liu and X. F. Sun	Low-Temperature Heat Transport in the Quasi-Two-Dimensional Multiferroic CuFeO₂
15P-C012	C6	C0408	K.K. Cong, Y. Ji, S.L. Wang, Z.C. Xia, L. Chen, and J.H. Zhao	Hole density of (Ga,Mn)As across its Curie temperature studied via pulsed high magnetic field
15P-C013	C6	C0410	W. Bazela, M. Dul, V. Diakonov, L. Gondek, A. Hoser, B. Penc, A. Szytula	Neutron diffraction studies of the polycrystalline and nano particle TbMnO₃
15P-C014	C6	C0416	V. Dyakonov, A. Szytula, R. Szymczak, E. Zubov, Z. Kravchenko, W.	Phase transitions in TbMnO₃

15P-C015	C6	C0425	H. Niki, Y. Okada, M. Oshiro, K. Higa, M. Yogi, and S. Tomiyoshi	NMR studies of Heusler-type intermetallic antiferromagnet Mn₃Si
15P-C016	C6	C0497	G. H. Hu, I. Umebara, X. Shuang, S. X. Cao, S. Yuan	Pressure Effect in Multiferroic Phase Transition of Perovskite Ferrite Crystals NdFeO₃ and ErFeO₃
15P-C017	C6	C0546	Y. P. Chin, S. Mukherjee, C. C. Chou, J. H. Zhang, C. C. Yeh, H. Berger, and	Magnetic and magnetodielectric properties in frustrated Cu₂Te₂O₅Br₂
15P-C018	C6	C0553	Wei Yi, Alexei A. Belik	Bi_{3-x}M₃O_{11+δ} (M=Cr, Rh, Ir, Pt, Pd), A series of new KSbO₃-type structural magnetic materials
15P-C019	C6	C0588	T. Katsufuji, M. Ikeda, J. Miyazaki, T. Kajita, K. Takubo, Y. Nagamine, S. Mori, K.	Three-dimensionally aligned V trimers in various vanadates
15P-C020	C6	C0709	S. Kimura, K. Watanabe, T. Fujita, M. Hagiwara, H. Yamaguchi, T.	Electromagnon excitation in the triangular lattice antiferromagnet CuFeO₃
15P-C021	C6	C0895	S. Yano, Y. Nishikawa, Y. Kousaka, J. Akimitsu, K. Taniguchi, H. Sagayama, T.	Magnetic Structure of Ba₂Mg₂Fe₁₂O₂₂ in Ferroelectric Phase.
15P-C022	C6	C0934	K. Yoshidaa, K. Watanabe, and H. Shimizu	Nb-substitution effects in half-metallic double perovskite Ba₂FeMoO₆
15P-C023	C6	C0997	R. Puzniak, J. Wieckowski, M. Gutowska, A. Szewczyk, J. Molenda,	Size effect on magnetic properties of LiFePO₄ particles
15P-C024	C6	C1008	H. Iwamoto, M. Ehara, M. Akaki, and H. Kuwahara	Magnetolectric property in 3d transition metal oxide with tetrahedral structure
15P-C025	C6	C1012	K. H. Wu, H.-J. Chen, J. B. Zeng, C. W. Luo, T. M. Uen, J. Y. Juang, J.-Y. Lin, T. Kobayashi	Ultrafast magnetoelastic and thermoelastic dynamics in hexagonal YbMnO₃ single crystals observed by femtosecond
15P-C026	C6	C1014	H. Z. Chen, M. C. Kao, S. L. Young, B. N. Chuang, W. W. Jiang and J. S. Song	The ferroelectric and leakage current properties of Sm-Ta co-doped Bi₄Ti₃O₁₂ Ferroelectric Thin films
15P-C027	C6	C1052	A. Koda, M. Miyazaki, M. Hiraishi, T. Masuda, K.M. Kojima, R. Kadono, N. Abe, T.	Spin Dynamics in Multiferroic Rare-Earth Mangnites Probed by Muon Spin Relaxation
15P-C028	C6	C1375	N. Furukawa and S. Miyahara	Electromagnons and non-reciprocal directional dichroism in Ba₂CoGe₂O₇

15P-D001	D5	D0312	Hyunho Noh, Lee-Seul Park, Eun-Kyoung Jeon, Jeong-O Lee, Jin Seok Lee, Jinhee	Observation of Supercurrent through Topological Insulator Nanowires of Bi₂Se₃
15P-D002	D5	D0367	Kai Chang, Z. H. Wu, J. J. Zhu, and L. B. Zhang	All-electrical control of Dirac electron transport
15P-D003	D5	D0384	Heon-Jung Kim et al.	Transport properties of defect-controlled Bi₂Te₃ single crystals:
15P-D004	D5	D0409	Xiang-lin Zhang and Huai-ming Guo	Disorder Effect in Two-dimensional Topological Insulator
15P-D005	D5	D0413	Xiang-lin Zhang and Huai-ming Guo	Disorder Effect in Two-dimensional Topological Insulator
15P-D006	D5	D0551	Yoshiki Imai, Katsunori Wakabayashi and Manfred Sigrist	Magnetism of Multi-Orbital Edge States in Sr₂RuO₄
15P-D007	D5	D0575	K. Kobayashi, T. Ohtsuki and K. Slevin	Critical Exponent for the Quantum Spin-Hall Transition
15P-D008	D5	D0656	A. Yazdani, S. Zarrini	The Fluctuation Character on the Existance of Magnetocaloric Effect
15P-D009	D5	D0687	M.L.Tian, J.Wang, M.Singh, and M.H.W.Chan	Electrical transport properties of single-crystal Bi₂Te₃ nanowires
15P-D010	D5	D0718	A. Yamakage, Ken Nomura, K.-I. Imura, Y. Kuramoto	Z₂ topological Anderson insulator
15P-D011	D5	D0725	K.-I. Imura, Y. Takane and A. Tanaka	Topological insulator with dislocation lines
15P-D012	D5	D0737	CHEN chaoyu	Coexistence of Topological Order and Quantum Well States on Topological Insulators
15P-D013	D5	D0800	Fan Yang, Yue Ding, Fanming Qu, Jie Shen, Jun Chen, Zhongchao Wei, Zhongqing Ji,	Superconducting Proximity Effect and Conductance Anomalies in Sn-Bi₂Se₃ Junctions
15P-D014	D5	D0808	K.Shiozaki and S.Fujimoto	Majorana edge modes at topological insulator-superconductor-junctions in three dimension

15P-D015	D5	D0841	Wei Zhang	Fractional Topological Excitations and Quantum Phase Transition in a Bilayer 2DEG Adjacent to a Superconductor Film
15P-D016	D5	D0974	J. Chen, X.Y. He, K.H. Wu, Z.Q. Ji, L. Lu, J.R. Shi, J.H. Smet, and Y.Q. Li	Gate Tunable Surface Conductance in Bi₂Se₃
15P-D017	D5	D1130	G. Remenyi, S. Sahling, K. Biljaković, D. Starežinić, J. E. Lorenzo, P. Monceau	On the low vibrational states seen in the heat capacity of incommensurate ThBr₄
15P-D018	D5	D1146	Wenwen Zhou, Yoshinori Okada, D. Walkup, Chetan Dhalal, Stephen D. Wilson and	Quasiparticle Interference in Fe doped Bi₂Te₃ by Scanning Tunneling Spectroscopy
15P-D019	D5	D1147	Yoshinori Okada, Wenwen Zhou, D. Walkup, Chetan Dhalal, Stephen D. Wilson,	The observation of the novel stripe phase in Bi₂Te₃
15P-D020	D5	D1148	D. Walkup, Yoshinori Okada, Wenwen Zhou, Chetan Dhalal, Stephen D. Wilson, and V.	Examination of inhomogeneous electronic structure in 3D topological insulator Bi₂Te₃
15P-D021	D5	D1361	Tao Dong	Optical spectroscopy study on the normal-state properties of superconducting doped topological Insulator Cu_xBi₂Se₃
15P-D022	D5	D1394	Jason N. Hancock, J. L. M. van Mechelen, Alexey B. Kuzmenko, Dirk van der Marel,	Surface state charge dynamics of a high-mobility three dimensional topological insulator
15P-D023	D5	D1502	J. Chen, X.Y. He, H.J. Qin, L. Lu, K.H. Wu, and Y.Q. Li	Identifying surface transport on 3D topological insulators with weak antilocalization
15P-D024	D7	D0075	C.H. Chung, K.V.P. Latha, K. Le Hur, M. Vojta, P. Woelfle	Tunable Kondo-Luttinger systems far from equilibrium
15P-D025	D7	D0102	H.L. Hortensius, A. Ozturk, P. Zeng, E.F.C. Driessens and T.M. Klapwijk	Thermovoltage of a Suspended Carbon Nanotube Heated by Terahertz Radiation
15P-D026	D7	D0215	Yi Sun, Rui Xu, Hui Yan, Jiacai Nie and Lin He*	Scanning Tunnelling Microscope Studies of nanowires and nanoparticles
15P-D027	D7	D0253	J. Voutilainen, T. T. Heikkilä	Energy relaxation in a diffusive SNS junction in an AC field
15P-D028	D7	D0543	J.R. Owers-Bradley, K. Lulla, C.J. Mellor, A.D. Armour, R. Cousins, M. Patton, A.	Dissipation in Stressed Silicon Nitride Beams at very low Temperatures

15P-D029	D7	D0578	J. Mucha, A. Je?owski, H. Misiorek, I.A. Smirnov, L.S. Parfen'eva	Influence of microstructure on the thermal properties of Si3N4/BN fiber monoliths.
15P-D030	D7	D0635	A. Jezowski, J. Mucha, H. Misiorek, I.A. Smirnov, and L.S. Parfeneva	Transport Properties of Bioceramics Type Bio-C/Cu
15P-D031	D7	D0814	I en a g a Koichiro, Tomohiko Yokota, Naoya Nakashima, Yuji Inagaki, Tatsuya	Electron tunneling measurements in atomic scale gap filled with liquid \$^4\$He below 4.2K
15P-D032	D7	D0865	I. Kanazawa	Fermion Zero Modes and Induced-charge on a Domain Wall of a Narrow-gap Semiconductor-Dot
15P-D033	D7	D0893	Yuh Tomio, Hidekatsu Suzuura and Tsuneya Ando	Fano Effect on Dynamical Conductivity for Perpendicular Polarization in Double-Wall Carbon Nanotubes
15P-D034	D7	D0917	M.T. Deng, H.A. Nilsson, P. Caroff, and H.Q. Xu	Hole transport in an InSb nanowire quantum dot with superconductor contacts
15P-D035	D7	D1006	H. Z. Chen, S. L. Young, C. Y. Kung, and C. C. Lin	Preparations and Photovoltaic properties of dye-sensitized solar cell based on ZnO nanowire electrode
15P-D036	D7	D1172	Akira Oguri, and Yoichi Tanaka	Fermi liquid description for Andreev-Kondo transport through a quantum dot coupled to normal and superconducting leads
15P-D037	D7	D1310	E. Condreaa, A. Gilewskib, and A. Nicoricia	Low-temperature oscillations of the thermopower in bismuth nanowires
15P-D038	D7	D1354	S. Nawaz, F. Lombardi, T. Bauch	Approaching the Depairing Current in YBCO Nanowires and Ultra-low-noise nanoSQUIDs
15P-D039	D7	D1403	Harold Meerwaldt, Samir Etaki, Gary Steele, Herre van der Zant	Electro mechanics of suspended carbon nanotube weak links in a SQUID configuration.
15P-E001	E4	E0150	Yantao Su, Yu Sui, Jinguang Cheng, Xianjie Wang, Yang Wang, and Wanfa Liu	Magnetocaloric Properties of Single Crystalline YbTiO3 with Second Order Phase Transition
15P-E002	E4	E0229	K. M. Omambac*, J. Porquez, R. B. Jaculbia, M.H.M. Balgos, M. Defensor,	Epitaxially lifted-off tensile strained InAs quantum dots with bimodal size distribution
15P-E003	E4	E0441	M. J. Prest, J. T. Muñonen, M. Prunnila, D. Gunnarsson, J. S. Richardson-Bullock, V.	Strain Enhancement of Electron Cooling in Silicon-Superconductor Tunnel Junctions

15P-E004	E4	E0482	Xiang Zheng, Sergio Y. Rodriguez, and Joseph H. Ross, Jr.	Low temperature NMR relaxation and rattling phonons in type-I Ba₈Ga₁₆Sn₃₀ clathrates
15P-E005	E4	E0574	Takeda T, Okamoto M, Miyazaki T and Katagiri K	Performance of the Helium Circulation System (HCS) on a Commercialized MEG
15P-E006	E4	E0591	Peter J. E. M. van der Linden, Ricardo Steinmann	Cryogenics for third generation X-ray research
15P-E007	E4	E0601	Gustav Teleberg, Anthony Matthews, Graham Batey	Dr
15P-E008	E4	E0698	D.H. Nguyen, S. Paschen, A. Sidorenko, M. Müller, A. Waard and G.	The Vienna Nuclear Demagnetization Refrigerator
15P-E009	E4	E0724	K. Matsumoto, K. Asamoto, R. Nishimura, Y. Zhu, S. Abe and T. Numazawa	Magnetocaloric Effect of RM₂ (R=rare earth, M=Ni, Al) Intermetallic Compounds Made by Centrifugal Atomization Process for
15P-E010	E4	E0741	T. Oota, K. Okidono, T. Nishioka, H. Kato, M. Matsumura, O. Sasaki	Suppression of temperature oscillation of GM cryocooler
15P-E011	E4	E0928	Ho Hyoun Kim, B.J. Mean, Ki Hyeok Kang, Jung Seok Sim, B. Ndiaye, Moohee Lee	\$¹H NMR Study of Proton Dynamics in the Ferroelastic Transition of K₄LiHS₃(SO₄)₄ Single Crystal
15P-E012	E4	E1030	F.M. Piegsa, B. van den Brandt and K. Kirch	A Cryogen-Free Laboratory Cryostat With Easy Sample Exchange
15P-E013	E4	E1076	M. Zech, C. Boedefeld, D. Andres, C. Mitzkus, and K. Karrai	Low temperature scanning probe microscopy at high magnetic fields in closed cycle systems: from 4K down to mK
15P-E014	E4	E1171	T. Oota, K. Okidono, T. Sumida, T. Nishioka, H. Kato, M. Matsumura, O. Sasaki	Suppression of temperature oscillation of GM cryocooler
15P-E015	E4	E1359	R. Halla, R. Mitchella, G. Frossattib, and A.R. Hamiltonc	A novel system for providing a 4.5 Tesla rotating vector with ultra low temperature
15P-E016	E4	E1360	R. Halla, R. Mitchella, G. Frossattib, and A.R. Hamiltonc	A novel system for providing a 4.5 Tesla rotating vector with ultra low temperature
15P-E017	E4	E1372	K. Watanabe, K. Saito, M. Yagi, T. Miya, T. Igarashi, S. Donuma, S. Harada and	Low T Study of PdH_x System by Torsional Oscillator Measurements using a New Refrigerator

15P-E018	E4	E1450	K.Watanabe, K.Saito, M.Yagi, T.Miya, T.Igarashi, S.Donuma, S.Harada and	Low T Study of PdHx System by Torsional Oscillator Measurements using a New Refrigerator
15P-E019	E5	E0119	M. ?love?ko, S. N. Fisher, G. Foulds, D. Garg, E. Guise, D. Schmoranzer, L.	Viscous and Acoustic Damping on Tuning Forks Oscillating in Liquid Helium-4
15P-E020	E5	E0151	K. Shunkeev, E. Sarmukhanov, A. Bekeshev, Sh. Sagimbaeva, K.	The cryostat for deformation of crystals at low temperature
15P-E021	E5	E0155	N. Zhanturina, K. Shunkeyev	Rate of the exciton self-trapping in KI and Rbl at different temperatures
15P-E022	E5	E0174	H. Matsuda, T. Iwata, Y. Miyachi, N. Doshita, K.H. Kondo, S. Ishimoto and T.	Inhibition of outgassing from a surface of CFRP (Carbon Fiber Reinforced Plastics) with nano-sized silver paint for COMPASS
15P-E023	E5	E0319	Chomsin S Widodo, Xun Xu, Muneaki Fujii, Yuji Kojima, Kenji Hosoyama	A Cryostat Suitable for Thermal Conductivity Measurements under High Pressure
15P-E024	E5	E0386	S.T. Boldarev, R.B. Gusev, S.I. Danilin, A.Ya. Parshin	The Potentialities of Quartz Tuning Fork as a Thermometer in Dilution Refrigerator
15P-E025	E5	E0560	Z. Geng and I. J. Maasilta	Development of an Inductive SINIS Thermometer
15P-E026	E5	E0726	T. Shigematsu, B. Ono, T. Kawae, H. Shimada, Y. Johno, K. Nakashima, S.	Temperature Dependent Measurement of Metals Contained Hydrogen by Vibrating Reed Method
15P-E027	E5	E0809	L. Roschier, D. Gunnarsson, M. Meschke, A. Savin, J. Penttil?, M. Prunnila	Primary CBT thermometer technology
15P-E028	E5	E1049	W.A. Bosch, O.W.B. Benningshof, O. Usenko and R. Jochemsen	SRD1000, a 13-point reference device for precision thermometry below 8 K
15P-E029	E5	E1104	M. Rostichera, Vu Dinh Lamb, J.C. Villegierc, F.R. Ladana, and J.P. Manevala	Temperatures of Phase-Slip Centers and Hot Spots in current-driven Superconducting Strips
15P-E030	E5	E1127	S.Uchaikin, A.Likhachev, F.Cioata, J.C.Petroff, C.Rich, P.Spear, I.Singh,	3D magnetometer for a dilution refrigerator
15P-E031	E5	E1129	S.Uchaikin, A.Eltony, X.Han	8-coils system to produce an uniform magnetic field in a dilution refrigerator

15P-E032	E5	E1226	A. Fleischmann, L. Gastaldo, S. Heuser, A. Kampk?tter, S. Kempf, C. Pies, J.-P.	Physics, micro-fabrication and applications of metallic magnetic calorimeters
15P-E033	E5	E1271	J. Engert, D. Heyer, J. Beyer, and H.-J. Barthelmess	Noise Thermometry at Low Temperatures: MFFT Measurements in the Temperature Range From 1.6 K to Below 1 mK

Tuesday Aug.16

Time Slot	Category	ABSN	Name	Title
Half Plenary Session(16H1)				
16H1-1			Gilbert Lonzarich	
16H1-2		E1482	Artru Luukanen	Applications of superconducting bolometers in security imaging
16H1-3		D1463	HeHendrik Bluhm	Coherence and coupling of two-electron-spin qubits in GaAs
Half Plenary Session(16H2)				
16H2-1			Ivan Bozovic	
16H2-2			Qi-Kun Xue	
16H2-3		B1263	Tetsuo Hanaguri	Spectroscopic-Imaging STM Studies of Superconducting Gap in Unconventional
Parallel Session(16m-A) Superfluid-He-3				
16m-A1		A1418	Peter Skyba	Anomalous spin relaxation and quasiparticle damping in superfluid 3He-B at very low
16m-A2		A1427	Shaun Fisher	Experiments on Quantum Turbulence in Superfluid 3He-B at very low temperatures
16m-A3		A1071	P. Gumann	Simultaneous torsional osciallator and NMR study of solid ³He-⁴He mixtures at low
16m-A4		A1420	Takeshi Mizushima	Majorana Fermions Bound at Vortices and Surface of Superfluid ³He
16m-A5		A0787	H. Ikegami	Ultra-low Temperature Mobility of Electron Bubbles Formed below the Free Surface of
Parallel Session(16m-B) Superconductivity, mostly Cuprates				
16m-B1			Masao Ogata	
16m-B2		B0355	T. K. Lee	Inhomogeneity in the Extended t-J Model: The Cases of Hole- and Electron-doped Cuprates
16m-B3			Makoto Hashimoto	
16m-B4		B0405	Manuel Nunez Regueiro	The relationship between the normal state Fermi liquid scattering rate and the
16m-B5			Xiao-Li Dong	
Parallel Session(16m-C) Magnetic Materials and Devices				
16m-C1		C0673	Xiufeng Han	Coulomb Blockade Magnetoresistance in Magnetic Tunnel Junctions
16m-C2		C1327	Vikram Tripathi	An Unusual Kondo Effect with a Topological Transition in the Honeycomb Kitaev Model
16m-C3		C1382	Changqing Jin	Pressure induced superconductivity in Topological Compounds
16m-C4			Dai Aoki	

16m-C5		C0907	E. Blackburn	Exploring the antiferromagnetic superconducting phase in CeCoIn5
Parallel Session(16m-D₁) 2DEG-related Transport and Devices				
16m-D ₁ 1		D1260	Lars Tiemann	The spin polarization of the v=5/2 fractional quantum Hall state
16m-D ₁ 2			Rui-Rui Du	
16m-D ₁ 3		D0446	J. L. Yu	Investigation of cavity mode and excitonic transition in an InGaAs/GaAs/AlGaAs vertical-
16m-D ₁ 4		D0053	Christian Flindt	Factorial cumulants reveal interactions in counting statistics
16m-D ₁ 5			Pei-Qing Jin	Lasing and Transport in a Quantum Dot-Resonator System
Parallel Session(16m-D₂) Nanowires & Molecular Electronics				
16m-D ₂ 1		D0357	Markus Gaass	Universality of the Kondo effect in quantum dots with ferromagnetic leads
16m-D ₂ 2		D0643	Tian Gang	Novel 2D spin system and its interaction with conduction electrons
16m-D ₂ 3			Tristan Meunier	
Parallel Session(16a-A) Phase Transition in Novel Systems				
16m-A1		A1276	D. M. Lee	Spin Wave Resonances Excited by Moving Domain Walls in Polarized Dilute Liquid 3He
16m-A2		A1393	Frank Gasparini	Confinement and Collective Behavior of 4He near the Superfluid Transition
16m-A3		A1475	J. Dupont-Roc	Observation of metastable solid helium-4 below its melting pressure
16m-A4		A1428	G. Gervais	Hydrodynamics of Superfluid Flow through a Nanohole: Towards the 1D Regime
16m-A5			Gary Williams	
Parallel Session(16a-B) Physical properties of Fe-based and Cuprate superconductors III				
16a-B1		B1434	H. Z. Arham	Novel Ordered Region Preceding The Magnetic And Structural Transition In Underdoped Ba(F
16a-B2		B0225	Hai-Hu Wen	Anisotropic Superconducting Gap Revealed by Angle Resolved Specific Heat, Point Contact
16a-B3		B1201	Teppei Yoshida	An energy scale directly related to superconductivity in the high-T_c cuprate
16a-B4		B0708	Masahito Yoshizawa	Quantum Criticality and Superconductivity in Ba(Fe_{1-x}Cox)₂As₂ Investigated by Ultrasonic
16a-B5		B1321	Takasada Shibauchi	Nodal s-wave superconductivity in BaFe₂(As,P)₂
Parallel Session(16a-C) Magnetism & Superconductivity				
16a-C1		C1350	Huihai Zhao	Quantum spin liquid phase in the spin-1 bilinear-biquadratic Heisenberg model on a
16a-C2			Mikhail Eremets	

16a-C3		C0803	H. Ohta	Developments of Multi-Extreme Terahertz ESR System at Low Temperature
16a-C4			Dragan Mihailovic	

Parallel Session(12a-D) Graphene / Dirac Electrons

16a-D1			Cory Dean	
16a-D2		D1409	Alberto Morpurgo	Gate tunable normal and superconducting transport through a 3D topological insulator
16a-D3			Jianhao Chen	
16a-D4		D1219	Adrien Allain	Tunable Superconductor-Insulator transition in tin-doped Graphene
16a-D5		D0127	Dmytro Fil	Magnetoexciton Superfluidity in Graphene-Dielectric-Graphene Structures

Parallel Session(12a-E) Novel Devices and Applications

16m-E1		E1325	Tetsushi Biwa	Thermoacoustic devices
16m-E2			L. Skrbek	Quartz tuning fork as a multipurpose tool for low temperature research - recent development
16m-E3		E0093	Yu.A. Pashkin	Single-electron devices with a mechanical degree of freedom
16m-E4		E0045	Oleg Kirichek	New Generation of Cryogen Free Superconducting Magnets for Neutron
16m-E5		B1257	Liangzhen Lin	A 630kVA/10.5kV superconductor substation

Poster Session

16P-A001	A7	A0065	S. N. Burmistrov	Oscillation Spectra of a Crystal 4He Facet and Its Destruction with Generating Crystallization Waves
16P-A002	A7	A0069	O. Kirichek, N.D. Vasilev, T.R. Charlton, C.J. Kinane, R.M. Dagliesh, A. Ganshin,	Neutron Reflection from the Surface of a Liquid \$^{3}\\$He--\$^{4}\\$He mixture
16P-A003	A7	A0118	I.V. Tanatarov, I.N. Adamenko, K.E. Nemchenko and A.F.G. Wyatt	Bulk and Surface Excitations of He II at Interfaces
16P-A004	A7	A0161	P. Stipanovic, L. Vranjes Markic , I. Beslic, and T. Martinic	Adsorption of 4HeN and 4HeN 3He clusters on cesium
16P-A005	A7	A0316	R. Nomura, H. Matsuda, R. Masumoto, K. Ueno, and Y. Okuda	Self-organized Criticality in Quantum Growth Regime of \$^4\$He Crystals in Aerogel
16P-A006	A7	A0333	V. Lebedev, P. Moroshkin and A. Weis	Vibronic spectra of atomic bubbles in liquid and solid He

16P-A007	A7	A0348	O.W.B. Benningshof and R. Jochemsen	Spin waves in the B-phase of superfluid Helium-3
16P-A008	A7	A0412	Y. Tsutsumi, T. Mizushima, M. Ichioka and K. Machida	On Intrinsic Angular Momentum due to Edge Mass Current for Superfluid ${}^3\text{He}$ A-Phase
16P-A009	A7	A0415	S. Higashitani, S. Matsuo, Y. Nagato and K. Nagai	Odd-Frequency Cooper Pairs near the Surfaces of Superfluid ${}^3\text{He}$-B
16P-A010	A7	A0428	H. Matsuda, R. Masumoto, R. Nomura, and Y. Okuda	Critical Overpressure for Nucleation of ${}^4\text{He}$ Crystals in Aerogel
16P-A011	A7	A0447	T. Mizushima and K. Machida	Magnetic Field Induced A-B Phase Transition and Edge States of Superfluid ${}^3\text{He}$ Confined in a Slab Geometry
16P-A012	A7	A0452	M.S.Tagirov, E.M.Alakshin, R.R.Gazizulin, A.V.Klochkov,	${}^3\text{He}$ adsorption processes on aerogel surface and their influence on ${}^3\text{He}$ spin kinetics
16P-A013	A7	A0517	L.V. Abdurakhimov, M.Yu. Brazhnikov, I.A. Remizov, and A.A. Levchenko	Two Different Regimes of the Turbulent Wave Cascade Decay on the Surface of Quantum Liquids
16P-A014	A7	A0744	D. G. Rees, I. Kuroda, C. A. Marrache-Kikuchi, M. Hofer, P. Leiderer, H. Totsuji and	Point-Contact Transport Properties of Classical Electrons on Helium
16P-A015	A7	A0900	L. Vranjes Markic, I. Beslic, P. Stipanovic, R. E. Zillich	${}^4\text{He}$ clusters adsorbed on graphene
16P-A016	A7	A0985	F. A. Shaban, J. Kalb, J. Engelhardt, J. Gleixner and P. Leiderer	Investigation of surface state electrons on He films at high densities
16P-A017	A7	A1035	P.Sharma, A.Corcoles, R.G.Bennett, J.M.Parpia, B.Cowan, A.Casey, J.Saunders	Effect of rough walls on transport in mesoscopic ${}^3\text{He}$ films
16P-A018	A7	A1068	T. Arai, S. Yamanaka, H. Yayama, A. Sawada, and A. Fukuda	Linewidth Broadening in Edge-magnetoplasmon Resonance of Helium Surface State Electrons
16P-A019	A7	A1121	L. V. Levitin, R. G. Bennett, A. J. Casey, B. Cowan, J. Parpia, E. V. Surovtsev, and J.	Superfluid Phases of ${}^3\text{He}$ Confined in a Single 0.6 Micron Slab
16P-A020	A7	A1420	T. Mizushima, T. Kawakami, Y. Tsutsumi, M. Ichioka, and K. Machida	Majorana Fermions Bound at Vortices and Surface of Superfluid ${}^3\text{He}$

16P-A021	A7	A1492	Tetsuo Nakajima	A New Rightful Gapless Dispersion Surfaces instead of the Conventional Erroneous Gappy Dispersion Ones in the Dynamical Theory of X-
16P-A022	E6	A1158	Norbert Mulders	Operation of Attocube Motors at Low Temperature
16P-B001	B4	B0025	Marcin Matusiak, Zbigniew Bukowski, and Janusz Karpinski	Doping dependence of the Nernst effect in Eu(Fe1?xCox)2As2 - departure from Dirac fermion physics
16P-B002	B4	B0115	J.M. Chen, S.C. Haw, J.M. Lee, S.A. Chen, K.T. Lu, Y.C. Liang, N. Hiraoka, H. Ishii, and	Pressure Dependence of Electron Structures and Spin States in Fe1.01Se Superconductors
16P-B003	B4	B0286	T. Oka, Z. Li, S. Kawasaki, G. F. Chen, N. L. Wang, G. -q. Zheng	\$^{75}As\$-NQR study of Superconductivity in LaFeAsO\$_{1-x}\$F\$_x\$
16P-B004	B4	B0335	M. Sato,a-c Y. Kobayashi,b, c S. Satomi,cT. Kawamata,b, c M.	Impurity Effects on the Superconducting Transition Temperatures of Fe pnictides and Superconducting Symmetry of the Order
16P-B005	B4	B0359	G. Li, G. Grissonanche, B. Conner, A. Gurevich S. Weyeneth, P. Moll, N.	Metamagnetism, superconducting properties, and intrinsic vortex pinning in 1111 Fe arsenide single crystals probed by torque magnetometry
16P-B006	B4	B0364	M. Sato, T. Kawamata, Y. Kobayashi, Y. YasuiT. Iida, S. Suzuki, M. Itoh, T. Moyoshi, K.	Study of Magnetic Excitation Spectra of Several Fe-pnictide Systems
16P-B007	B4	B0366	Y. Kobayashi, T. Iida, K. Suzuki, E. Satomi, T. Kawamata, M. Itoh, and M. Sato	NMR Studies on Iron Pnictide Superconductors of LaFeAsO0.89F0.11 and Ca-Fe-Pt-As
16P-B008	B4	B0485	Debtanu De, Carlos Diaz-Pinto, Zheng Wu, Pei-Herng Hor, Haibing Peng	Andreev reflection spectroscopy for Fe\$_{1+y}\$Te\$_{1-x}\$Se\$_x\$ in nano-scale metal-superconductor junctions
16P-B009	B4	B0490	I. Tsukada, M. Hanawa, S. Komiya, A. Ichinose, T. Akiike, F. Nabeshima, Y. Imai	Hall-effect study on multiband nature in FeSe\$_{1-x}\$Te\$_x\$ thin films
16P-B010	B4	B0502	Z.R. Ye, Yan. Zhang, M. Xu, Q.Q. Ge, F. Chen, Juan. Jiang, B.P. Xie, D.H. Lu, X.Y.	Phosphor induced heavy hole-doping in BaFe2(As1-xPx)2 superconductor
16P-B011	B4	B0530	K. Suzuki, H. Usui, K. Kuroki	The origin of the electron-hole asymmetry of the spin fluctuation and its effect on superconductivity in iron-based
16P-B012	B4	B0539	H. Usui and K. Kuroki	Effective five band analysis on \$T_c\$ vs. lattice structure correlation in iron pnictides

16P-B013	B4	B0544	Y. Nakajima, Y. Kurosaki, and T. Tamegai	Enhancement of Thermal Conductivity in the Superconducting State of Co-doped BaFe₂As₂
16P-B014	B4	B0585	P. Belova, I. Zakharchuk, K. B. Traito, and E. Lahderanta	Effects of the order parameter symmetry on the vortex core structure in the iron pnictides
16P-B015	B4	B0586	P. Belova, I. Zakharchuk, K. B. Traito, and E. Lahderanta	Cutoff parameter versus Ginzburg-Landau coherence length in the mixed state of high-
16P-B016	B4	B0620	D. Kimura, T. Chiba, Y. Nakanishi, K. Kihou, M. Nakajima, C. H. Lee, A. Iyo, H. Eisaki, S.	Elastic Anomalies Associated with Structural and Superconducting transitions in Iron-based Superconductor Ba(Fe_{1-x}Cox)2As₂
16P-B017	B4	B0621	S. Orozco, M. A. Ortiz, R. M. M'endez, Gabriela Murguia	A Multiband Model for SmFeAsO_{1-x}F_x
16P-B018	B4	B0646	Y.M. Dai, B. Xu, A. Forget, D. Colson, B. Shen, H.H. Wen, R.P.S.M Lobo, and	Optical properties of electron and hole-doped 122
16P-B019	B4	B0735	K. Ohishi, Y. Ishii, I. Watanabe, H. Fukazawa, T. Saito, Y. Kohori, K. Kihou, C.H.	Flux-Line Lattice State in FeAs-Based Superconductor (Ba,K)Fe₂As₂
16P-B020	B4	B0739	H. Takahashi, Y. Imai, T. Okada, S. Komiya, K. Kitagawa, K. Matsubayashi, N.	Microwave Surface Impedance Measurements of LiFeAs and FeSe_{0.4}Te_{0.6}
16P-B021	B4	B0753	Y. Imai, F. Nabeshima, Y. Kobayashi, M. Hanawa, I. Tsukada, and A. Maeda	Effects of Co Doping on the Transport Behaviors and Superconducting Transition Temperature of FeSe_{0.4}Te_{0.6} single
16P-B022	B4	B0801	K. K. Huynh, Y. Tanabe, T. Urata, R. Nouchi, N. Mitoma, S. Heguri, J. Xu, G. Mu	Evidence for Quantum Magnetotransport of Dirac Cone States in Ba(FeAs)₂
16P-B023	B4	B1051	H. Kawano-Furukawa, C. Bowell, R.W. Heslop, E.M. Forgan, A.S. Cameron, J. S.	Field Angle Dependence of Vortex Lattice Structure in KFe₂As₂
16P-B024	B4	B1057	D.V.Efremov, M.M.Korshunov, O.V.Dolgov, A.A.Golubov,P.J.Hirsch	Disorder induced transition between s-(pm) and s-++ states in two-band superconductors
16P-B025	B4	B1108	T. Goto, R. Kurihara, K. Araki, K. Mitsumoto, M. Akatsu, Y. Nemoto, S. Tatematsu, and M.	Ultrasonic Investigations on Layerd Iron Pnictide Superconductor Ba(Fe_{0.9}Co_{0.1})₂As₂
16P-B026	B4	B1109	O.V. Dolgov, A.A. Golubov, D.V. Efremov, M.M. Korshunov, A.V. Boris	Multiband Eliashberg model for pnictides

16P-B027	B4	B1124	H. Mukuda, M. Nitta, M. Yashima, Y. Kitaoka, P. M. Shirage, H. Eisaki, and A. Iyo	\$^{57}\text{Fe-NMR}/{}^{75}\text{As-NQR studies in LaFeAsO-based Superconductors}
16P-B028	B4	B1188	T. Yoshida, A. Fujimori, S. Ideta, I. Nishi, T. Shimojima, W. Malaeb, S. Shin, Y. Nakashima,	Three-dimensional Fermi surfaces and their nesting properties in the iron pnictide superconductor BaFe₂(As_{1-x}P_x)₂
16P-B029	B4	B1240	A. Aperis, P. Kotetes, G. Varelogiannis and P.M. Oppeneer	Momentum dependent \$s_{\pm pm}\$ superconductivity and isotope effect in electron and hole doped iron pnictides from the small-q
16P-B030	B4	B1267	B.Cheng,Z.G.Chen,C.L.Zhang,R.H.Yuan,T.Do ng,B.F.Hu,W.T.Guo,S. S.Miao,J.L.Luo,G.Xu,P.	C-axis Polarized Optical Study on Thick Ba_{0.67}K_{0.33}Fe₂As₂ Single Crystal
16P-B031	B4	B1308	M. Hirano, Y. Yamada, T. Saito, Y. Murano, R. Nagashima, H. Fukazawa, Y. Kohori,	NMR study of hole-doped iron-pnictide superconductor Ba_{1-x}K_{x}Fe_{2}As_{2} (x = 0.27 - 1)
16P-B032	B4	B1329	T. Kida, M. Kotani, M. Ishikado, H. Eisaki and M. Hagiwara	Transport Properties of the Iron-Oxypnictide Superconductor PrFeAsO_{1-y} in High Magnetic Fields
16P-B033	B5	B0027	D. Beckmann, F. Hübler, M. J. Wolf, H. v. Löhneysen	Observation of Andreev bound states at spin-active interfaces
16P-B034	B5	B0032	A.Farooq, M.Kamran, H.F.Yang and X.G.Qiu	Fractional matching effect in superconducting Nb thin film of square array of antidots
16P-B035	B5	B0059	E.M. Rudenko, D.A. Luzhbin, Y.V. Kudryavtsev, I.V. Korotash, D.S. Dubina,	Critical currents in superconductor-ferromagnet heterostructures subjected to the injection of spin-polarized tunneling current
16P-B036	B5	B0080	V. Taufour, H. Kotegawa, D. Aoki, G. Knebel, J. Flouquet	Metamagnetism in ferromagnetic superconductors
16P-B037	B5	B0088	Yu. Proshin and M. Khusainov	The Prediction of the Solitary Reentrant Superconductivity in the Asymmetrical Ferromagnet-Superconductor-Ferromagnet
16P-B038	B5	B0129	I.A. Rudnev, Yu.Yu. Sedin, M.A. Osipov, S.V. Pokrovskiy, A.I. Podlivaev	Low-Temperature Magneto-Optical Studies of Magnetic Flux Local Penetration into HTSC Films on Magnetic and Nonmagnetic
16P-B039	B5	B0142	Yu. Proshin and V. Tumanov	Influence of proximity effect with Umklapp processes on the Josephson current in the SFS nanostructure
16P-B040	B5	B0154	Sunao Shimizu, Hidekazu Mukuda, Yoshio Kitaoka, Parasharam M.	Superconducting transition under long-range ordered antiferromagnetic state in high-T_c cuprates Ba₂Ca₄Cu₅O₁₀(F,O)₂: Cu- and F-

16P-B041	B5	B0159	Kh. A. Ziq	Magnetic and transport properties of FeT(As, Se and Te)
16P-B042	B5	B0180	Y. F. Guo, X. X. Wang, K. Yamaura and E. Takayama-Muromachi	Magnetic moment in single crystalline BaFe_{2-x}Zn_xAs₂
16P-B043	B5	B0205	V. Kataev, A. Alfonsov, G. Lang, N. Leps, L. Wang, A. Kondrat, C. Hess, S. Wurmehl, G.	High-Field ESR Spectroscopy on GdO{1-x}F{x}FeAs Superconductors
16P-B044	B5	B0210	I. Felner and I. Nowik	Superconductivity and Magnetism of Fe-based AFe₂As₂ and BxFe₂Se₂ Systems Studied by Magnetization and M?ssbauer Spectroscopy
16P-B045	B5	B0239	G. Seibold,	Magnetic structure of electronic inhomogeneities in cuprates: Competition between stripes and spirals
16P-B046	B5	B0344	Hidetoshi Ozawa, Akihiro Shimizu, Ikuo Ichinose and Tetsuo Matsui	Phase Structure of Superconductors Coexisting with Ferromagnetism
16P-B047	B5	B0398	V. Grinenko, S.-L. Drechsler, K. Kikoin, G. Fuchs, K. Nenkov, F. Hammerath, G. Lang,	Vacancies, local moments and Pauli limiting in Fe-pnictide superconductors
16P-B048	B5	B0420	Yoshiki Hori and Akira Goto	Competition between Singlet and Triplet Superconductivity in the Extended Hubbard Model with Exchange Interaction on a Square
16P-B049	B5	B0427	Masato Imaizumi, Takashi Noji, Tadashi Adachi, Kazuki Ohishi, Isao Watanabe and	Superconductivity and magnetism of annealed FeSe_{1-x}Tex (0.6≤x≤1) single crystals studied by specific heat and μSR
16P-B050	B5	B0449	M. Jirsa, M. Muralidhar, M. Rames, Th. Wolf	Interplay of Paramagnetic Signal with the Superconductive Environment of (Nd,Eu,Gd)BaCuO Superconductors
16P-B051	B5	B0463	Dao-Xin Yao	Magnetism and multiorbital models in the iron-based superconductors
16P-B052	B5	B0480	Mauro M. Doria, Alfredo Vargas-Paredes, Jos'e Abdala Helay'l Neto	The principle of local rotational invariance and the coexistence of magnetism, charge and superconductivity
16P-B053	B5	B0484	Goryunov Yuriy	Superconducting heterostructure (FeCr_xFe)VFe: new view on old experiment
16P-B054	B5	B0486	T. Wakamura, K. Ohnishi, Y. Niimi and Y. Otani	Generation of Large Spin Accumulation in S/N/S Josephson Junctions

16P-B055	B5	B0500	I. P. Nevirkovets, M. A. Belogolovskii, O. Chernyashevskyy, and J. B. Ketterson	Anomalous zero-bias conductivity in superconductor-ferromagnet-insulator-superconductor tunnel junctions
16P-B056	B5	B0511	C. He, Y. Zhang, B. P. Xie, X. F. Wang, L. X. Yang, B. Zhou, F. Chen, X. H. Chen, M.	Electronic structure transition: the driving force behind magnetic and lattice structure transitions in NaFeAs
16P-B057	B5	B0590	V. H. Tran, D. T. Adroja, A. D. Hillier, D. Kaczorowski	Coexistence of magnetic fluctuations and superconductivity in an unconventional superconductor Ce\$2\$PdIn\$8\$
16P-B058	B5	B0626	R. Mohan, S. J. Kim, N. K. Gaur, S. Bhattacharya, and S. K. Gupta	Dr
16P-B059	B5	B0631	V. Chandrasekhar, M. Mehta, D. Dikin, C. W. Bark, C. Folkman, and C. B. Eom	Hysteretic Hall resistance at the LaAlO₃-SrTiO₃ interface - interplay between superconducting and ferromagnetic properties
16P-B060	B5	B0637	A. Yu. Aladyshkin, J. Fritzsche, Stefan Guénon, R. B. G. Kramer, I. M. Nefedov, V. V.	Visualization of Different Regimes of Localized Superconductivity in Superconductor-Ferromagnet-Hybrids by Low-Temperature
16P-B061	B5	B0668	M. Kamran, S. K. He, X.G. Qiu	Enhanced fractional matching fields in superconducting NbN film with periodic array of antidots
16P-B062	B5	B0677	T. Herrmannsdoerfer, R. Skrotzki, J. Wosnitza, D. Koehler, R. Boldt, M. Ruck	Coexistence of ferromagnetism and superconductivity of nanostructured single-phase Bi\$3\$Ni
16P-B063	B5	B0693	G. Annunziata, C. Autieri, M. Cuoco, P. Gentile, C. Noce, and A. Romano	Atomic scale properties of chiral spin-triplet pairing at the interface with normal or magnetic systems
16P-B064	B5	B0734	J. Sun, H. Watanabe, M. Hamabe, T. Kawahara, A. Iiyoshi and S. Yamauchi	Critical Current Measurements of a Tape in the Hybrid Multi-Stacking High Tc Superconducting Tapes
16P-B065	B5	B0840	T. Gaber, M. Weides, H. Kohlstedt, R. Kleiner, D. Koelle and E. Goldobin	Escape rate measurements of 0. \$\pi\$ and 0-\$\pi\$ ferromagnetic Josephson junctions
16P-B066	B5	B0862	T. Adachi, Y. Tanabe, K. Suzuki, T. Kawamata, Risdiana, T. Suzuki, I. Watanabe,	Similar Effects of Nonmagnetic and Electrostatic Impurities on the Cu-Spin Correlation and Superconductivity in La-214
16P-B067	B5	B0871	M. Hiraishi, R. Kadono, M. Miyazaki, A. Koda, K. M. Kojima, M. Ishikado, S. Shamoto,	Anomalous correlation between superconductivity and magnetism in iron pnictide superconductor LaFeAsO_{1-x}F_x near
16P-B068	B5	B0888	L. Zhao, X. J. Zhou	Unusual Doping Dependence of Magnetic Ordering and Electronic Band in Co-Doped BaFe₂As₂

16P-B069	B5	B0889	S. Miyasaka, W. Hirata, A. Takemori and S. Tajima	Charge Dynamics in SDW state of AFe₂As₂
16P-B070	B5	B0920	K. Sugimoto, E. Kaneshita and T. Tohyama	In-Plain Anisotropy of Charge Dynamics in Parent Compounds of Iron Pnictide Superconductors
16P-B071	B5	B0943	A. Djaglo and Q. Gu	Diamagnetism of quasi-2D charged Bose gases under
16P-B072	B5	B0956	M. Sutherland, D. Hills, B. Tan, M. Altarawneh, N. Harrison, J. Gillett, E. O'Farrell, S. Goh, T.	Evidence for Dirac-like excitations in SrFe₂As₂ from Quantum Oscillation Experiments
16P-B073	B5	B0963	V.I. Zdravkov, J. Kehrle, G. Obermeier, C. Müller, R. Morari, A.S. Sidorenko, S.	A Superconducting Spin Valve Core Structure based on the FFLO Like State: Studies on Bilayers and Trilayers of Superconductors and
16P-B074	B5	B0986	T. Yu. Karminskaya, A. A. Golubov, M. Yu. Kupriyanov, S. Prischepa	Interplay between spin-singlet and spin-triplet ordering in SFF spin valves
16P-B075	B5	B1003	M. Nakao	Two-Dimensional CrFe-Based Half-Metallic Antiferromagnets
16P-B076	B5	B1032	M.R. Eskildsen , P. Das, A.T. Holmes, E.M. Forgan, A.D. Bianchi, J.S. White, S. Gerber,	Vortex Lattice Studies in CeCoIn₅ with H perpendicular to the c-axis
16P-B077	B5	B1050	D. Hykel, C. Paulsen, D. Aoki, J. R. Kirtley, K. Hasselbach	Imaging of Magnetic Domains above the surface of the Superconducting Ferromagnet UCoGe
16P-B078	B5	B1054	A.T. Holmes, A.S. Cameron, E. Blackburn, E.M. Forgan, J.S.White,	SANS Studies of the Flux Lattice in YBa₂Cu₃O₇ at Very High Fields
16P-B079	B5	B1072	Hiroshi Akiba, Kento Nobori, Kazuo Shimada, Yutaka Nishio, Koji Kajita,	Magnetic Field Effect on Antiferromagnetic Insulating State of lambda-(BETS)2FeCl₄
16P-B080	B5	B1075	Ryo Ishikawa, H. Taniguchi, S. K. Goh, S. Yonezawa, F. Nakamura, and Y.	Control of the electronic state of Ca₂RuO₄ by uniaxial pressure
16P-B081	B5	B1080	N. Qureshi, P. Steffens, Y. Dress, A.C. Komarek, Y. Sidis, D. Lamago, M.T.	Magnetic excitations in the FeAs based superconductors
16P-B082	B5	B1081	S. -i. Tabata, S.Shimizu, H.Mukuda, Y.Kitaoka, P. M. Shirage, and A.Iyo	Antiferromagnetic order and high temperature superconductivity in underdoped Hg-based Five-layered Cuprates

16P-B083	B5	B1089	T. Wu, M.-H. Julien, H. Mayaffre, S. Kramer, M. Horvatic, C. Berthier, C.T. Lin, V.	NMR study of the interplay between magnetic order and superconductivity in YBa₂Cu₃O_{6.45}
16P-B084	B5	B1095	I. A. Zaliznyak, Z. J. Xu, J. M. Tranquada, G. D. Gu, A. M. Tsvelik, and M. B.	Unconventional temperature-enhanced magnetism in Fe(1.1)Te
16P-B085	B5	B1118	A. Yaresko, L. Boeri and O.K. Andersen	On the nature of an energy barrier between? (?pi,0?) ?and? (?0,pi) ?magnetic? ?orders in? ?Fe? ?pnictides
16P-B086	B5	B1133	H. Kinouchi, H. Mukuda, M. Yashima, Y. Kitaoka, P. M. Shirage, H. Kito, H.	Antiferromagnetic spin fluctuations and s+ - wave Superconductivity (Ca₄Al₂O_{6-y})(Fe₂As₂) probed by As NQR
16P-B087	B5	B1230	Wei Ku, W.-G. Yin, and C.-C. Lee	What do the rich magnetic structures of iron-based superconductors teach us about their electronic structure?
16P-B088	B5	B1283	Lev S. Mazov	From Low \$T_c\$ to Room \$T_c\$ in Cuprate- and Pnictide-Like
16P-B089	B5	B1290	G. W. Ataklti, W. Gillijns, A. V. Silhanek, J. Van de Vondel , A.Yu. Aladyshkin, I.M.	Mesoscopic cross-film cryotrons: Vortex trapping and dc-Josephson-like oscillations of the critical current
16P-B090	B5	B1298	K. J. Zhou, Y. B. Huang, C. Monney, N. L. Wang, P. C. Dai, X. Dai, J. van den Brink,	Dispersive high-energy spin excitations in iron-based superconductors
16P-B091	B5	B1318	S.-H. Lee	Crystal structure and magnetic correlations of Fe_{1+y}Te_{1-x}Se_x under ambient and applied pressure
16P-B092	B5	B1324	Jihong Qin and Yu Lan	Spin Dynamics in the Pressure-induced Two-leg Ladder Cuprate Superconductors
16P-B093	B5	B1343	Yu Lan, Jihong Qin	Doping dependence of spin dynamics in bilayer cuprate superconductors
16P-B094	B5	B1465	Tetsuo Oka, Hirotaka Seki, Daichi Ishiduka, Jun Ogawa, Satoshi Fukui, Takao Sato,	Field trapping property of HTS bulk magnet with reduced voids in pulsed
16P-C001	C7	C0078	T. A. Zaleski and T. K. Kope?	Spectral functions in the two-dimensional Hubbard model within a spin-charge rotating frame approach
16P-C002	C7	C0170	C. Ciccarelli, A. Irvine, J. Wunderlich, R. Campion, B.L. Gallagher, and A.J.	Ultra-sensitive measurement of magnetisation dependent chemical potential in ferromagnetic materials

16P-C003	C7	C0769	V. Badaut, T. Shirakawa and S. Yunoki	A Haldane-Anderson model study for the iron spin and charge state in Myoglobin
16P-C004	C7	C0770	Yuki Tokuda, Syuya Hirano, Eiji Ohmichi and Hitoshi Ohta	Cantilever-detected high-frequency ESR measurement using a backward wave traveling oscillator
16P-C005	C7	C0820	V. Badaut, T. Shirakawa, and S. Yunoki	A Haldane-Anderson model study for the iron spin and charge state in Myoglobin
16P-C006	C8	C0940	Toshio Ono, Hidekazu Tanaka, Kazumitsu Sakai and Masaki Oshikawa	Low-Temperature Specific Heat of Quantum sine-Gordon Spin System KCuGaF₆
16P-C007	C8	C0147	D.O. Ledenyov a, J.E. Mazierska a, V.O. Ledenyov b, O.P. Ledenyov c,	On the Nature of Nonlinearities in HTS Thin Films at Microwaves
16P-C008	C8	C0878	S. Ilkovic , M. Reiffers , V. Seben , K. Sterbakova , V. Burger , L. Parma , O. Cobal ,	Heat capacity and electrical resistivity of (Pby Sn_{1-y})₂P₂S₆ chalcogenides
16P-C009	C8	C0691	H. Nishihara, T. Harada, T. Kanomata, and T. Wada	Magnetization Process near the Curie Temperature of an Itinerant Ferromagnet CoS₂
16P-C010	C8	C0145	A. Bonanni, W. Stefanowicz, T. Devillers, M. Sawicki, B. Faina, Tian Li, T. E.	Experimental Probing of Exchange Interactions between Localized Spins in a Dilute Magnetic Insulator (Ga,Mn)N
16P-C011	C8	C1340	H. Nishihara, T. Baba, T. Kanomata, K. Kobayashi, R.Y. Umetsu, and R.	Zero-field NMR of ⁵⁹Co and ⁵⁵Mn in a Heusler Alloy Co₂MnGa
16P-C012	C8	C1313	M. A. Anisimov, A. V. Bogach, V. V. Glushkov, S. V. Demishev, N. A.	Heat capacity analysis of LaB₆
16P-C013	C8	C0824	F. Ishikawa, Y. Okawara, A. Ohmura, A. Nakayama, Yuh Yamada, T. Naka, and	Effect of nonstoichiometric aluminum composition on magnetic properties of Fe₂VAI system
16P-C014	C8	C0402	G. E. Volovik	BEC of Non-Equilibrium Quasiparticles in 3He and Beyond
16P-C015	C8	C0121	A.V. Andreev, Y. Skourski, S. Yasin, S. Zherlitsyn, J. Wosnitza	High-field study of magnetization and magnetoacoustics in UCo₂Si₂
16P-C016	C8	C0559	T. Toriyama, T. Konishi, Y. Ohta	Mechanism of the metal-insulator transition of hollandite vanadate K₂V₈O₁₆

16P-C017	C8	C0488	T. Tajiri, S. Hohdai, K. Hamamoto, H. Deguchi, M. Mito and A. Kohno	Magnetic Properties of La_{2-x}S_xCuO₄ Nanoparticles in Mesoporous Silica
16P-C018	C8	C1042	Yuanjie Huang, Zhaorong Yang, Yuheng Zhang	Orbital glass state and magnetic anomalies in CoV\$ 2\$O\$ 4\$
16P-C019	C8	C1058	Ran Tong, Zhaorong Yang, Chen Shen, Xuebing Zhu, Yuping Sun, Li Li, Shile Zhang,	Disorder Induced Orbital Glass State in FeCr₂S₄
16P-C020	C8	C0954	T. Hamasaki, K. Zenmyo and H. Kubo	Magnetic Phase Transition of the Mixed Antiferromagnets Ni\$ 1-x\$A\$ x\$Cl\$ 2\cdot H\$ 2\$O (A=Co, Mn)
16P-C021	C8	C0168	Carlos F. Baldo III	Low-lying spin excitations due to Next-Nearest Neighbour interactions in Ferromagnetic lattices
16P-C022	C8	C0957	I. Shigeta, S. Urakawa, M. Ito and M. Hiroi	Magnetization and spin polarization of Cox-2FexMnSi Heusler alloys
16P-C023	C8	C1203	I. Shigetaa, Y. Tanaka, A. A. Golubov and M. Hiro	Spin polarized conductance in ferromagnet / insulator / conventional superconductor junctions
16P-C024	C8	C1103	M. Akatsu, S. Baba, T. Goto, S. Komatsu, K. Horie, K. Mitsumoto, T. Ogawa, Y. Nemoto,	Ultrasonic Investigation of Ground State of Vacancy Orbital in Boron-Doped Silicon
16P-C025	C8	C0021	Takahashi Masao	Conduction Electron States and Ferromagnetism of Electron-doped EuO
16P-C026	C8	C0023	V.G.Peschansky, O.V.Kirichenko	Diamagnetism and electron transport in organic layered
16P-D001	D4	D0033	Sybous1, A. El kaaouachi1, R. Abdia1, A. Narjis1, G. Biskupski2, J.	Quantum interference and localized magnetic moments in NbSi amorphous alloys at very low temperature with magnetic field
16P-D002	D4	D0034	A. Narjis1, A. El kaaouachi1, , J. Hemine3, A. Sybous1 , G. Biskupski 2, L.	Negative magneto conductivity in hydrogenated amorphous silicon-nickel alloys a-Si1-yNi_y:H at very low temperature with magnetic field.
16P-D003	D4	D0041	I.S. Burmistrov, I.V. Gronyi, A.D. Mirlin	Enhancement of superconductivity by Anderson localization
16P-D004	D4	D0042	Ya.I. Rodionov, I.S. Burmistrov	Out-of-Equilibrium Admittance of Single Electron Box Under Strong Coulomb Blockade

16P-D005	D4	D0094	I.Yu. Smirnov, I.L. Drichko, A.V. Suslov, O.A. Mironov and D.R. Leadley	Ferromagnetic-Paramagnetic Transition in a Tilted Magnetic Field in p-Si/ SiGe/Si Quantum Wells
16P-D006	D4	D0166	R. Gammag and C. Villagonzalo	The Interplay of Rashba Spin-Orbit Interaction and Landau Level Broadening on a Two-Dimensional Electron Gas Under a Tilted
16P-D007	D4	D0177	Xin Wan, Ki Hoon Lee, Zi-Xiang Hu, Kun Yang, E. H. Rezayi	Quasiparticle tunneling in fractional Quantum Hall liquids
16P-D008	D4	D0199	A.Fukuda, D.Terasawa, T.Morikawa, Y. D.Zheng, T.Arai, Z. F.	Activated tranport in the $\nu=1$ bilayer quantum Hall states with small tunneling energy $\Delta_{\text{SAS}} = 1 \text{ mK}$
16P-D009	D4	D0200	K. Iwata, A. Fukuda, M. Morino, and A. Sawada	Anisotropic nuclear spin relaxation and dynamic polarization rates in the $\nu=2/3$ quantum Hall states
16P-D010	D4	D0207	Ezawa Junichi	Meron-Pair Excitations in Imbalanced Bilayer Quantum Hall Systems
16P-D011	D4	D0222	A. O. Badruttinov, S. M. Huang, K. Kono, K. Ono, D. A. Tayurskii	Extremely long relaxation times of dynamically polarized nuclei in 3-electron spin blockade regime in GaAs vertical double quantum dot
16P-D012	D4	D0224	L.H. Willems van Beveren, H. Huebl, R. de Sousa, and A. Morello	Spin-Dependent Scattering in a Phosphorus Doped Silicon MOSFET
16P-D013	D4	D0307	A.V. Suslov, M. Kharitonov, M.V. Yakunin, I.Yu. Smirnov, S.A. Dvoretsky, and	Coincidence of the Landau levels in wide HgTe quantum well
16P-D014	D4	D0331	E.Grémion, D.Niepce, A.Cavanna, U.Gennser, and Y.Jin	Quantum Point Contact Transistor and Ballistic Field-Effect Transistors
16P-D015	D4	D0382	B. Shinozaki, S. Ezaki, K. Hidaka, K. Makise, T. Asano, N. Kokubo, K. Yamada, K. Yano,	Depression of positive magneto-conductance due to anti-weak localization effect in annealed In₂O₃-ZnO thick
16P-D016	D4	D0418	Xuan Qian, Yang Ji and Vladimir Umansky	Observation of dynamic nuclear polarization in a high-mobility low-density two-dimensional electron system
16P-D017	D4	D0492	C.Y. jiang, H. Ma, Y. Liu, J.L. Yu, Y.H. Chen	Radiation modulation effect of circular photogalvanic effect in two-dimensional electron gas system
16P-D018	D4	D0548	H. Ikegami, H. Akimoto, and K. Kono	Nonlinear Transports of Electrons on Liquid ⁴He in a 1.6 μm Channel

16P-D019	D4	D0605	P.-Q. Jin, M. Marthaler, J. H. Cole, A. Shnirman, G. Sch?n	Lasing and Transport in a Quantum Dot-Resonator System
16P-D020	D4	D0607	R. Peng, H.C. Xu, B. Zhou, J.F. Zhao, and D.L. Feng	Pervoskite AB₃ Thin Film Growth by Ozone Assisted Molecular Beam Epitaxy
16P-D021	D4	D0622	Ryoma Kobayashi and Hideki Yayama	Mobility of Electrons on Helium Film Capillary Condensed on a Two-Dimensionally Corrugated Surface of Solid Substrate
16P-D022	D4	D0638	C.H. Jung, K.M. Liu, V. Umansky, and S.Y. Hsu	Magnetotransport of gate confined cavities
16P-D023	D4	D0655	M. Z. Tahar, D. I. Popov and S. A. Nemov	Transport Properties of \$Sn\$ and \$SbI_{\{3\}}\$ Doped Single Crystal p-\$Bi_{\{2\}}Te_{\{3\}}\$
16P-D024	D4	D0665	K. W. Chan, M. Mottonen, A. Kemppinen, N. S. Lai, K. Y. Tan, W. H. Lim,	Single-electron shuttle in a silicon quantum dot
16P-D025	D4	D0748	M. Yamamoto, S. Takada, K. Watanabe, C. Baeuerle, A. D. Wieck and S. Tarucha	Electrical Control of a Flying Charge Qubit
16P-D026	D4	D0757	L. C. Li, S. K. Su, Y. W. Suen, J. Y. Wu, H. R. Kuo, Y. T. Sung, and C. P. Lee	Low Temperature and High Magnetic Field Ellipsometry System
16P-D027	D4	D0816	R. Okuyama and M. Eto	Superradiance in Transport through Ensemble of Double Quantum Dots
16P-D028	D4	D0975	M. A. Laakso, T. T. Heikkil?, and Y. V. Nazarov	Giant current fluctuations in an overheated single electron transistor
16P-D029	D4	D1005	Xiaoqing Zhou, B. Schmidt, L.W. Engel, C. Proust, G. Gervais, L.N. Pfeiffer, and K.W.	Parallel field induced novel phenomena in a weakly interacting 2D electron gas
16P-D030	D4	D1028	Y. Hirata, M. Nakajima, T. Suemoto, H. Tajima, Y. Kiuchi, Y. Matsushita, and K.	Electronic Properties of Polar-Metallic Iridium Oxides
16P-D031	D4	D1113	Gertrud Zwicknagl, Brendan E. Coughlan and Lars Musiol	Kondo effect in double quantum dots with magnetic field-tuned coupling
16P-D032	D4	D1131	F.D. Parmentier, A. Anthore, H. le Sueur, S. Jezouin, U. Gennser, A. Cavanna,	Strong back-action of a linear environment on a single electronic quantum channel

16P-D033	D4	D1169	K.M. Shen, E.J. Monkman, J.W. Harter, D.E. Shai, C. Adamo, L. Maritato, D.G.	New Frontiers for Einstein's Electrons : Photoemission Studies of Novel Correlated Materials and Artificial Heterostructures
16P-D034	D4	D1248	Y. Utsumi, D. Golubev, M. Marthaler, and G. Schoen	Effective temperature of the fluctuation theorem in single-electron counting
16P-D035	D4	D1320	Y. Yamane and M. Itoh	Boltzmann Description of Non-Interacting Electrons in Weakly Localized Regime
16P-D036	D4	D1330	Y. Hamamoto, T. Jonckheere, T. Kato and T. Martin	Breakdown of Universal Dynamical Resistance of a Mesoscopic Capacitor
16P-D037	D4	D1332	Jian Huang, L.N. Pfeiffer, K.W. West	Interaction-driven effects in strongly correlated GaAs Two-dimensional systems
16P-D038	D6	D0185	S. G. Cheng, H. Zhang and Q. F. Sun	Effect of electron-hole inhomogeneity on specular Andreev
16P-D039	D6	D0242	Yositake Takane and Ken-Ichiro Imura	Stationary Josephson effect in ballistic graphene junctions: effects of inhomogeneous carrier density
16P-D040	D6	D0284	He Long, Sun Jian and Yun Song	A Numerical Study of the Electronic Properties of Graphene
16P-D041	D6	D0356	Ya-Fen Hsu and Guang-Yu Guo	Anomalous integer quantum Hall effect in AA-stacked bilayer graphene
16P-D042	D6	D0368	Zhongqin Yang	Anomalous transport and spin filtering effect in graphene nanojunctions
16P-D043	D6	D0371	Shijie Hu, Wei Du, Guiping Zhang, Miao Gao, Zhong-Yi	Exact results for intrinsic electronic transport in graphene
16P-D044	D6	D0499	Wen-Min Huang, Jian-Ming Tang and Hsiu-Hau Lin	Power-law singularity in the local density of states induced by the point defect in graphene
16P-D045	D6	D0615	GuoPing Guo	Quantum transport of graphene nanostructure and its application in quantum information
16P-D046	D6	D0623	Y. Hamamoto, Y. Hatsugai, and H. Aoki	Chiral Symmetry and Electron-Electron Interaction in Many-Body Gap Formation

16P-D047	D6	D0644	Gunasekaran Venugopal and Sang Jae Kim	Low Temperature Electrical Transport and Field Effect Transistor Characteristics of Graphene- oxide Thin Films
16P-D048	D6	D0689	A.F Young, C.R. Dean, K.L Shepard, J. Hone, P. Kim	Quantum Hall ferromagnetism in graphene on hexa-Boron Nitride substrates
16P-D049	D6	D0692	M. Lewkowicz, B. Rosenstein and D. Nghiem	Two distinct ballistic processes in graphene at Dirac point: short time ultra-relativistic vs long time nonrelativistic
16P-D050	D6	D0750	H. Yoshioka and Y. Mochizuki	Properties of Graphene Nanoribbon with Zigzag Edges Attached to Two Normal Metals
16P-D051	D6	D0818	T. Morimoto and H. Aoki	Flow diagram of the longitudinal and Hall conductivities in ac regime in the disordered graphene quantum Hall system
16P-D052	D6	D0837	Wei Zhang	Quasienergy Spectra of a Charged Particle in Planar Honeycomb Lattices
16P-D053	D6	D0911	K. Tsumura, M. Ohsugi, T. Hayashi, S. Nomura, E. Watanabe, D. Tsuya, and H.	Development of superconducting interference device based on graphene
16P-D054	D6	D0947	B. Rosenstein, M. Lewkowicz and H.C. Kao	Signature of Schwinger's pair creation rate via radiation generated in graphene by a strong electric current
16P-D055	D6	D0952	H. Shioya, M. Yamamoto, S. Russo, M. F. Craciun and S. Tarucha	Bilayer graphene pn junction devices
16P-D056	D6	D1084	J. K. Vlijas, A. Fay, M. Wiesner and P. J. Hakonen	Self heating and nonlinear current-voltage characteristics in bilayer graphene
16P-D057	D6	D1115	A. Fay, R. Danneau, J. K. Viljas, F. Wu, M. Y. Tomi, M. Wiesner, and P. J. Hakonen	Electron-optical phonon interactions in bilayer graphene
16P-D058	D6	D1116	A. Fay, R. Danneau, J. K. Viljas, F. Wu, M. Y. Tomi, M. Wiesner, and P. J. Hakonen	Electron-optical phonon interactions in bilayer graphene
16P-D059	D6	D1157	T. Kaneko and H. Imamura	First-Principles Calculations of Graphene on Ti/Au Surface
16P-D060	D6	D1221	Z. Han, A. Allain, V.Bouchiat	Graphene Membranes for Cryogenic Nano- Electro-Mechanical Resonator

16P-D061	D6	D1309	Rui Zhu, Huiming Chen, and Maoli Lai	Pumped current and shot noise in adiabatically modulated graphene-based double-barrier structures
16P-D062	D6	D1391	C. Yanik, A. G. Demirkol, C. Celebi and I. I. Kaya	Breakdown of Quantum Hall Effect in Graphene
16P-D062	D8	D0060	D.A. Luzhbin	Small carbon clusters as molecular switches: modeling and working principles
16P-D063	D8	D0642	A. Yazdani, N. Kamali Sarvestani	Quantum Critical Point At Critical Conduction Electron Concentration
16P-D064	D8	D0653	A. Yazdani, S. Nabavi	A Critical Point at Which Magnetocaloric Effect Can Be Manifested
16P-D065	D8	D0784	R. F. Dou, F. Lin, F. W. Liu, Y. Sun, J.Y. Yang, B. F. Lin, L. He, C.M. Xiong and J.C. Nie	Comparative Study of the Structure and Electronic Property of Molecular
16P-D066	D8	D0844	Cheng-Wei Jiang, I-Chi Ni, Shien-Der Tzeng, Watson Kuo	Observation of single electron tunneling in strongly coupled gold-nanoparticle assembly.
16P-D067	D8	D0950	T. Lofwander, A. Bergvall, S. Kubatkin	Graphene Nanogap for Coherent Molecular Electronics
16P-D068	D8	D1173	Wei L. Wang, S. Bhandari, D. Bell, E. Kaxiras, R. Westervelt	Fabrication of Suspended Graphene Nanodevices
16P-D069	D8	D1341	Ray Ren	Spin polarization transport properties in ZnO/La₂/3Sr₁/3MnO₃ heterostructures
16P-D070	D8	D1390	A. G. Demirkol and I. I. Kaya	Fabrication of metallic nanogaps using in-situ controlled thermal evaporation
16P-E001	E6	E0061	D.Xu,P.Xu,L.F.Li,L.H.Gong	An apparatus for the measurements of thermal conductivity and thermal expansion based on GM cryocooler
16P-E002	E6	E0146	Y.X. Liang, Q. Dong, U. Gennser, A. Cavanna, and Y. Jin	Specific HEMTs for deep cryogenic high-impedance and low-frequency readout electronics
16P-E003	E6	E0302	P. Smeibidl, M. Bird, H. Ehmler and A. Tennant	New Hybrid Magnet System for Structure Research at Highest Magnetic Fields and Temperatures in the Millikelvin Region

16P-E004	E6	E0304	K. V. SRINIVASAN	Operation of cryogenic facility in e-way at Tata Institute of Fundamental Research, Mumbai, INDIA
16P-E005	E6	E0396	L. Skrbek, P. Urban and V. Musilova	Efficiency of Heat Transfer in High Rayleigh Number Cryogenic Helium Turbulent Convection
16P-E006	E6	E0423	Yu. M. Bunkov, E. Collin, J. Elbs and H. Godfrin	Dark Matter Detector on the Basis of Superfluid ^3He.
16P-E007	E6	E0580	I. Zivkovic, J. Piatek, I. Levatic, H.M. Ronnow	A new SQUID-based magnetometer for temperatures below 1 K implementing an extended motion piezo-motor for the sample
16P-E008	E6	E0624	E. Smith, M. Deshmukh, V. P. Adiga, H. S. Solanki, V. Singh, R. Bennett, N.	Compact, Inexpensive Coaxial Terminators for Low Temperature RF applications
16P-E009	E6	E0679	X. Wei, C. Bass, A. D'Angelo, A. Deur, G. Dezern, T. Kageya, M. Khandaker, D. Kashy,	HDice, Highly Polarized Low-Background Frozen-Spin HD Target for CLAS
16P-E010	E6	E0747	H. Kawasaki, T. Shigematsu, K. Imasaka, T. Ohshima, Y. Yagyu, and Y. Suda	Discharge characteristics in liquid helium, liquid nitrogen and pure water preparatory to fabrication of carbon nanomaterials
16P-E011	E6	E1037	A. Matsubara, T. Ueno, A. Sawada, K. Kono	Micro NMR Coil for Liquid ^3He at Ultra Low Temperature
16P-E012	E6	E1163	M. Keiderling, P. Gumann, D. Ruffner and H. Kojima	Compound Torsion Oscillator Driven Simultaneously at Two Frequencies
16P-E013	E6	E1317	Feng-jin Xia, Yue-ju Fu, Bo Xu, Yu-mei Wang, Jie Yuan, Hao Wu, Bei-yi Zhu, Xiang-	Preparation and Rectification Function of Multilayer Oxide p-i-n Junctions
16P-E014	E6	E1469	Guoqing Zhang,Ling Zhao,Feipeng Ning,Xiaojie Du,Zian Zhu	A design for high-field MRI main magnet based on the low temperature stability of NbTi superconducting wire
16P-E015	E6	E1498	Ozgur Karci, Gizem Durak, Munir Dede, Yury Bugoslavsky, Renny Hall, Ahmet	Low Temperature Scanning Probe Microscope (LT-SPM) operating in a Cryogen-Free Cryostat, 1.5-300K
16P-E016	E6	E1499	Munir Dede, Ozgur Karci and Ahmet Oral	mK-Scanning Probe Microscope(mK-SPM) operating in a Cryogen-Free Dilution Refrigerator at 20mK
16P-E017	E6	E1500	Zhongkun Hu, Minkang Zhou, Xiaochun Duan and Jun Luo	A cold atom interferometer for precise gravity measurements

16P-E018	E6	E1501	Minkang Zhou, Zhongkun Hu, Xiaochun Duan and Jun Luo	<u>Precisely mapping the magnetic field gradient in vacuum with a cold atom Interferometer</u>
----------	----	-------	---	--

Wednesday Aug.17

Time Slot	Category	ABSN	Name	Title
Plenary Session(11P)				
11P-1			Christophe Salomon	
11P-2		B1407	Peter Johnson	High Resolution Photoemission Studies of High T_c Superconductivity
11P-3			Leo Kouwenhoven	
11P-4			Alain Benoit	
Ending				

LT26

The 26th International Conference
on Low Temperature Physics
<http://lt26.iphy.ac.cn/>

